

DAYANANDA SAGAR COLLEGE OF ENGINEERING

(An autonomous Institute affiliated to Visvesvaraya Technological University, approved by AICTE & UGC, Accredited by NAAC with 'A' gradeandISO 9001-2015 Certified Institution)

DEPARTMENT OF AERONAUTICAL ENGINEERING

(Accredited by National Board of Accreditation, NBA)



A Project Report on

“APPLICATION OF THRUST VECTOR CONTROL FOR SOLID ROCKET MOTOR” (Sub Code: AE83)

Submitted in partial fulfillment for the award of the degree

**BACHELOR OF ENGINEERING
in
AERONAUTICAL ENGINEERING.**

Submitted By

AISHWARYA K (1DS16AE003)

KAVYA PATIL (1DS16AE021)

PRAJWAL NAYAK (1DS16AE030)

PRAJWAL P (1DS16AE031)

Under the guidance of

**SURESH P, M.E. (AERONAUTICAL ENGINEERING)
Assistant professor, Department of Aeronautical Engg.
Dayananda Sagar College of Engineering
Bengaluru-560078**

2019-20

DAYANANDA SAGAR COLLEGE OF ENGINEERING

(An autonomous Institute affiliated to Visvesvaraya Technological University, approved by AICTE & UGC, Accredited by NAAC with 'A' grade and ISO 9001-2015 Certified Institution)

DEPARTMENT OF AERONAUTICAL ENGINEERING

(Accredited by National Board of Accreditation, NBA)



CERTIFICATE

Certified that the project work entitled "**Application Of Thrust Vector Control For Solid Rocket Motor**" carried out by Ms. Aishwarya K (1DS16AE003), Ms. Kavya Patil (1DS16AE021), Mr. Prajwal Nayak (1DS16AE030), Mr. Prajwal P (1DS16AE031), in partial fulfillment for the award of **Bachelor of Engineering in Aeronautical Engineering**, during the academic year 2019-20. It is certified that all corrections/suggestions indicated for internal assessment have been incorporated in the report deposited in the departmental library. The project report has been approved as it satisfies the academic requirements in respect of project work prescribed for the said degree.

Signature of the Guide
(Suresh P)

Signature of the HOD
(Dr. Hareesha N G)

Signature of the Principal
(Dr. C P S Prakash)

Name of the examiners

1)

2)

Signature

DECLARATION

We, Ms.Aishwarya K (1DS16AE003), Ms. Kavya Patil (1DS16AE021), Mr. Prajwal Nayak (1DS16AE030), Mr. Prajwal P (1DS16AE031)], hereby declare that, this dissertation work entitled “Applicationof Thrust Vector Control for Solid Rocket Motor”has been carried out by us under the guidance of Suresh P, Assistant professor, Department of Aeronautical Engineering, in partial fulfillment of the requirement of the degree Bachelor of Engineering in Aeronautical Engineering.

Place: Bangalore

Aishwarya K (1DS16AE003)

Date:

Kavya Patil (1DS16AE021)

Prajwal Nayak (1DS16AE030)

Prajwal P (1DS16AE031)

ACKNOWLEDGEMENT

Before introducing our thesis work, we would like to thank the people without whom the success of this thesis would have been only a dream.

We express our deep sense of gratitude and indebtedness to **Suresh P**,Assistant Professor, Department of Aeronautical Engineering, for his valuable guidance, continuous assistance in the critical appraisal of the thesis.

We express our sincere thanks to **Dr. Hareesha N G**,Associate Professor and HOD, Department of Aeronautical Engineering, for providing the facilities required for the completion of this project work.

It is with great pleasure, we extend our gratitude and thanks to **Dr.C P S Prakash**, Principal, Dayananda Sagar College of Engineering, for his encouragement throughout the project.

It was a honor to work with **Dr. R Pandiyan**,Professor, Department of aeronautical engineering, for his valuable guidance through all the phases of our project and his valuable help in the controlling and guidance part of the project work.

We are also thankful to, **Anutha M A**, Assistant professor, Department of Aeronautical Engineering for her guidance and motivation towards successful completion of the project work.

We are also thankful to, **Naresh D C**, Project coordinator, Department of aeronautical engineering for his encouragement towards completion of this project

We feel short words to express our heartfelt thanks to all our family members and friends and all those who have directly or indirectly helped me during our course.

Aishwarya K (1DS16AE003)

Kavya Patil (1DS16AE021)

Prajwal Nayak (1DS16AE030)

Prajwal P (1DS16AE031)

ABSTRACT

The high launch cost of commercial rockets has led to a great interest into the development of reusable rockets. With this motivation, two aerospace companies have already developed technologies and successfully landed their first stages of rocket back onto the ground. However, the first stage rocket re-entry trajectory is pre-planned and controlled to accomplish recovery of stages. Such missions were achieved with the use of liquid engine thrust vectoring as it is relatively easy to vary the level of thrust. In this paper, we explore the concept of reusability to solid propellant motors by way of designing a rocket with a pre-defined thrust profile.

Firstly, a solid rocket motor has been designed with a goal to reach a maximum of 10 Km altitude which is planned to be used as a sounding rocket. It is aimed that the solid rocket motor is to be recovered so that it can be reused for subsequent launches. The recovery has to take place using a designed recovery rocket motor which has a pre-defined thrust profile. The rocket system also has an attitude control system to maintain the stability of the rocket while landing on the ground. The entire design process has assumed that the motion takes place in a plane and only one angular motion in the plane need to be controlled for clean landing. Thus, the equations of motion are representing just 3-degrees of freedom, two translational and one rotational motion. For simplicity, the earth is assumed to be flat and with constant acceleration due to gravity. The rocket motor for ascent and descent have been designed and simulations of control have been carried out using MATLAB® and Simulink® by assuming that the rocket is a point mass system for the thrust and motor design and a 6 DOF with all design constraints for controller response simulation. The simulation results indicate that the ascent motor is meeting the design goal of reaching 10 Km altitude clearly and the descent motor works perfectly to bring the structural portion of the rocket to the ground with closer to zero velocity.

For demonstration purposes of thrust vector control, a model rocket is also built which is controlled by two servo motors, operated by a micro controller. It has a ‘G’ class motor with a relatively low specific impulse propellant. A PID controller has been implemented to correct for the disturbances in pitch and yaw.

TABLE OF CONTENTS

CHAPTER-1	1
INTRODUCTION.....	1
1.1 Project background	2
1.2 Objectives	3
1.3 Scope of the project.....	3
1.4 Outline of thesis	3
CHAPTER-2	5
LITERATURE REVIEW.....	5
2.1 Literature review.....	5
CHAPTER-3	7
ANALYTICAL CALCULATIONS.....	7
3.1 Methodology	7
3.2 Prediction of propellant mass required to reach an altitude of 10km.....	8
3.2.1 Prediction of best mass.....	8
3.3 Formulae used for calculation of motor dimensions.....	10
3.3.1 MATLAB code used for calculation of motor dimensions	14
3.4 Structural constraint	14
3.5 Motor case thickness clculations.....	15
CHAPTER-4	16
MATERIALS	16
4.1 Airframe materials	16
4.2 Motor case materials	16
4.3 Thermal insulation by heat resistant polymers.....	16
4.3.1 Calculation of heat transfer	18
CHAPTER-5	19
MOTOR DESIGN AND BURN SIMULATION	19
5.1 Motor design	19
5.1.1 Ascent motor design.....	20
5.1.2 Descent motor design	21
5.2 3D motor representation.....	21
5.3 Burn simulation.....	22
5.3.1 Ascend motor	22
5.3.2 Descent motor	23
CHAPTER – 6.....	24

ROCKET BODY DESIGN	24
6.1 Nose cone.....	24
6.2 Fin design.....	25
6.3 Rocket body	25
6.4 Nozzle	26
6.5 Stability of rocket.....	27
6.6 Design details.....	28
CHAPTER-7	29
COMPUTATIONAL FLUID ANALYSIS	29
7.1 Flow analysis over rocket body	29
7.1.1 Grid independent test.....	29
7.1.2 Results and discussion.....	30
7.2 Nozzle flow analysis	31
7.2.1 Geometry	32
7.2.2 Mesh	32
7.2.3 Boundary conditions.....	32
7.2.4 Grid independent test.....	33
7.2.5 Result and discussion	34
CHAPTER-8	36
1D – FLIGHT SIMULATION	36
8.1 List of formulae used in simulation	36
8.2 Flight simulation	37
8.3 Results.....	39
CHAPTER – 9.....	43
THRUST VECTOR CONTROL.....	43
9.1 Definition	43
9.2 TVC mechanism with single nozzle	44
9.3 Control algorithm.....	46
9.3.1 Proportional Integral Derivative (PID) controller	46
9.3.2 Optimal control	46
9.3.3 Linear quadratic regulator	47
9.3.4 Model predictive control	47
9.4 Comparison	47
9.5 Equation of motion.....	48
9.6 Controller design in SIMULINK	51

9.6.1	Description of SIMULINK blocks	52
9.6.2	Results and discussion.....	55
CHAPTER-10		58
MODEL ROCKET		58
10.1.	Introduction to Model Rocket.....	58
10.2.	Propellant Selection	59
10.3.	Selection of motor materials and motor fabrication	60
10.4.	Motor static test	61
10.5.	Rocket body material selEction	62
10.5.1	3D design and printed parts	62
10.6.	Component mass calculation:	63
10.7.	Electronics	64
10.8.	TVC code generation:.....	67
10.9.	PCB design	73
CHAPTER 11.....		79
CONCLUSION		79
11.1 Conclusion.....		79
11.2 Future scope.....		80
References		82
APPENDIX		83
Appendix 1: MATLAB code for theoretical calculation		83
Appendix 2: Nozzle dimension calculation MATLAB code		86
Appendix 3: 1D flight simulation MATLAB code		86
Appendix 4: TVC Arduino code compilation output		87

LIST OF TABLES

Table 3. 1 Variation of mass with altitude.....	9
Table 4. 1Properties of laminates made using six alternate layers of CCF and KP based EPDM prepgs.....	17
Table 5. 1 Composition of APCP	19
Table 6. 1 Design details and values of designing Plant.....	28
Table 7. 1 Boundary conditions for nozzle flow analysis.....	32
Table 10. 1 Mass of various components of rocket	63

LIST OF FIGURES

Fig 3.1 Variation of mass with altitude.....	9
Fig 4. 1 Photo of cross-section of a laminate consisting of six alternative layers of (CCF or KP) based prepgs.....	17
Fig 5. 1 Ascent motor design	20
Fig 5. 2 Descent motor grain configuration	21
Fig 5. 3 3D motor design (ISO view)	21
Fig 5. 4 Thrust curve for ascend motor.....	22
Fig 5. 5 Thrust curve for descend motor.....	23
Fig 6. 1 Design of nose cone.....	24
Fig 6. 2 Fin design	25
Fig 6. 3 Rocket body design	25
Fig 6. 4 Sectional view of rocket body excluding electronics and hydraulics.....	26
Fig 6. 5 Convergent-Divergent nozzle design	26
Fig 6. 6 Rocket stability and part details.....	27
Fig 7. 1 Mesh generated for rocket body	29
Fig 7. 2 Coefficient of drag vs Number of elements (Mach 0.5).....	30
Fig 7. 3 Coefficient of drag vs number of elements (Mach 1.5).....	30
Fig 7. 4 Velocity contour for Mach 1.5	30
Fig 7. 5 Pressure contour for Mach 1.5.....	31
Fig 7. 6 Pressure contour (left) and velocity contour(right) for Mach 0.5.....	31
Fig 7. 7 Meshing of the nozzle.....	32
Fig 7. 8 Throat pressure vs number of elements	33
Fig 7. 9 Exit velocity vs number of elements	34
Fig 7. 10 Pressure contour	34
Fig 7. 11 Velocity contour	35
Fig 8. 1 Simulink block and connections for simulation of flight	37
Fig 8. 2 Simulink blocks and connections to calculate engine thrust and weight	38

Fig 8. 3 Simulink block and connections to calculate subsonic drag	38
Fig 8. 4 Simulink block and connections to calculate supersonic drag	39
Fig 8. 5 Coefficient of drag variation with respect to Mach number.....	39
Fig 8. 6 Variation of altitude with time.....	39
Fig 8. 7 Variation of acceleration with time	40
Fig 8. 8 Variation of velocity with time.....	40
Fig 8. 9 Variation of thrust with time	40
Fig 8. 10 Variation of drag with time	41
Fig 8. 11 Variation of mass with time.....	41
Fig 9. 1 Control of rocket body using thrust vector control.....	43
Fig 9. 2 Axis of pitch, yaw and roll motion along rocket body	44
Fig 9. 3 Pivot points for flexible nozzle bearing.....	44
Fig 9. 4 Types of thrust vectoring using single nozzle	45
Fig 9. 5 Forces acting on rocket body.....	48
Fig 9. 6 Controller and Simulation model	52
Fig 9. 7 Rocket inertial system and propulsion system blocks	52
Fig 9. 8 motor configuration subsystem for both ascent and decent	53
Fig 9. 9 Moment of inertia calculation subsystem.....	53
Fig 9. 10 Force and moment measurement Subsystem.....	54
Fig 9. 11 6 DOF Quaternion and Result subsystem	54
Fig 9. 12 PID response for a step input of 1 (left) and 2 (right) degree of rotation	55
Fig 9. 13 Velocity change in XYZ direction (Red – X, Yellow – Y, Blue – Z)	55
Fig 9. 14 Trajectory of the rocket with respect to Time	56
Fig 9. 15 Force variation on the inertial frame of reference of rocket.....	56
Fig 9. 16 Response output for continuous disturbance	57
Fig 9. 17 Quaternion response test results – (green implies test passed) , and the band noise response (right).....	57
Fig 10. 1 Propellants selected for motor test.....	60
Fig 10. 2 Fabricated solid rocket motor	60
Fig 10. 3 Motor static test and its setup	61
Fig 10. 4 Thrust data recorded with respect to time	61
Fig 10. 5 Landing legs design and 3D printed part.....	62
Fig 10. 6 PCB mount design and 3D printed part.....	62
Fig 10. 7 TVC design and assembly of the Printed part	63

Fig 10. 8 Teensy 3.2.....	64
Fig 10. 9 BMP 280.....	65
Fig 10. 10 Micro SD card reader	65
Fig 10. 11 9g servos	65
Fig 10. 12 N channel MOSFET	66
Fig 10. 13 5V regulator.....	66
Fig 10. 14 Buzzer.....	66
Fig 10. 15 RGB light.....	67
Fig 10. 16 LIPO battery	67
Fig 10. 17 Teensy 3.2.....	74
Fig 10. 18 MPU 6050.....	74
Fig 10. 19 BMP 280.....	75
Fig 10. 20 Micro SD Card Reader	75
Fig 10. 21 Pyro channels.....	75
Fig 10. 22 Voltage Regulator, Battery Terminal and Switch	76
Fig 10. 23 Servo.....	76
Fig 10. 24 Buzzer and RGB LED	76
Fig 10. 25 Header Pins.....	76
Fig 10. 26 Voltage Measure.....	77
Fig 10. 27 Top and Bottom layer of PCB board	77
Fig 10. 28 Electronics connections arranged in breadboard for response outputs.....	78
Fig 10. 29 PID response signal and launch detection signal.....	78

LIST OF ABBREVIATIONS

Symbol	Description	Units
APCP	Ammonium perchlorate composite propellant	-
MIT	Massachusetts Institute of Technology	-
R _c	Burn rate co-efficient	-
ρ	Density	kg/m ³
n	Burn rate exponent	m/s
ISP	Specific impulse	Ns/kg
PDMS	Poly-di-methyl-siloxane	-
HTPB	Hydroxyl-terminated polybutadiene	-
RoManS	Rocketry Management software	-
COG	Centre of Gravity	-
Al	Aluminium	-
g	Acceleration due to gravity	m/s ²
AP	Ammonium perchlorate	-
CCF	Chopped carbon fibre	-
K _n	Ratio of burn area to throat area	-
V	Velocity	m/s
A	Area of rocket body	m ²
C _d	Co-efficient of drag	-
P	Pressure	N/m ²
M	Mach number	-
k	Specific heat ratio	-
F _i	Inertial force	N
T	Thrust force	N
F _d	Drag force	N
ṁ	Mass flow rate	kg/s
m	Mass	kg
a	Acceleration	m/s ²
D	Diameter of rocket body	m
V _{bo}	Burnout velocity	m/s
m _r	Rocket dead mass	kg

N	Drag influence number	-
t	Thickness	m
σ	Yield strength of Aluminium 6061 t6	N/m ²
FOS	Factor of safety	-
A _t	Nozzle throat area	m ²
A _b	Propellant burning area	m ²
ρ_p	Density of propellant	kg/ m ²
C*	Characteristic velocity	m/s
P _c	Chamber pressure	N/ m ²
r _b	Burning rate	mm/s
N _m	Mach number of propellant	-
P _e	Exit pressure	N/ m ²
γ	Specific heat of propellant	-
A _e	Nozzle exit area	m ²
D _e	Nozzle exit diameter	m
T _c	Chamber temperature	K
T _e	Exhaust temperature	K
V _e	Exhaust velocity	m/s
R	Gas constant	-
M	Molecular mass of propellant	-
P _t	Pressure at throat of nozzle	N/ m ²
\dot{m}	Mass flow rate of propellant	kg/s
F	Thrust produced by motor	N
P _a	Atmospheric pressure	N/ m ²
C _F	Thrust coefficient	-
I _{sp}	Specific impulse	Ns/kg
g	Acceleration due to gravity	m/s ²
I _{sm}	Average specific impulse	Ns/kg
ΔV	Change in velocity	m/s
\dot{m}_n	Flow rate through nozzle	kg/s
m _p	Mass of propellant	kg
w _f	Web fraction	-
w _t	Web thickness	m
V _f	Volumetric load fraction	-
V _p	Grain volume	m ³

V_c	Chamber volume	m^3
H	Altitude	m
W	Weight	N
F_t	Total force	N
m_e	Empty mass of rocket	kg
m_t	Total mass of rocket	kg
Acc	Accuracy	-
ANOVA	Analysis of Variance	-
Ao	Cost of replacement or repair	-
CNC	Computer Numerical Control	-
DOF	Degree of Freedom	-
DOE	Design of Experiments	-

CHAPTER-1

INTRODUCTION

Thrust vector control or TVC, is the ability of rocket, an aircraft or other vehicle to manipulate the direction of the thrust from its engine(s) or motor(s) to control the attitude or angular velocity of the vehicle. Model rockets have fins and launch quickly, but real space launch vehicles don't; they actively aim exhaust vector to steer the rocket. Usage of fins in traditional rockets and missiles increases the drag whereas implementing thrust vector control for solid rocket motor (SRM) for stability and guidance not only overcomes drag but is the key to propulsive landings. Thrust vectoring enables control over the direction of a rocket's engines during flight to change its trajectory and stabilize the vehicle.

Related to SpaceX's Falcon series of self-landing rockets where the first and second stage is automated to return to earth and land so that it can be reused. This is a recent field which was successful only in 2015 and very little information is available for rockets at a smaller scale for development. This project is to explore the possibility of control of a model solid propellant rocket motor at a smaller scale. Here, rocket achieves thrust vectoring by deflecting the nozzle or the entire motor which none of the amateur rocketeers have been able to successfully achieve.

These missions were achieved with the integration of thrust vectoring for liquid engines where it is relatively easy to vary the total thrust, this project will explore to see whether it is possible to achieve landing for solid propellant motor whose thrust remains almost constant.

Preliminary design of the rocket and rocket motor nozzle will be attempted and computer simulations will be carried out to prove the effectiveness of the concept. Further the project will attempt to experiment to land the rocket purely with the help of thrust vectoring. This will help us to apply most of the aerospace elements such as propulsion, performance, structures, aerodynamics, control and stability; to carry out experiments.

The project deals with selection of solid propellant, theoretical calculation of performance parameters, design and optimizing the nozzle for desired performance, computational analysis and simulation, wind tunnel test and finally aims at controlling the

thrust vector by gimbling the nozzle or the entire solid motor with the help of commercial micro-processor to provide pitch and yaw moments for stability.

In this project the dimensions for maximum optimized rocket motor are calculated from MATLAB code. Then the flight simulation is done such that the rocket reaches to an altitude of 10 km. Further, design and flow analysis over rocket body is done by using solid-works and ANSYS®. For thrust vector control, the simulation developed is in 2-dimensions only and hence a single rotational movement is needed. Finally, the flexible laminated bearing nozzle configuration which is similar to gimbal nozzle is adopted for TVC control of solid rocket motor.

1.1 PROJECT BACKGROUND

Solid propellant rocket is a rocket which uses solid propellants as fuel to produce thrust. The solid rocket motors were invented during 13th century, earlier they used black powder as fuel for rocket motors. Till 20th century almost all rockets used solid propellant but, later liquid rockets, hybrid rockets were used extensively because of their higher efficiency and these rockets can be controlled easily. Because of the simplicity in design and operation of solid rockets, they are still used today in many larger applications. The solid rockets also provide advantageous like they can be stored for long period of time and can be launched on short notice. And these solid rockets are frequently used in military applications like missiles.

Because of the low performance of solid rockets as compared to liquid rockets and hybrid rockets, the solid rockets are not used as the primary means of propulsion for modern medium to large launch vehicles which are used to orbit satellites and launch major space probe. Instead the solid rockets are used for instant and smaller applications like air to air and air to ground missiles, on model rockets and are used as boosters.

The vectored thrust started in the mid-1950s when a Frenchman, Michel Wibault, proposed a single seat fighter that he called the Gyroptere. This led to a new Bristol engine, the Pegasus, having 4 rotating nozzles. The rocket design has evolved in such a way that it is becoming more cheaper this motivates us to develop more economic launchers, NASA developed a SLS rocket booster that can be reused upto 20 times and they are more powerful. Thrust vectoring has been improved more in recent times for fin less launch of rocket which increase efficiency if the rocket, and they are easily controllable in case of emergency failure as per NASA publication.

1.2 OBJECTIVES

- To design the solid rocket motor through an iterative process and theoretical calculations.
- Validate the theoretical values with flight and burn computer simulation of solid rocket motor
- Implementation of thrust vector control for pitch and yaw moments and design of rocket for an altitude goal of 10km
- Development of guidance and control for rocket and simulation of control response in SIMULINK
- Development of TVC for two axis control and Arduino code for TVC
- Development of model rocket for TVC working validation.

1.3 SCOPE OF THE PROJECT

- Provides a comprehensive modelling approach or guidelines using TVC.
- Simplicity makes solid rockets a good choice.
- Reusable, Low orbit satellite launch.
- Provides methods to be followed for propulsive landing a solid rocket booster
- Provides information regarding development of controlling method and code generation for TVC operations.
- A step towards making rockets cheaper and more reliable.

1.4 OUTLINE OF THESIS

Chapter 1: This chapter gives the introduction about the development of thrust vector control for solid rocket motor, project background, objective and the scope of the present work.

Chapter 2: This chapter gives the reviews of the literature survey.

Chapter 3: This chapter deals with the calculations motor and rocket body dimensions, prediction of best mass, structural constraint, motor case thickness calculations. The preliminary work has done as development of MATLAB code for calculation of rocket body motor dimensions through iterative process.

Chapter 4: This chapter deals with the selection of airframe material, motor case material and thermal insulation material and its thickness calculations.

Chapter 5: This chapter gives the design of ascend and descend motor with burn simulations, 3D motor design, nozzle design.

Chapter 6: This chapter deals with the fin design, nose cone design and rocket body design and the design methodology used, and the structural constraints and other relative data and also design of thrust vector control

Chapter 7: This chapter gives the computational fluid analysis of the nozzle and its throat pressure calculation, computational fluid analysis over rocket body and its drag calculation for both subsonic and supersonic conditions.

Chapter 8: This chapter deals with the flight simulation by considering rocket body as a point mass in the MATLAB® coder and SIMULINK® environment.

Chapter 9: This chapter deals with controlling of rocket and the simulation of rocket in 3D with the help of quaternions and it also explains different controllers and TVC mechanism available and selection criteria of TVC

Chapter 11: This chapter deals with experimental part of the project, it explains the development of the model rocket, and generation of the Arduino code for the TVC and electronics required for the working of TVC

CHAPTER-2

LITERATURE REVIEW

2.1 LITERATURE REVIEW

The vectored thrust started in the mid-1950s when a Frenchman, Michel Wibault, proposed a single seat fighter that he called the Gyroptere. This led to a new Bristol engine, the Pegasus, having 4 rotating nozzles. With Blue Origin's New Shepard booster rocket making the first successful vertical landing on November 23, 2015 and SpaceX's Falcon 9 marking the first landing of a commercial orbital booster on December 22, 2015. After stage separation, the booster flips around, an optional boost back burn is done to reverse its course, a re-entry burn, controlling direction to arrive at the landing site and a landing burn to affect the final low-altitude deceleration and touchdown.

Master of Science thesis on A Robust Control Approach for Rocket Landing by Reuben Ferrante [1] demonstrates the design and compares classical and optimal control algorithms with machine learning algorithms with increasing sophistication. For simplification of the problem 3 degree of freedom body is considered that is having x and z as position variables and the other is pitch angle. For 2-dimensions, only a single rotational movement is needed.

A report prepared for jet propulsion laboratory by NASA ‘Study of selected thrust vector control systems for solid propellant motors’ [2], This study was conducted to evaluate several possible thrust vector control system/propellant combinations within the three concepts, liquid injection into rocket engine exhaust gases, auxiliary hot or cold gas systems, and gimballed nozzles. This helped in selecting the TVC methods for solid motors and design aspects of nozzle.

A student project report on ‘Design and Integration of a High-Powered Model Rocket’ [3] provides mechanical design, construction, integration and also structural, aerodynamic and thermal analysis of parts for a high-powered rocket, the aerodynamic and inertial forces acting on the rocket body were also calculated. These forces were then used to predict the stresses acting on the rocket during its flight, which helped in selection of material.

‘Two-Stage, High-Altitude Rocket with Internal Skeleton Design Entered in Advance Category of 7th ESRA IREC’^[4], describes the design of internal structure of the rocket, using this the rocket internal structures were designed followed by structural analysis in the Ansys and then assembled in Solid works.

‘Design Optimization and Analysis of Rocket Structure for Aerospace Applications’^[5] This project involves component design and fabrication, structural, aerodynamic, and thermal analysis as well as functionally testing. SolidWorks is used for component design and integration. ANSYS simulations provide the structural loads on components and safety factors. FLUENT simulations and analytical modelling determine the drag forces during ascent and decent.

‘Mechanical Properties of Glass Fibre Reinforced Polyester Composites’^[6], helped in determine the material properties.

‘Conceptual Design and Structural Analysis of Solid Rocket Motor Casing’^[7], helped in calculation of the required motor thickness which resists all the thermal loads during the combustion.

‘Rocket Fin Design’^[8] by Eric Hardester& Philip, explains the detailed design of rocket fin and this has been used to determine the dimension of the fins.

‘Thermal insulation by heat resistant polymers for solid rocket motor insulation’^[9] material for thermal protection, properties and thickness helps in selecting the motor insulation material.

‘Rocket propulsion elements’^[10] by George P Sutton helped in understanding different concept of solid rocket motor design including grain configuration, nozzle design, and the equations of motion of the rocket in different frame of reference, requirement of control for rocket. This equation is used to model the rocket in the MATLAB Simulink and simulate the rocket during ascend for its different parameters.

CHAPTER-3

ANALYTICAL CALCULATIONS

3.1 METHODOLOGY

- **LEVEL 1: Preliminary work**

Studying the Propulsion elements, Aerodynamics of solid rocket motor and thrust vector control from journals for formulation. Along with this, the necessary control engineering is referred for take-off.

- **LEVEL 2: Determination of propellant characteristics and availability**

Several propellants are formulated, and corresponding characteristics are determined from the ProPep-3 tool in order to select suitable propellant that satisfy the requirements for this project.

- **LEVEL 3: Design of solid rocket motor and flight simulation using SIMULINK**

Theoretical performance parameters are calculated using MATLAB by considering grain configuration and maximum chamber pressure. This results in the respective dimensions of motor casing and nozzle using the propellant characteristics.

- **LEVEL 4: Design of rocket body**

Design the outer cylindrical body and nose cone having less aerodynamic drag. Calculation the total mass, weight distribution, coefficient of pressure, lift, drag, keeping the center of gravity always ahead of center of pressure.

- **LEVEL 5: CFD analysis and simulation**

The rocket is modelled with SOLIDWORKS and analyzed using ANSYS. And flight parameters are simulated using MATLAB. The rocket nozzle is optimized to eliminate erosive burning by minimizing the peak mass flux.

- **LEVEL 6: Design of thrust vector control and Programming the control system**

The 3-D design of thrust vector mount is done and is printed to have vectoring in pitch and yaw, this done such that it bears the maximum thrust delivered by the motor. Flight computer is designed and programmed to control two servo motors.

- **LEVEL 7: Motor build and static test of a solid rocket motor with TVC**

The motor is built, and the propellant is added in the desired grain configuration. Then the static test is carried out to verify the response

3.2 PREDICTION OF PROPELLENT MASS REQUIRED TO REACH AN ALTITUDE OF 10KM

The spreadsheet designed by Richard. A. Nakka is intended as an easy-to-use design aid for model rockets. Unlike most simulation software, that estimates peak altitude for a given rocket and motor combination, this program instead considers peak altitude as a design goal and based on this goal, the program computes what motor size is required to reach this altitude.

The various parameters that describe the proposed rocket vehicle, as well as basic motor sizing parameters are given as inputs for subsonic flights. These inputs are as follows:

- Altitude Goal
- Rocket basic data: Body diameter, Empty mass and Drag coefficient
- Motor sizing data: Chamber Diameter, Propellant loading, Propellant type and Thrust time
- Propellant data: Density and Specific Impulse

This program is meant only for low-powered rockets propelled by propellant that has a specific impulse in the range of 100 to 150. For high-powered rockets that utilizes a propellant of specific impulse of >180 (used in our case), this spread-sheet is taken as a reference and has been modified. This resulted in the mass of 26.348 kg for APCP as propellant.

3.2.1 PREDICTION OF BEST MASS

Best mass is the mass that the rocket should have in order to reach maximum altitude propelled by certain mass of propellant. If the total mass is less than the best mass then, the rocket will not have enough momentum to travel further after burnout. If the total mass is greater than the best mass then, the rocket will have large momentum and will reach a lower altitude before burnout. Therefore, consideration of best mass is a crucial aspect.

The Simulink program is designed and simulated for propellant mass data from above and the best mass is tabulated as shown in Table 1.1.

Table 3. 1 Variation of mass with altitude

Mass (kg)	Altitude (m)
65.711	10140
63.711	10330
61.711	10390
59.711	10600
57.711	10630
55.711	10680
53.711	10710
51.711	10690
49.711	10650
47.711	10610
45.711	10520
43.711	10450
41.711	10340

A series of varying wet mass of the rocket for peak altitude is calculated.

1. Peak altitude of 10710 m for propellant mass of 26.348 kg
2. With this the total best mass of the Rocket (wet mass) = 53.711 kg

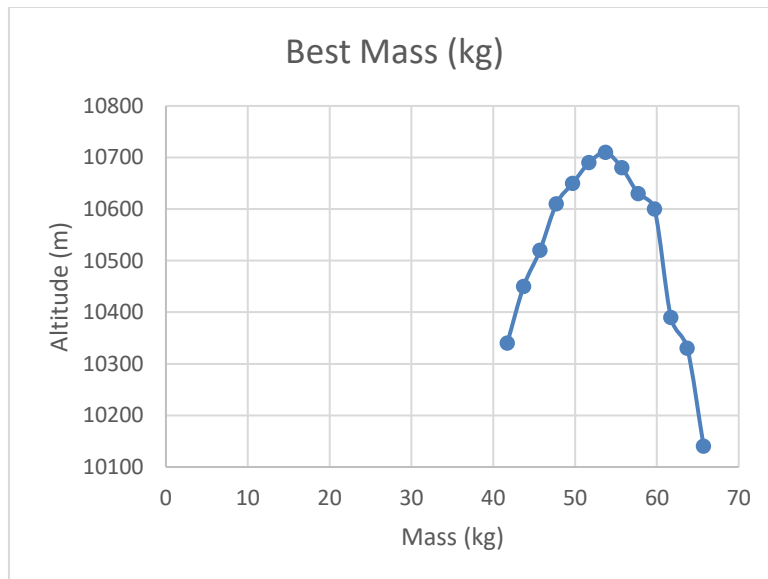


Fig 3.1 Variation of mass with altitude

The dry mass has to be around 27 kg and is designed and estimated in the later sections.

3.3 FORMULAE USED FOR CALCULATION OF MOTOR DIMENSIONS

In order to design a motor many design parameters, performances parameters has to be considered. Hence many formulas that are related to solid rocket motor design are taken from various sources and from these formulas the motor design has been tried in various ways. Although all the design parameters are available it is challenge to find the correct sequence to design the motor. It can only be done by optimization and iterative process. And the formulas that are used for design process are as follows:

- 1. Nozzle throat area:** This is the smallest cross section of nozzle and the exhaust flow is choked at the throat that is the Mach no. of exhaust flow becomes equal to 1.0 here.

$$A_t = \frac{A_b \times \rho_p \times a \times C^*}{P_c^{n-1}} \quad (3.1)$$

$$A_t = \frac{\dot{m}}{P_t} \sqrt{\frac{R \times T_t}{M \times \gamma}} \quad (3.2)$$

- 2. Chamber Pressure:** Many parameters are dependent upon the chamber pressure developed by the motor such as throat area, thrust developed, efficiency, burn rate.

$$P_c = \left[\frac{\rho_p \times A_b \times a \times C^*}{A_t} \right]^{\frac{1}{1-n}} \quad (3.3)$$

$$P_c^{n-1} = \frac{\rho_p \times A_b \times a}{C_D \times A_t} \quad (3.4)$$

$$P_c = \left(\frac{\gamma+1}{2(\gamma-1)} \right)^{\frac{\gamma+1}{2(\gamma-1)}} \times \frac{\sqrt{\gamma \times R \times T_c}}{\gamma \times A_t} \times \dot{m} \quad (3.5)$$

- 3. K_n:** It is the ratio of burning area to nozzle throat area.

$$K_n = \frac{A_b}{A_t} \quad (3.6)$$

- 4. Burning rate:** It determines the rate at which the propellant is burns and generates exhaust gas. Pressure and temperature are the parameters that affects the burn rate.

$$r_b = a \times P_c^n \quad (3.7)$$

$$r_b = \frac{P_c \times A_t}{\rho_p \times A_b \times C^*} \quad (3.8)$$

$$r_b = \frac{P_c}{\rho_p \times K_n \times C^*} \quad (3.9)$$

- 5. N_m :** Many properties and design parameters can be found if the Mach number is known and hence it is important to find the Mach number and can be done by the following formula where Mach number is expressed by N_m .

$$N_m = \sqrt{\frac{2}{\gamma-1} \times \left[\left(\frac{P_c}{P_a} \right)^{\frac{\gamma-1}{\gamma}} - 1 \right]} \quad (3.10)$$

- 6. Exit area of nozzle:** Nozzle exit pressure in terms of exit Mach number and throat area is given by the formula

$$A_e = \frac{A_t}{N_m} \times \left[\frac{1 + \left(\frac{\gamma-1}{2} \right) \times N_m^2}{\frac{\gamma+1}{2}} \right]^{\frac{\gamma+1}{2(\gamma-1)}} \quad (3.11)$$

- 7. Exit diameter:** Exit diameter can be obtained by exit area as follows

$$D_e = 2 \times \sqrt{\frac{A_e}{\pi}} \quad (3.12)$$

- 8. Exhaust temperature:** The exhaust temperature determines the exhaust speed of sound and helps in determining exhaust velocity and formula to find exhaust temperature is as follows

$$T_e = \frac{T_c}{1 + \left(\frac{\gamma-1}{2} \right) N_m^2} \quad (3.13)$$

- 9. Exit velocity:** Exit velocity helps in determining the amount of thrust produced.

$$V_e = N_m \times \sqrt{\gamma \times r \times T_e} \quad (3.14)$$

$$V_e = \sqrt{\frac{2 \times r \times T_c}{(\gamma-1)} \times \left[1 - \left(\frac{P_c}{P_a} \right)^{\frac{\gamma-1}{\gamma}} \right]} \quad (3.15)$$

$$r = \frac{R}{M}$$

Specific heat ratio at exit

r=R/M at exit

10. Throat Pressure: The throat pressure in terms of chamber pressure can be determined from the following formula

$$P_t = P_c \times \left(1 + \frac{\gamma-1}{2}\right)^{-\left[\frac{\gamma}{\gamma-1}\right]} \quad (3.16)$$

11. Throat Temperature: The formula for throat pressure in terms of chamber temperature is as follows

$$T_t = \frac{T_c}{\left(1 + \frac{\gamma-1}{2}\right)} \quad (3.17)$$

12. Mass flow rate: Mass flow rate is helpful in determining the thrust produced by the motor and mass flow rate can be determined from the following formula

$$\dot{m} = \frac{P_c \times A_t}{\sqrt{T_c}} \times \sqrt{\frac{\gamma}{r}} \times \left(\frac{\gamma+1}{2}\right)^{-\left[\frac{\gamma+1}{2(\gamma-1)}\right]} \quad (3.18)$$

13. Thrust: It is the force which helps the rocket to move in space and it can be determined in terms of exit velocity, mass flow rate and pressure as follows

$$F = \dot{m} \times V_e + (P_e - P_a) \times A_e \quad (3.19)$$

$$F = C_F \times P_c \times A_t \quad (3.20)$$

14. Thrust coefficient: It is a factor about which a thrust is multiplied by the nozzle and it is defined as the thrust per unit chamber pressure and throat area.

$$C_F = \sqrt{\frac{2 \times Y^2}{Y-1} \left(\frac{2}{Y+1}\right)^{\frac{Y+1}{Y}}} \left[1 - \left(\frac{P_e}{P_c}\right)^{\frac{Y-1}{Y}}\right] + \left(\frac{P_e - P_a}{P_c} \times \frac{A_e}{A_t}\right) \quad (3.21)$$

15. Specific impulse: It is the measure of how effectively the mass of the propellant has been utilized that is it indicates the efficiency of the engine. The engine with high specific impulse produces more thrust compared to other engines with less specific impulse for same weight of propellant.

$$I_{sp} = \frac{F}{\dot{m} \times g} = \frac{P_c \times C_F \times A_t}{g \times P_c \times C_D \times A_t} = \frac{C_F}{g \times C_D} \quad (3.22)$$

$$I_{sp} = \frac{1}{g} \sqrt{2 \times T_c \times r \times \left(\frac{\gamma}{\gamma-1}\right) \left[1 - \left[\frac{P_e}{P_c}\right]^{\frac{\gamma-1}{\gamma}}\right]} \quad (3.23)$$

16. Average specific impulse:

$$I_{sm} = \frac{\int_0^{t_c} F \times dt}{g \int_0^{t_c} \dot{m} \times dt} = \frac{\int_0^{t_c} F \times dt}{g \times m_p} = \frac{I_t}{g \times m_p} \quad (3.24)$$

17. Change in velocity:

$$\Delta V = g_0 \times I_s \times \ln\left(1 + \frac{\rho_p \times V_p}{m_a}\right) + g \times t_c = g_0 \times I_s \times \ln\left(\frac{m_t}{m_a}\right) + g \times t_c \quad (3.25)$$

18. Propellant grain flow rate:

$$\dot{m} = \rho_p \times A_b \times r_b \quad (3.26)$$

19. Flow rate through nozzle:

$$\dot{m}_n = \frac{P_c \times A_t}{C^*} \quad (3.27)$$

20. Discharge coefficient: It is a measure of losses that occur in chamber and nozzle and coefficient of discharge in terms of chamber temperature is given below

$$C_D = \frac{\tau(\gamma)}{\sqrt{\gamma \times r \times T_c}} \quad (3.28)$$

$$r = \frac{R}{M} \quad (3.29)$$

$$\tau(\gamma) = \gamma \times \left(\frac{2}{\gamma+1}\right)^{\frac{\gamma+1}{2(\gamma-1)}} \quad (3.30)$$

$$C_D = \frac{m_p}{\int_0^{t_c} P_c(t) \times A_t(t) \times dt} \quad (3.31)$$

21. Temperature ratio:

$$\frac{T_a}{T_c} = \left(1 + \frac{\gamma-1}{2} N_m^2\right)^{\frac{\gamma}{\gamma-1}} \quad (3.32)$$

22. Web fraction: More the web fraction more will the rate of burn, and it is a ratio of web thickness of propellant and outer radius of propellant.

$$w_f = \frac{w_t}{r} \quad (3.33)$$

23. Volumetric load fraction: It indicates volumetric and performance efficiencies of motor and is a ratio of propellant/grain volume to volume of chamber.

$$V_f = \frac{V_p}{V_c} \quad (3.34)$$

$$V_f = \frac{I_t}{I_s \times \rho_p \times g \times V_c} \quad (3.35)$$

24. Characteristic velocity: It is used to compare between various propellants and is dependent on performance of nozzle and indicated combustion performance.

$$C^* = \frac{1}{c_D} = \sqrt{\frac{(R/M) \times T_c}{\gamma \times \left(\frac{2}{\gamma+1}\right)^{\gamma-1}}} \quad (3.36)$$

25. Expansion ratio: More the expansion ration less will be the pressure of gas inside the nozzle and it is defined as the ratio of exit area to the throat area.

$$\frac{A_e}{A_t} = \frac{1}{N_m} \times \left[\frac{1 + \left(\frac{\gamma-1}{2}\right) \times N_m^2}{\frac{\gamma+1}{2}} \right]^{\frac{\gamma+1}{2(\gamma-1)}} \quad (3.37)$$

3.3.1 MATLAB CODE USED FOR CALCULATION OF MOTOR DIMENSIONS

It is important to know the sequence of calculation during design of the motor; many calculation patterns have been tried. Later chamber pressure of 500psi has been considered with some assumptions which will be explained in further section and following code has been run in MATLAB to get various dimensions and performance parameters. It is not possible to get results at the first run and hence iterative process has been adopted in the design. The MATLAB code is depicted in the Appendix 1 and 2.

3.4 STRUCTURAL CONSTRAINT

As far as the cylindrical column is not extensively long (that is, $L / D > 15$) that may result in failure by buckling, thin-walled cylinders will fail in a collapsing, or crippling, mode. This is beneficial, as this means that the structure will remain mostly undeformed till collapse. Therefore, the rocket body has L/D ratio of 15, so that it is easier to control when a controller is implemented in further research. From ascend motor design,

the outer diameter of the rocket is estimated to be 0.25 m and therefore the total length is 3.75m.

3.5 MOTOR CASE THICKNESS CALCULATIONS

The thickness of the motor case is calculated using hoop stress for a maximum chamber pressure of 550 psi and factor of safety of 2.5. The material for the motor case is Aluminium T-6.

$$t = \frac{P \times D}{2 \times \sigma} \times FOS \quad (3.8)$$

$$t = \frac{550 \times 0.16}{2 \times 35000} \times 2.5$$

$$t = 3.2 \text{ mm}$$

CHAPTER-4

MATERIALS

4.1 AIRFRAME MATERIALS

The conventional airframe materials for high-powered rockets are non-metallic, composite materials having high strength to weight ratio like fiberglass, carbon-fiber, phenolic and PVC (rules of National Association of Rocketry).

For this project the fiberglass is chosen as airframe material since it has corrosion resistance property, good structural strength, superior strength to weight ratio and it is cost effective-especially for complex shapes.

4.2 MOTOR CASE MATERIALS

1. Cardboard is used for small black powder model motors
2. Aluminium is used for larger composite-fuel hobby motors
3. Steel was used for the space shuttle boosters
4. Filament-wound graphite epoxy casings are used for high-performance motors

Aluminium T6 is preferred as motor case material. 6061-T6 Aluminium has good structural strength and toughness and offers good finishing characteristics.

4.3 THERMAL INSULATION BY HEAT RESISTANT POLYMERS

The flame temperature of APCP is 2700 K. It is vital to include thermal insulation for the motor case for it to bear this high temperature. Thermal insulation consists of chopped carbon fiber (CCF) and aramid fiber in pulp form as reinforcement for ethylene propylene diene monomer (EPDM) combined with ammonium polyphosphate (AP) flame retardant agent. Six millimeters long CCFs and/or Kevlar pulp (KP) are dispersed in the EPDM polymeric matrix that results in a homogenous master batch for curing purpose. The new method involves the development of two types of prepgs and the lamination of these types of prepgs. The first one consists of CCF/EPDM/AP and the second type of

prepreg KP/EPDM/AP. Six alternative laminates composed of these prepgs are shown to exhibit better thermal, mechanical, physical, and ablative properties when compared to non-laminated counterparts.

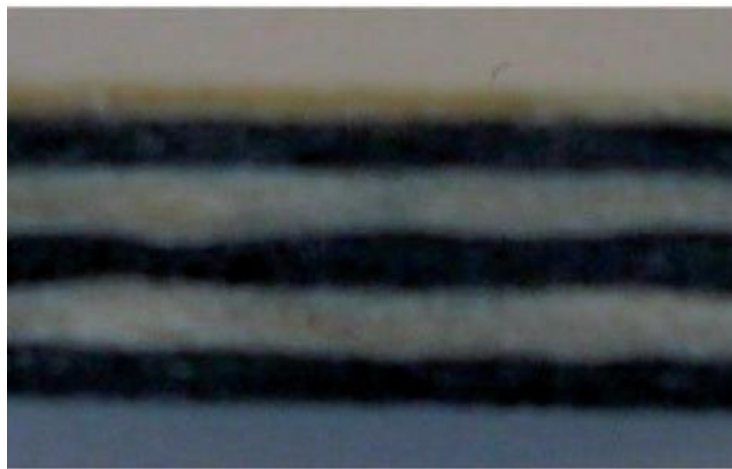


Fig 4. 1 Photo of cross-section of a laminate consisting of six alternative layers of (CCF or KP) based prepgs.

Table 4. 1Properties of laminates made using six alternate layers of CCF and KP based EPDM prepgs

Property	unit	Test value for laminate	Test value for hybrid (25 phr CCF+ 25 phr KP)
Tensile strength	MPa	7.8±0.5	11
Elongation	%	12.1±1.2	7.4
Hardness	Shore	88.9±0.2	96.4
Density	gm/cm ³	1.239	1.256
Specific heat capacity	j/kg-K	1691±4	1973
Thermal diffusivity	mm ² /s	0.085±0.002	0.08
Thermal conductivity	W/m-K	0.178±0.001	0.198
Ablation rate	mm/s	0.006±0.0002	0.005
Outer case temperature	°C	39.1±0.5	82
TGA remaining weight	%	27±0.5	24

4.3.1 CALCULATION OF HEAT TRANSFER

To calculate the total heat transfer across the insulation and to check if the motor casing can withstand this high temperature we use Fourier law of heat conduction, we have,

$$Q = \frac{K \times A \times \Delta T}{\Delta x} \times t \quad (4.1)$$

Taking the burn time as 13 s,

And Area,

$$A = 2 \times \pi \times 0.08 \times 0.96$$

$$A = 0.4825 \text{ m}^2$$

$$Q = \frac{0.178 \times 0.4825 \times (2700 - 300)}{0.006} \times 13$$

$$Q = 446.64 \text{ kJ}$$

Specific heat of material of case = 1000 J/kg

Total mass of motor casing = 6 kg

This gives,

$$\Delta T = \frac{446.64 \times 10^3}{6000} = 74 K$$

Hence the change in temperature is 74 K, which is well below the melting point of the material (855 – 925 K).

CHAPTER-5

MOTOR DESIGN AND BURN SIMULATION

5.1 MOTOR DESIGN

Ammonium perchlorate composite propellant (APCP), a compound propellant that has both fuel and oxidizer mixed with a binder as shown in Table 5.1 usually of a rubbery nature, also known as ‘Cherry Limeade’, developed by MIT Rocketry team suits best and hence has been selected to power the rocket. The propellant contains ammonium perchlorate as the oxidant and hydroxyl-terminated polybutadiene (HTPB) as an elastomer binder. It includes Aluminum, which along with the binder, which serves as the fuel. Usually, it is used in aerospace missions since it is easy to handle, store and has good propulsive characteristics.

Table 5. 1 Composition of APCP

Ingredient	Percentage
Binder	17.1%
Caster oil	0.3%
PDMS	0.05%
Triton X100	0.05%
Al	7.5%
200 AP	65.5%
90 AP	9.5%

Performance and Combustion Properties:

Density: 1688.4742 kg/m³

Rc: 0.0006346444 m/s

n: 0.327392

Typical ISP: 225 s

The motor configuration that provides the optimum performance to reach this altitude is designed via burn simulation. The dimensions for maximum optimized rocket motor are calculated from MATLAB code. This iterative design is done such that the following constraints are satisfied:

- Port to throat area ratio > 2
- Peak mass flux < 0.907185 kg/s
- Maximum combustion chamber pressure = 3.792×10^6 pa
- Burn/Throat area ratio is between 180 to 250

Which is subjected to fallowing assumptions:

- No erosive burning
- Nozzle efficiency = 1 (Nozzle exit pressure = Atmospheric pressure)
- Throat erosion coefficient = 0
- Slag build-up coefficient = 0

5.1.1 ASCENT MOTOR DESIGN

The ascend motor has two different grain configurations are used that is; finocyl and bates. This grain configuration provides almost neutral burn, as the surface area remains fairly constant throughout the burn. To get greater efficiency in delivering total impulse from a rocket motor, neutral burning is usually preferred and also the nozzle operates efficiently when chamber pressure is constant. The ascend motor is designed in SOLIDWORKS® as shown in Fig 5.1.

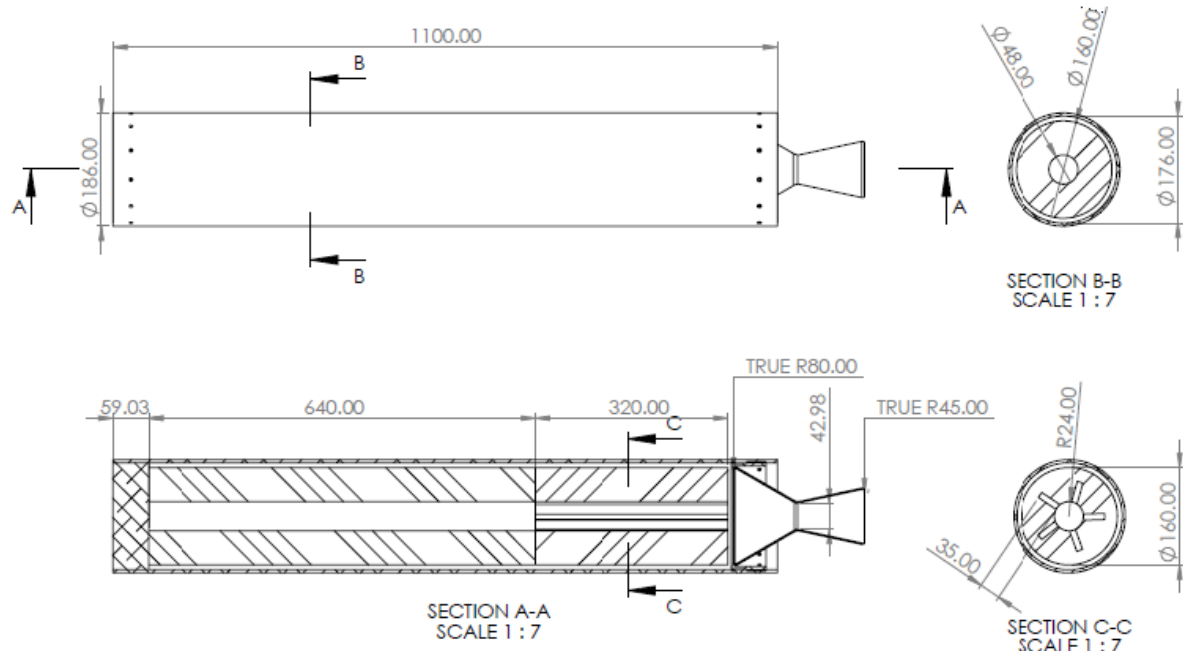


Fig 5. 1Ascent motor design

5.1.2 DESCENT MOTOR DESIGN

For descend motor an end burning grain configuration best suits because for propulsive landing, the thrust level should be low, it should have long duration of burn and constant thrust profile makes it easy to control. The descend motor grain configuration is also designed in SOLIDWORKS® as shown in Fig 5.2.

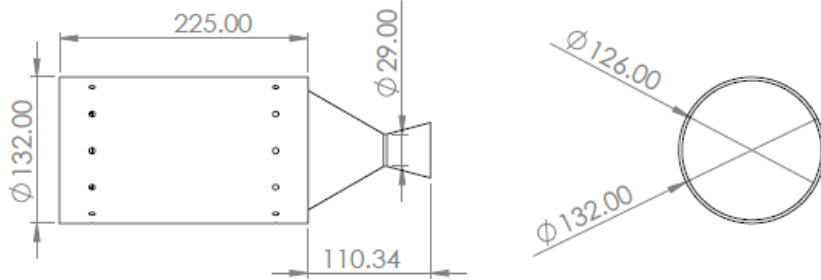


Fig 5. 2Descent motor grain configuration

5.2 3D MOTOR REPRESENTATION

For motor casing Aluminium T-6 alloy, A CCF coating for thermal insulation is used, the design also includes several O-rings for pressure fits. The motor case thickness required to sustain a maximum chamber pressure of 3.627×10^6 Pa was found to be 3.2mm as per the calculations shown in section 3.4. The design also considers the allowable pressure limits to upper case and nozzle connections, The grain materials are consolidated to one single formula to help the burn back simulation for future scope as shown in Fig 5.3.

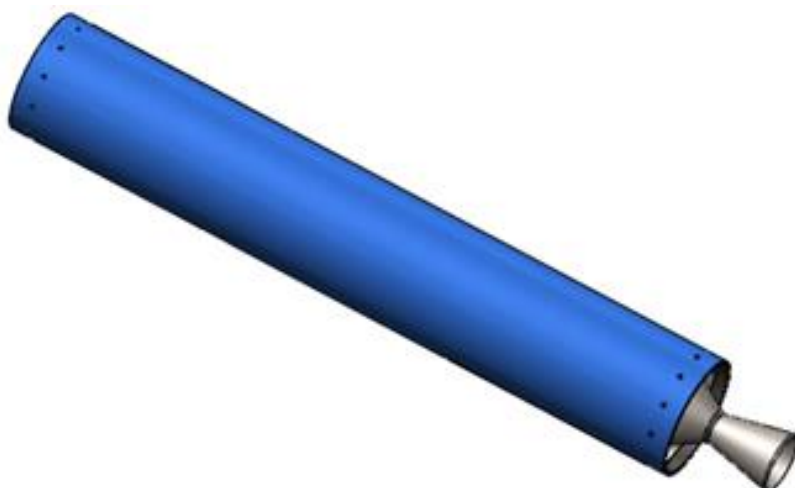


Fig 5. 33D motor design (ISO view)

5.3 BURN SIMULATION

The combustion parameters are obtained from burn simulation in OPENMOTOR®. This software takes type of propellant, grain configuration and its dimensions as input and this software is used to calculate the optimised nozzle dimensions that gives maximum specific impulse. This is achieved by giving the inputs obtained from MATLAB® code, burn simulation is carried out and following results were obtained.

5.3.1 ASCEND MOTOR

Motor statistics

- Total Impulse = 62031.636 Ns
- Burn time = 12.5 s
- Average Pressure = 2.564×10^6 Pa
- Peak Pressure = 3.852×10^6 Pa
- Peak Kn = 254.61
- Propellant mass = 26.35 kg
- Propellant length = 0.849 m
- Port/Throat Ratio = 2.969

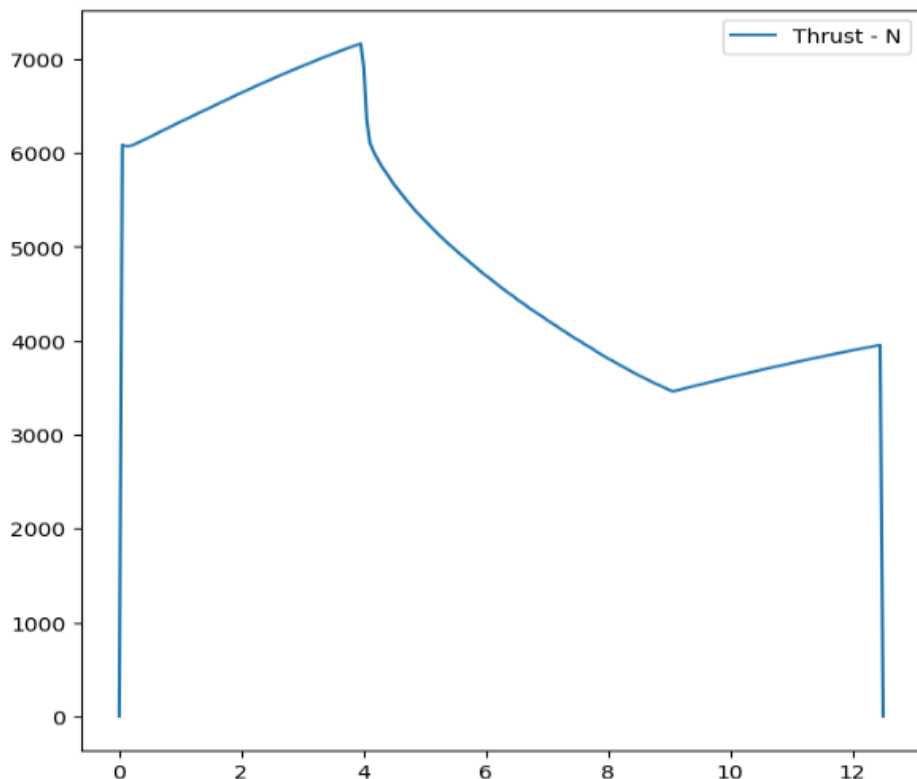


Fig 5. 4Thrust curve for ascend motor

5.3.2 DESCENT MOTOR

Motor statistics

- Total Impulse = 8848.67 Ns
- Burn time = 39.65 s
- Average Pressure = 2.806×10^6 Pa
- Peak Pressure = 2.810×10^6 Pa
- Peak Kn = 216.263
- Propellant mass = 3.711 kg
- Propellant length = 0.1799 m

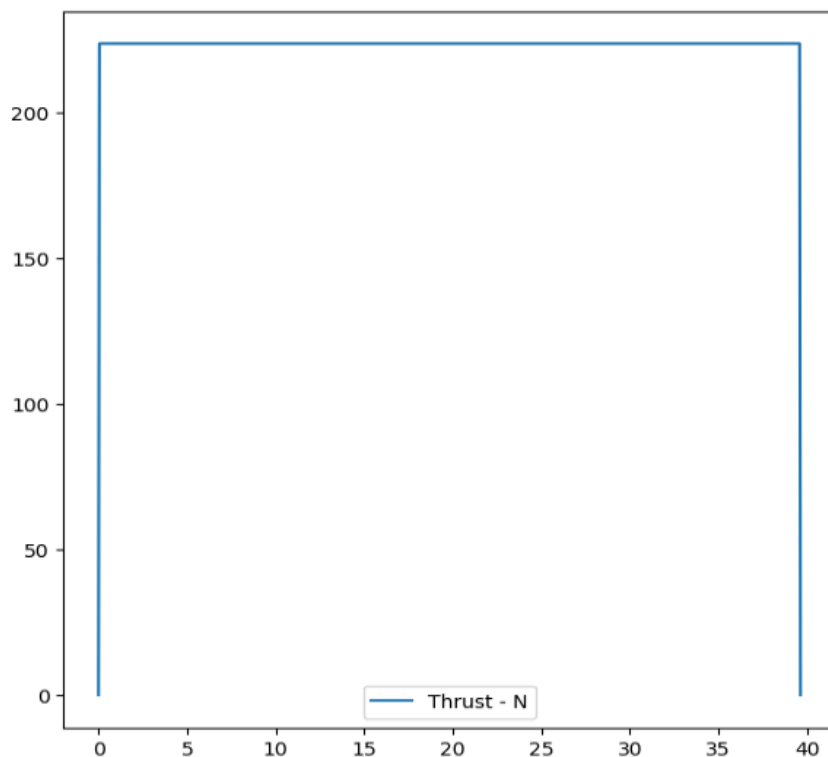


Fig 5. 5Thrust curve for descend motor

CHAPTER- 6**ROCKET BODY DESIGN****6.1 NOSE CONE**

The ogival shape nose has been considered in this project since it has many advantages over other shape nose cone like it provides higher volume compared to others for the same base and length and blunter nose provides lower drag and structural superiority. The tangent ogive has been considered to design a nose cone and shape of this profile is formed by the part of the circle that the body of the rocket is tangent to the nose cone curve at its base and radius of circle forms the base of the nose cone.

Ogive (R_o) radius is the radius of the circle that forms the ogive and it can be related to length (L_o) and radius of base(r_o) of the nose cone as follows

$$R_o = \frac{r_o^2 + L_o^2}{2r_o} \quad (6.1)$$

Considering $r_o=25\text{cm}$ and $L_o=75\text{cm}$ and calculating' for R_o we get

$$R_o = \frac{25^2 + 75^2}{2 \times 25}$$

$$R_o = 125\text{cm}$$

All the above dimensions are optimized for the rocket length to achieve minimum drag and by considering above dimensions nose cone has been designed in SOLIDWORKS® and is shown in Fig6.1.

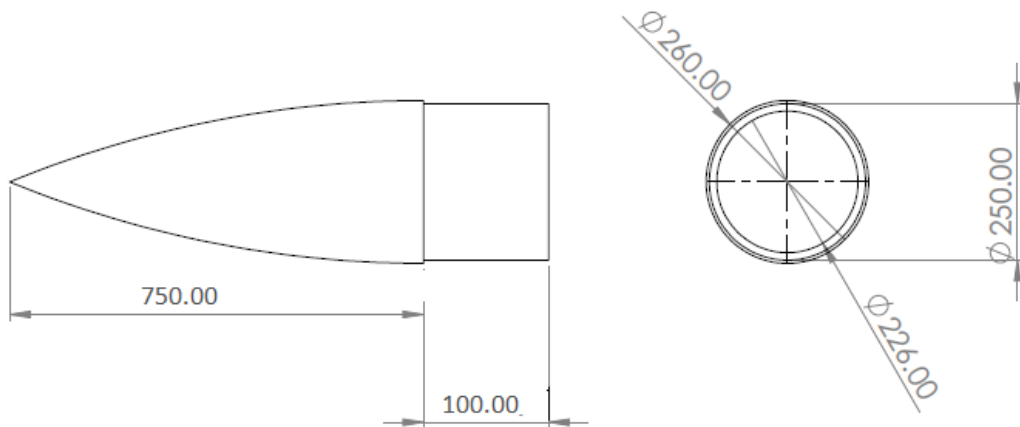


Fig 6. 1 Design of nose cone

6.2 FIN DESIGN

Although the rocket is equipped with TVC, in order to have at least neutral stability, presence of fins are essential. Therefore, fins are designed such that the rocket has neutral stability. There has been a attachment given to fix this into rocket body which is structurally very stable and can handle all the bending stress applied on the fins. The fins dimensions are aerodynamically designed to get maximum efficiency as shown in Fig 6.2.

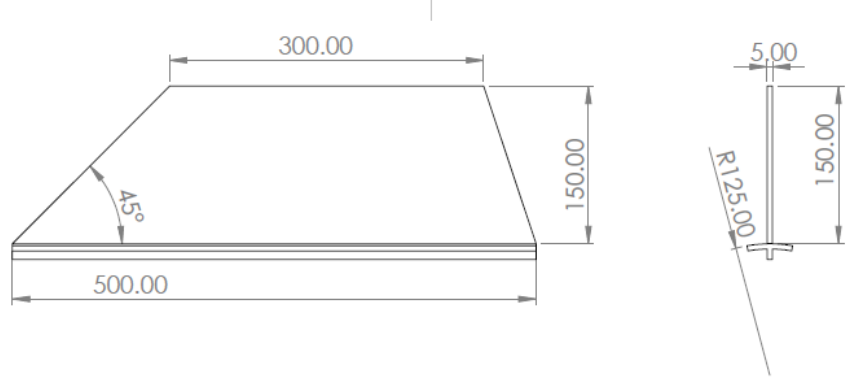


Fig 6. 2Fin design

6.3 ROCKET BODY

Considering the dimensions of the motor, the rocket body design is optimized in OPEN ROCKET®. Then, the rocket body is designed in SOLIDWORKS® and thickness of the rocket body is calculated using hoop stress. The total length of the rocket is 3.75 m. The fins are designed such that the centre of pressure is located just behind the centre of gravity for the rocket to be stable or coincide to have neutral stability.

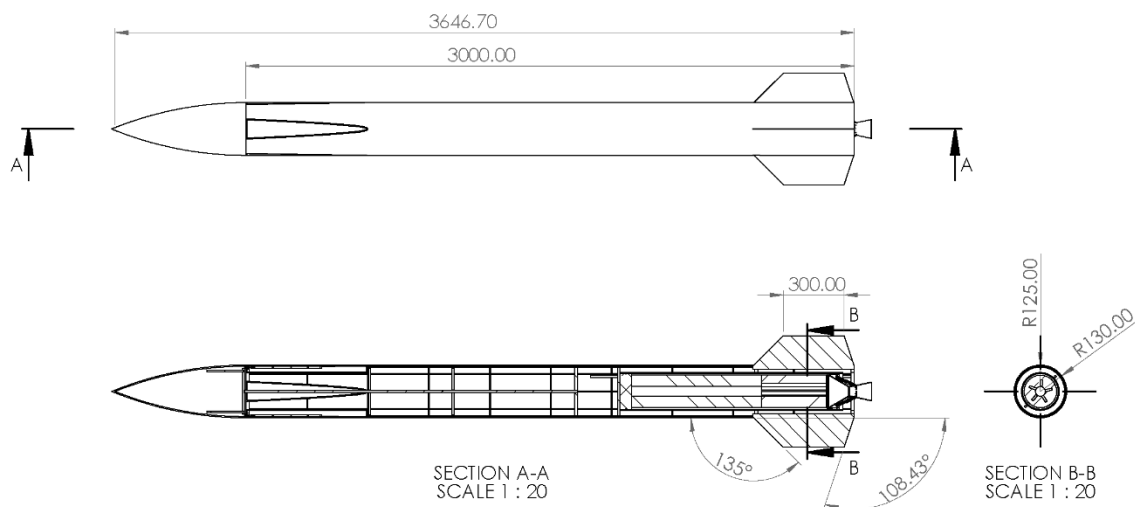


Fig 6. 3Rocket body design

Landing legs has been installed at the upper part of the rocket body near nose cone. Once the rocket reaches the apogee it turns for 180^0 to support the landing of the rocket and hence the landing legs are placed at the upper part of the rocket body as shown in Fig 6.3. The landing legs are aerodynamically attached to ensure minimum drag during ascent and maximum possible interference during decent, and they are attached with hydraulic gears for their movement in a separate housing.

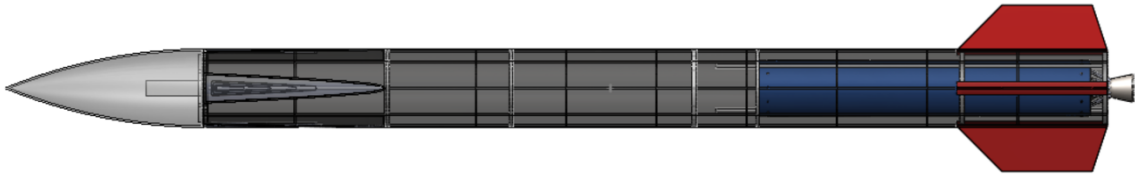


Fig 6. 4 Sectional view of rocket body excluding electronics and hydraulics

6.4 NOZZLE

A nozzle is a generally basic device, only an exceptionally molded cylinder through which hot gases flow. Since the stream is supersonic, the nozzle utilized is a convergent-divergent nozzle. Flexible laminated bearing are used to throat section for gimbaling the nozzle and is by all accounts the best choice if there should be an occurrence of solid rocket engine. It is assumed that no erosion takes places during the burn. The dimensions considered for nozzle design are as follows:

Inlet diameter: 160mm

Throat diameter: 43mm

Exit diameter: 90mm

Divergence half angle: 12 degree

Convergence half angle: 30degree

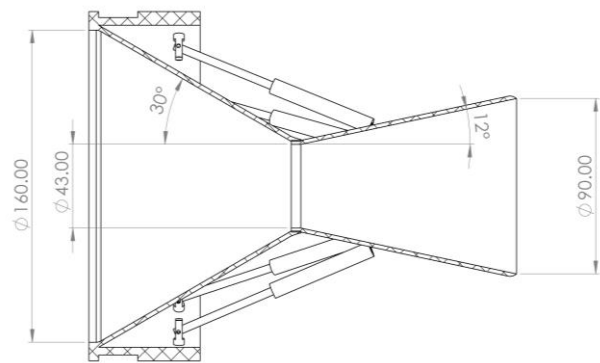
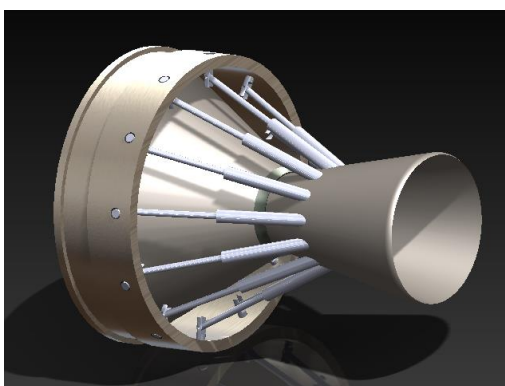


Fig 6. 5Convergent-Divergent nozzle design

6.5 STABILITY OF ROCKET

The rocket is designed in OPENROCKET to calculate the stability. This software makes use of Barrowman equations to calculate center of pressure and it is seen that the rocket is neutrally stable for this configuration. CG and CP coincide at a point 243 cm away from the tip of the nose giving 0 caliber of stability. The stability criteria is very much necessary in designing the control algorithm, the rocket body is also tested for its neutral stability even after burnout and at apogee. For the simplification of calculation all the electronics mass has been consolidated and placed in longitudinal axis ensuring equal mass distribution. The design for the calculation and its mass distribution is as shown in Fig 6.6 and it can be observed that the payload capacity of up to 3.6kg is achieved for a total mass of 32.5kg of fuel which is more economic.

Rocket Design



Rocket

Stages: 1

Mass (Empty): 53457 g

Stability: 0 cal

CG: 243 cm

CP: 243 cm

Parts Detail

Stage

	Nose cone	Fiberglass (1.85 g/cm³)	Ogive	Len: 75 cm	Mass: 1098 g
	Payload		Dia _{out} 2.5 cm		Mass: 3600 g
	Landing legs		Dia _{out} 25 cm		Mass: 3300 g
	Body tube	Fiberglass (1.85 g/cm³)	Dia _{in} 24.7 cm Dia _{out} 25 cm	Len: 300 cm	Mass: 6499 g
	Fin set (4)	Acrylic (1.19 g/cm³)	Thick: 0.5 cm		Mass: 960 g
	Ascent Motor		Dia _{out} 17.6 cm		Mass: 32500 g
	Descent Motor		Dia _{out} 13.2 cm		Mass: 5500 g

Fig 6. 6Rocket stability and part details

6.6 DESIGN DETAILS

Table 6. 1 Design details and values of designing Plant

Sl. No.		Unit	Values
01	Total length	mm	3750
02	Total mass	kg	599.76
03	Propellant mass for ascend	kg	236.7
04	Propellant mass for descend	kg	4.5
05	Structural weight	kg	31.806
06	Location of cg from base	mm	1284.25
07	Location of control thrusters from CG	mm	1667.57
08	Length of swivelling nozzle	mm	110.56
09	Moment of inertia of the rocket with all propellant for ascend, I_{xx}	kg/mm ²	422295.199
10	Moment of inertia of the rocket with all propellant for ascend, I_{yy}	kg/mm ²	154719228.560
11	Moment of inertia of the rocket with all propellant for ascend, I_{zz}	kg/mm ²	154719233.532
12	Moment of inertia after reaching required height, I_{xx}	kg/mm ²	316016.570
13	Moment of inertia after reaching required height, I_{yy}	kg/mm ²	154719228.560
14	Moment of inertia after reaching required height, I_{zz}	kg/mm ²	154719233.532
15	Moment of inertia of only structural portion, I_{xx}	kg/mm ²	227981.821
16	Moment of inertia of only structural portion, I_{yy}	kg/mm ²	4038301.247
17	Moment of inertia of only structural portion, I_{zz}	kg/mm ²	40383016.217
18	CG shifts during propellant burning	mm	555.47

COMPUTATIONAL FLUID ANALYSIS

7.1 FLOW ANALYSIS OVER ROCKET BODY

The rocket body is designed in SOLIDWORKS®, The model is oriented such that the length of the rocket is in X-axis. The model is assumed to be smooth and the motor configuration are removed to aid the CFD analysis. Mesh has been generated for the selected 3D domain with inlet normal to nose cone direction as shown in Fig 7.1, mesh has a 2*2*8 m domain and total of 193235 elements with 55432 nodes, there has been a 10 layer of inflation given at rocket body to ensure shock capture at high Mach number.

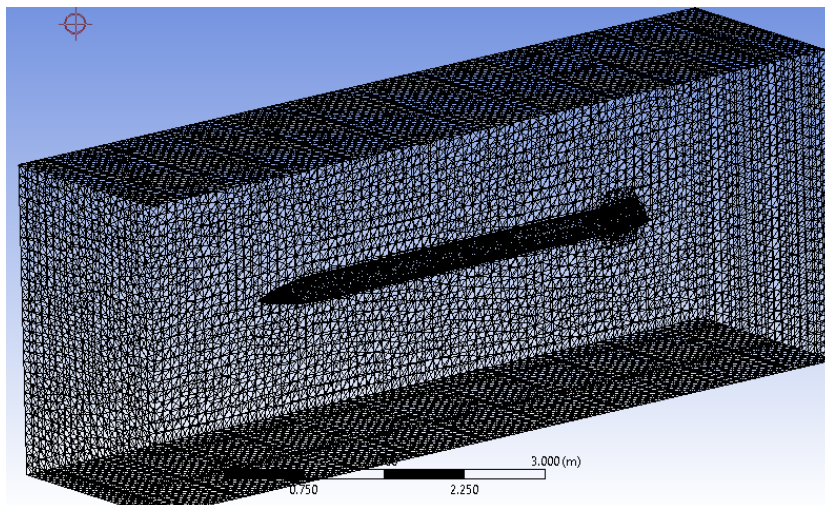


Fig 7. 1 Mesh generated for rocket body

7.1.1 GRID INDEPENDENT TEST

The normal CFD technique is to start with a coarse mesh and gradually refine it until the changes observed in the results are smaller than a pre-defined acceptable error. Initially a course mesh is analyzed and the error has been calculated comparing to theoretical calculation, the mesh has been made fine until we get more accurate and comparable results All the measured quantities are then plotted in a Excel sheet to visualize the error in measurement. The grid independent test for the analysis done for seven different number of elements from course mesh to fine mesh size and the corresponding Cd values plotted as shown in Fig 7.2 and 7.3 for both Mach 0.5 and Mach 1.5

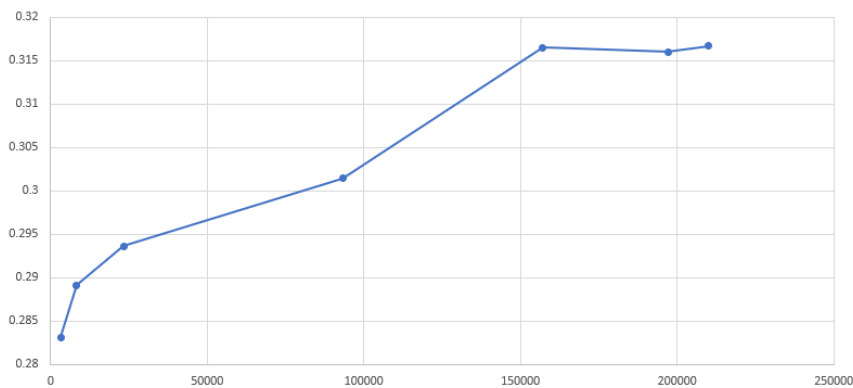


Fig 7. 2Coefficient of drag vs Number of elements (Mach 0.5)

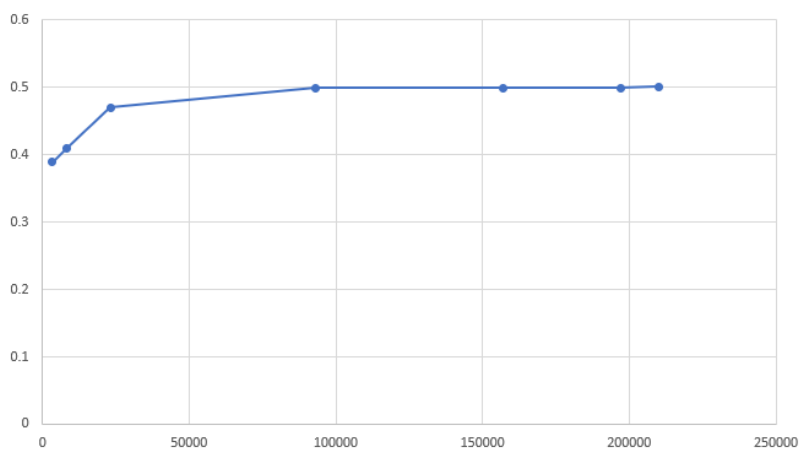


Fig 7. 3Coefficient of drag vs number of elements (Mach 1.5)

7.1.2 RESULTS AND DISCUSSION

The flow over the rocket body is simulated in SOLIDWORKS® for Mach 1.5. and In Ansys Fluent for Mach 0.5 with the same mesh file to reduce the computational time. The rocket body is treated as a no-slip wall. Since the rocket is fixed in its reference frame, the velocity at the solid boundary is zero. The simulations are carried with Transition SST viscous model, with material density selected based on the atmospheric model.

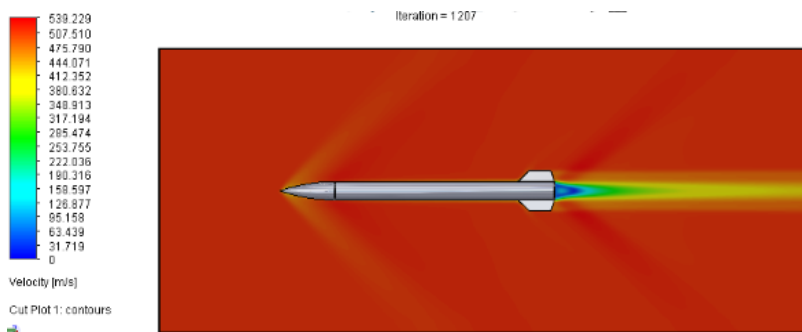
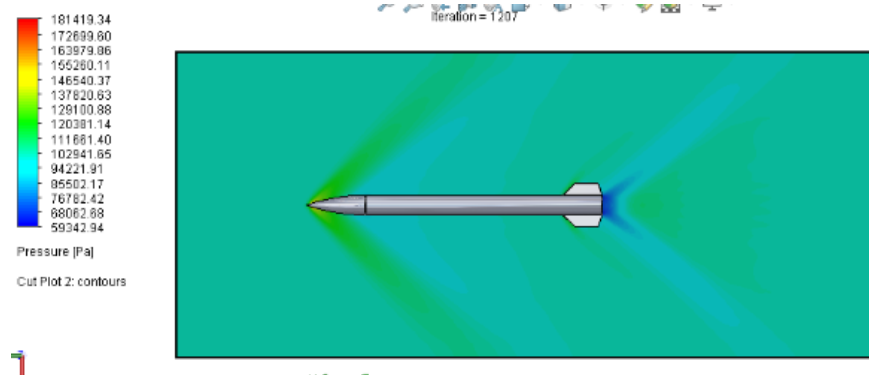
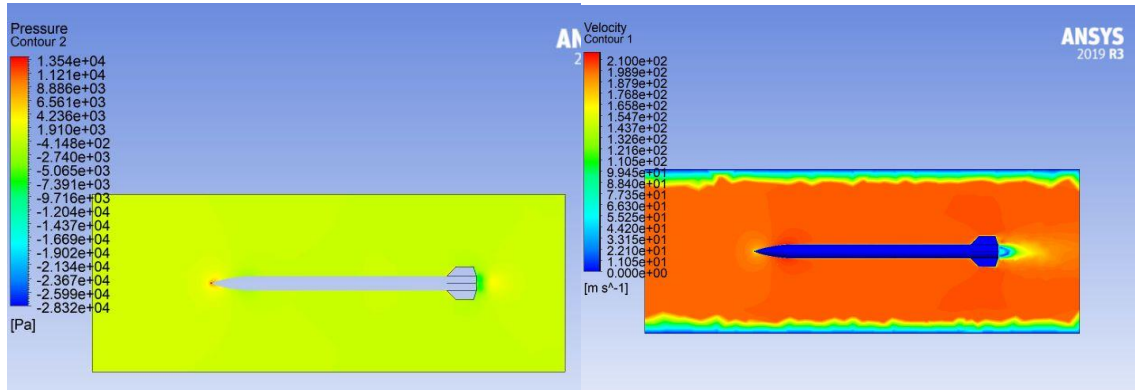


Fig 7. 4Velocity contour for Mach 1.5

**Fig 7. 5 Pressure contour for Mach 1.5**

From Fig 7.4 and Fig 7.5 it can be observed that there is an oblique shock at the nose cone and the strength of the shock is weak, so the structure can handle the shock without much vibrations. Drag obtained in this simulation are used as reference for MATLAB program.

**Fig 7. 6 Pressure contour (left) and velocity contour(right) for Mach 0.5**

From Fig 7.6 it can be observed that the flow is smooth and the drag is less (drag coefficient of 0.02) and pressure contour says that the profile is uniform and from velocity contour it can be observed that the flow over the surface is smooth and there is no vortex formation on the surface.

7.2 NOZZLE FLOW ANALYSIS

The analysis of flow inside the nozzle has been carried out in Ansys 2019[®] and following results were obtained. The hot fumes leave the ignition chamber and combines down to the base region, or throat of the nozzle. The throat diameter is selected such that the flow is choked at this section and set the mass flow rate through the system. The exit velocity, pressure, and mass flow through the nozzle decides the measure of thrust delivered by the nozzle.

7.2.1 GEOMETRY

The 2D nozzle was designed in ANSYS design modeler® using surface from sketches. The dimensions of the nozzle is as shown in Fig 6.5. The inlet is from the larger wall and the throat section is split at equal intervals for fine meshing and the outlets are at the smaller diameter as per the previous design

7.2.2 MESH

Initially the surface of nozzle is divided into 4 faces because, the throat is critical region where mesh has to be very fine. Then all the edges (inlet, outlet and walls) are separately meshed with edge sizing. Later face meshing is applied to entire surface. Structured mesh is finally obtained as shown in Fig 7.8, and the mesh stats are as shown below,

STATISTICS

Nodes	16688
Elements	16493

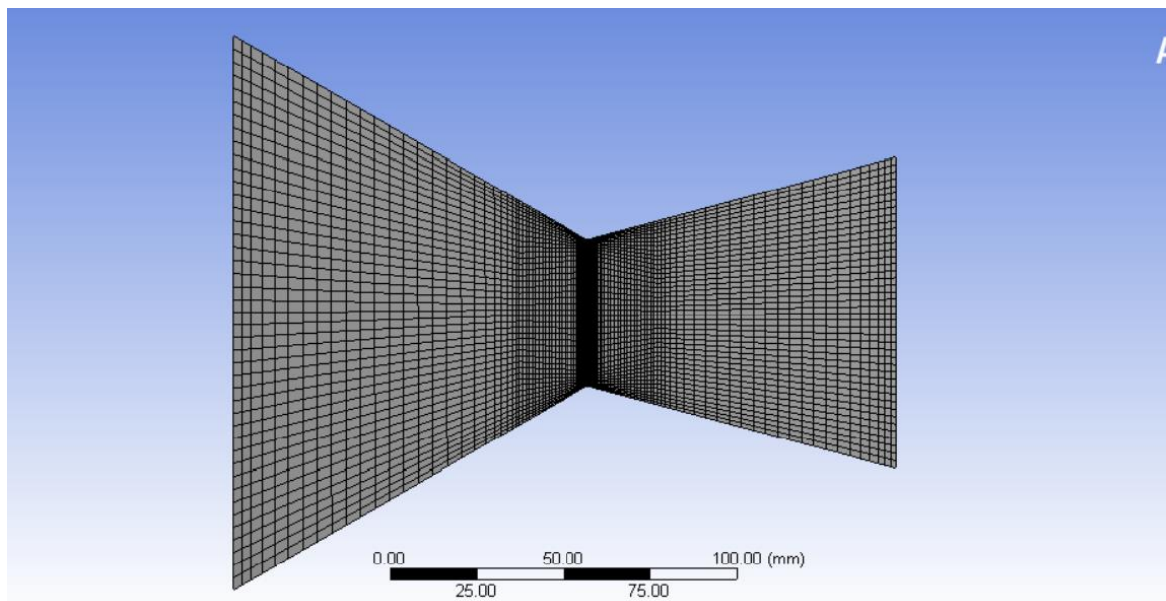


Fig 7. 7 Meshing of the nozzle

7.2.3 BOUNDARY CONDITIONS

Table 7. 1 Boundary conditions for nozzle flow analysis

Sl. No.	Boundary conditions	
01	Model	SST k-omega viscous model
02	Fluid	Ideal gas

03	Inlet	Pressure inlet=500pascal
04	Outlet	Pressure outlet
05	Symmetry	Symmetry
06	Energy equation	On
07	Solver	Density based

7.2.4 GRID INDEPENDENT TEST

The normal CFD technique is to start with a coarse mesh and gradually refine it until the changes observed in the results are smaller than a pre-defined acceptable error. Initially a course mesh is analyzed and the error has been calculated comparing to theoretical calculation, the mesh has been made fine until we get more accurate and comparable results, Throat pressure and exit velocity has been calculated using force Calculator in CFX, All the measured quantities are then plotted in a Excel sheet to visualize the error in measurementas shown in Fig 7.9 and 7.10 and it is found that the results obtained are more accurate to calculations for a finer mesh.

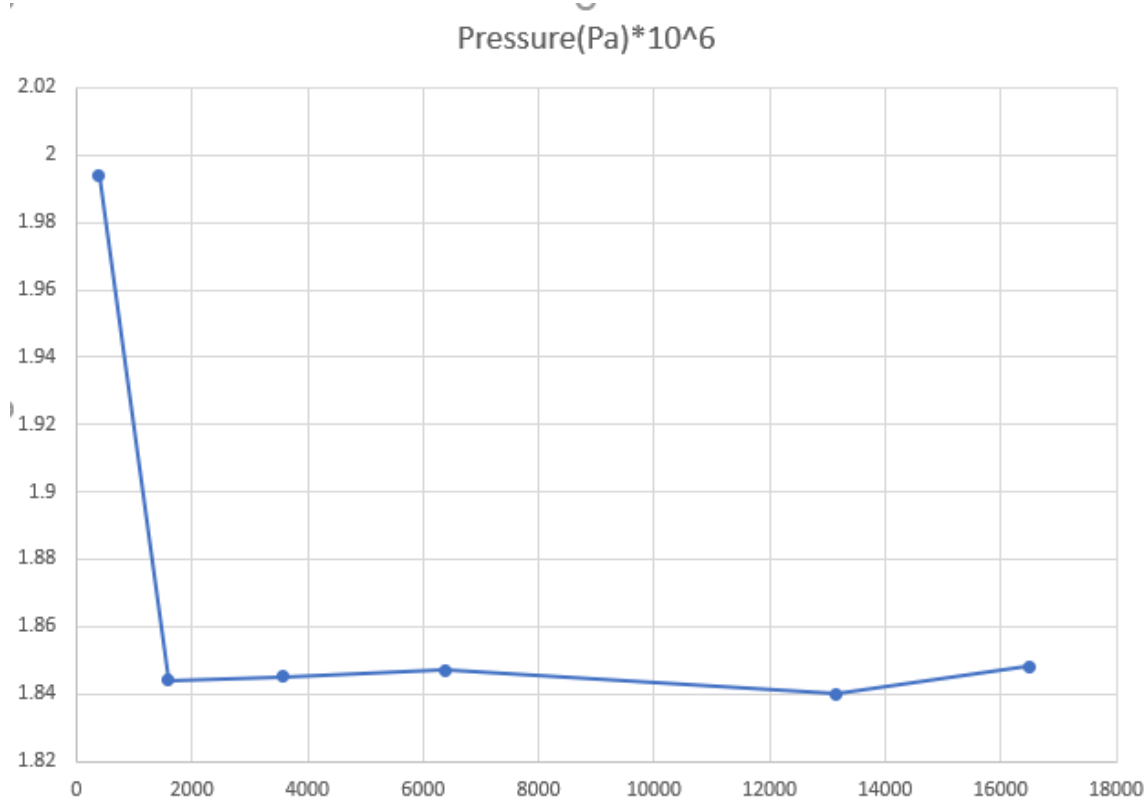
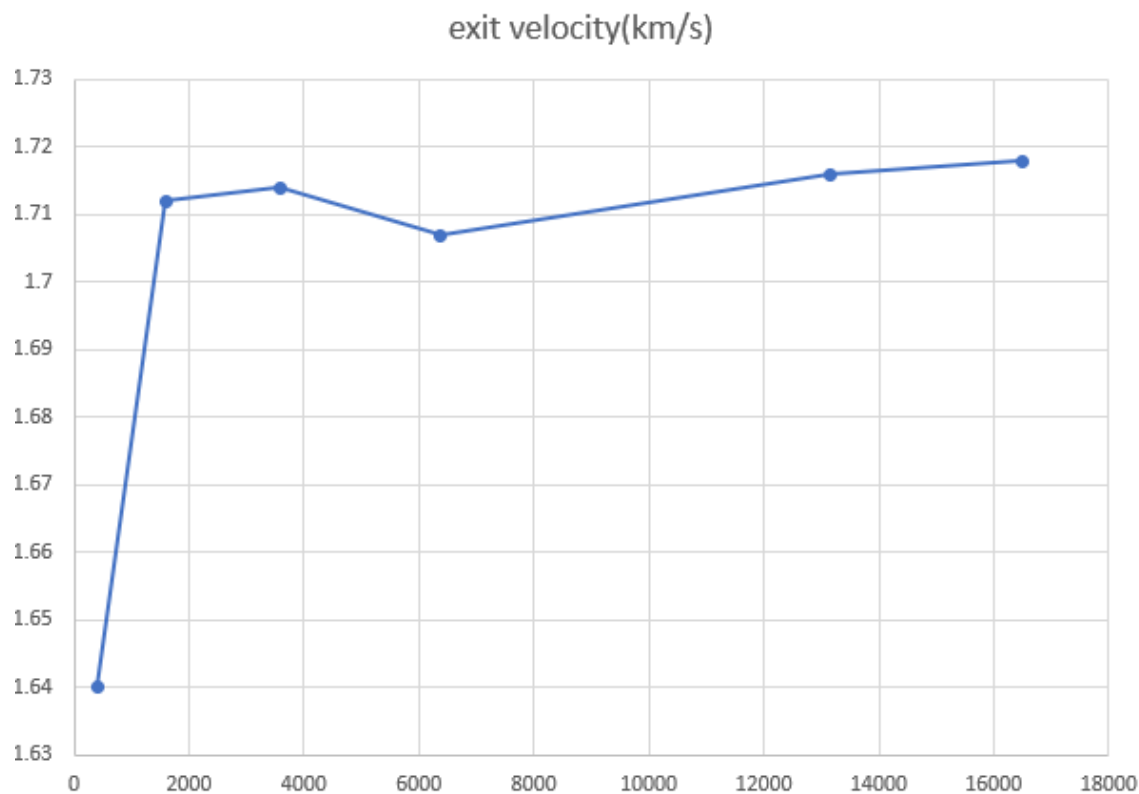
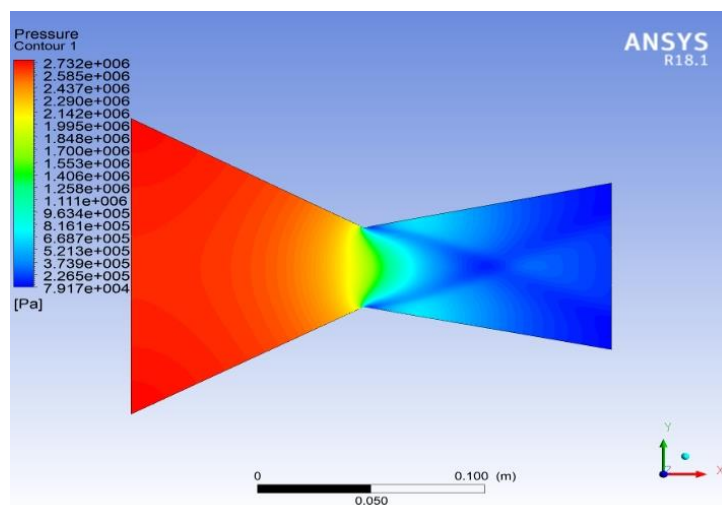


Fig 7. 8 Throat pressure vs number of elements

**Fig 7. 9 Exit velocity vs number of elements**

7.2.5 RESULT AND DISCUSSION

The expansion of a supersonic flow causes the decrease in static pressure and temperature from the throat to the exit, so the exit pressure and temperature are determined by amount of the expansion. The maximum pressure in nozzle is 2.732×10^6 Pa which is comparable with value obtained in analytical calculations.

**Fig 7. 10 Pressure contour**

The stream in the throat is sonic which implies the Mach number is equivalent to one at the throat. In the divergent section, the geometry stalls and the flow isentropically expanded to Mach number at around Mach 5. The observed shock is due to gimbling angle and is done purposefully to simulate the results during gimbling and to ensure shock exits without reflecting.

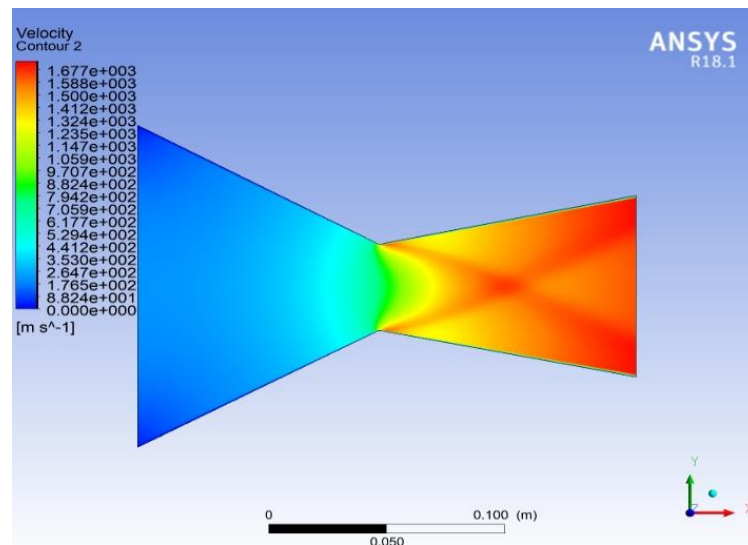


Fig 7. 11Velocity contour

CHAPTER-8

1D – FLIGHT SIMULATION

8.1 LIST OF FORMULAE USED IN SIMULATION

The flight simulation is done such that the rocket reaches an altitude of 10 km and then perfectly land to ground. The flight simulation is done considering a point mass in Simulink and the formulas used for flight simulation are as follows:

- **Total mass**

$$m_t = m_e + m_p \quad (8.1)$$

- **Weight**

$$W = m_t \times g \quad (8.2)$$

- **Inertial force**

$$F_i = m_t \times a \quad (8.3)$$

- **Drag force**

Subsonic drag force:

$$F_d = \frac{1}{2} \rho V^2 A C_d \quad (8.4)$$

Supersonic drag force

$$F_d = \frac{1}{2} k P M^2 A C_d \quad (8.5)$$

- **Total force**

$$F_t = T - F_d - W \quad (8.6)$$

- **Acceleration**

$$a = \frac{F_t}{M_t} \quad (8.7)$$

- **Velocity**

$$V = \int a dt \quad (8.8)$$

- **Altitude**

$$h = \int V dt \quad (8.9)$$

8.2 FLIGHT SIMULATION

The flight simulation is done such that the rocket reaches an altitude of 10 km and then perfectly land to ground. The flight simulation is done considering a point mass in Simulink. It includes two subsystems namely, Engine and Aerodynamic drag to reduce the complex design of Simulink block. With the initial inputs such as thrust curve, engine mass, propellant mass the sum of forces acting on the rocket body has been calculated using eq 8.6. Then using newton's second law of motion (eq 8.7) the acceleration of the vehicle is calculated. Then by integration the velocity and altitude reached by rocket body is determined (eq 8.9). In the simulation, initially the drag is considered as 0 then from the calculated velocity the drag is determined as a closed loop. The results are discussed below.

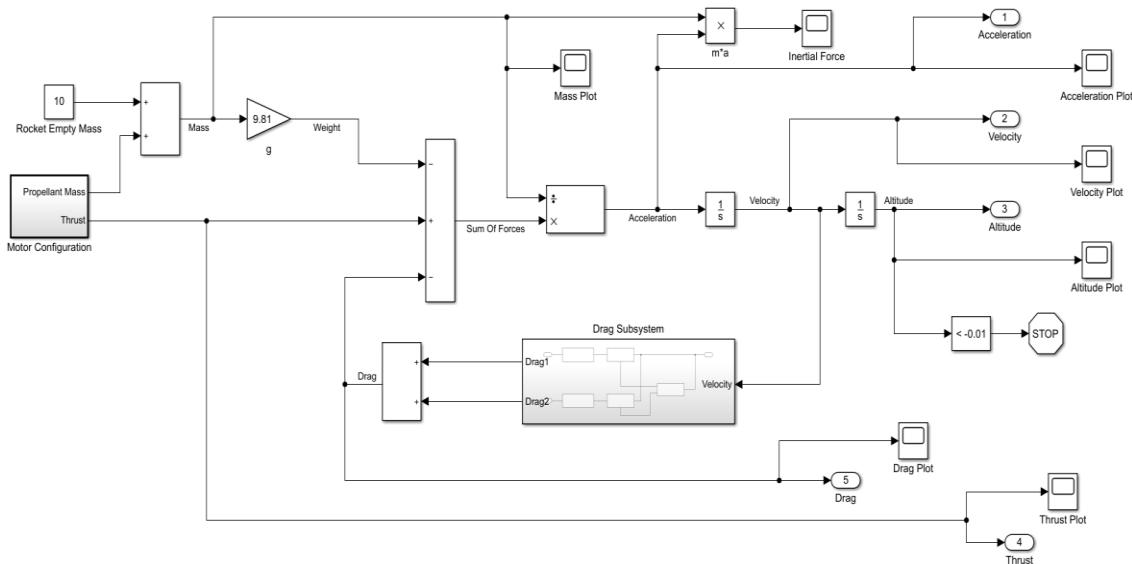
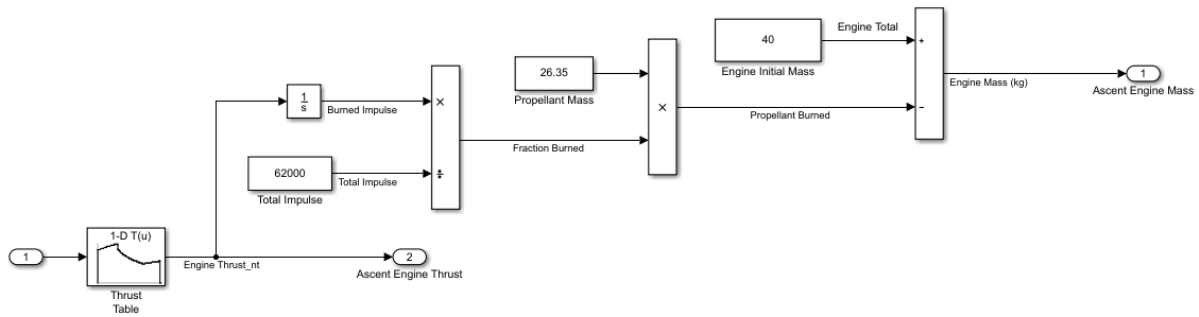
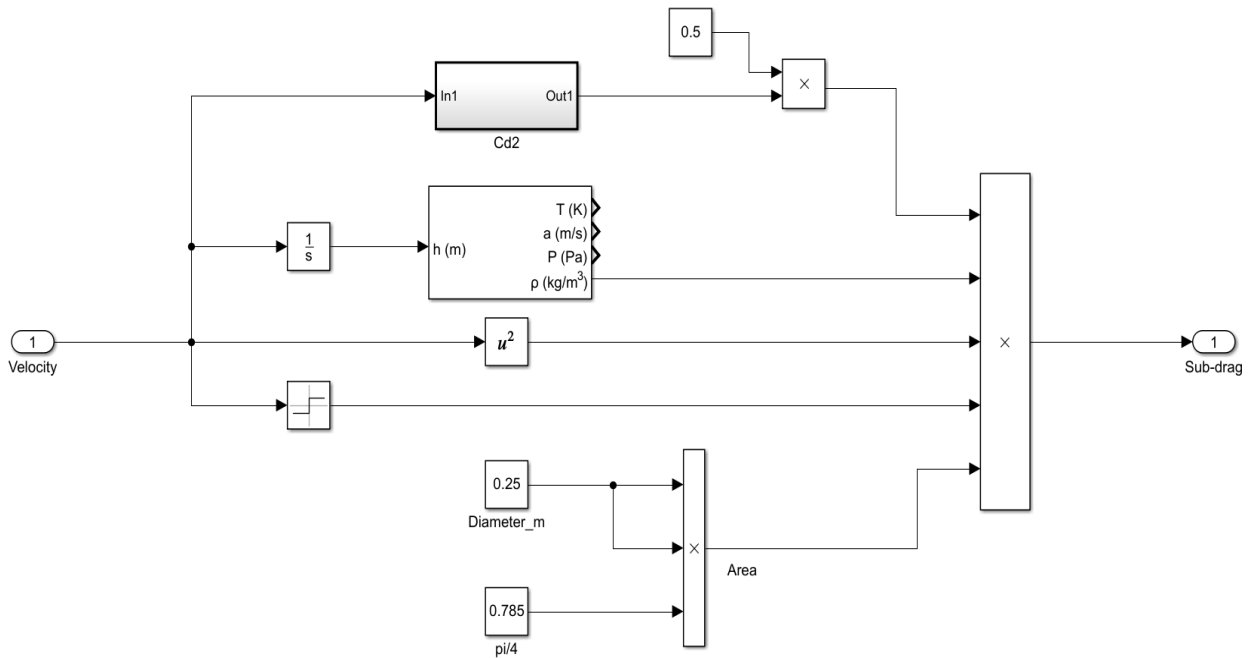


Fig 8. 1Simulink block and connections for simulation of flight

The thrust variation with a time step of 0.05 s is imported to MATLAB workspace from the code shown in Appendix 3,The Simulink block named Lookup table has been used in simulation in order to import thrust values with respect to time from excel sheet. Then the fraction of the propellant burned is calculated. The Rocket empty weight is added from the estimation of best mass. Multiplying the total mass with acceleration due to gravity gives the force of gravity.


Fig 8. 2Simulink blocks and connections to calculate engine thrust and weight

The variation of air density, pressure and speed of sound with altitude is also considered. For this, the international standard atmosphere model (ISA) block is taken. It is observed that the rocket is supersonic during its flight path and hence the variation of coefficient of drag with Mach number is implemented as shown in Fig 8.5. This data is taken from RASAero-2®. The drag experienced by the rocket body with respect to altitude has been calculated by using eq 8.4 & eq 8.5. and the Simulink blocks are as shown in Fig 8.3 and 8.4.


Fig 8. 3Simulink block and connections to calculate subsonic drag

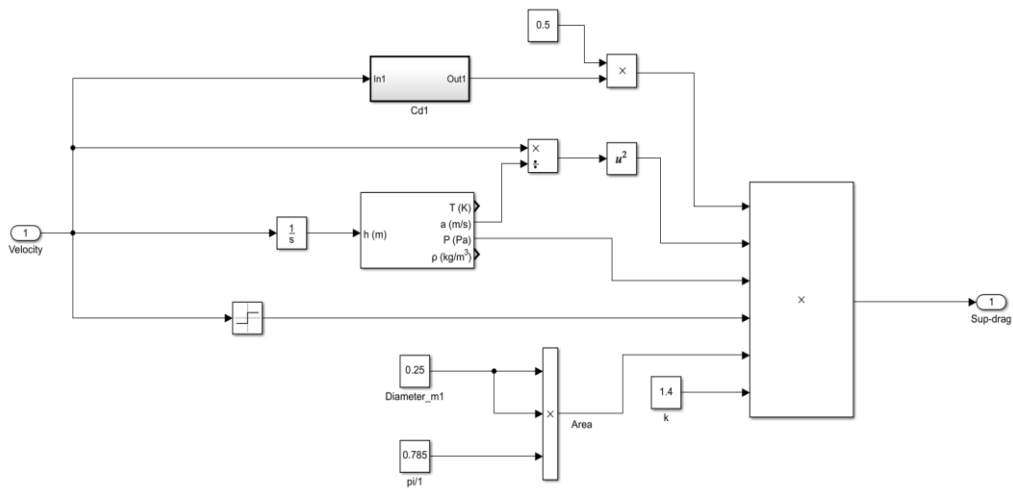


Fig 8. 4Simulink block and connections to calculate supersonic drag

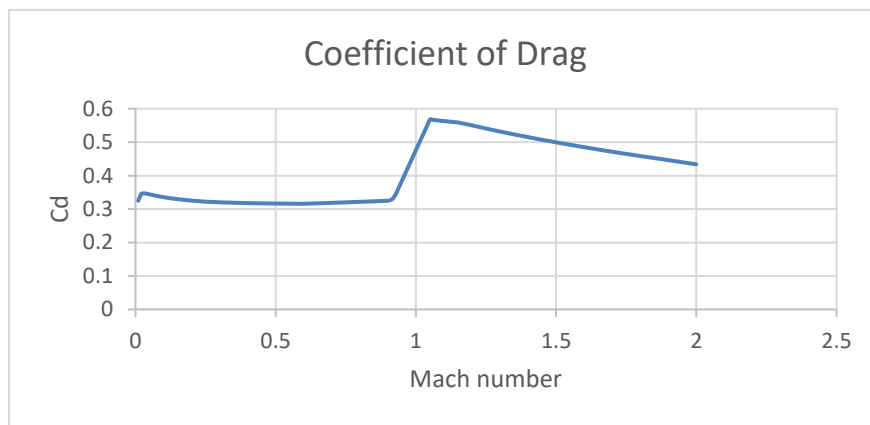


Fig 8. 5Coefficient of drag variation with respect to Mach number

8.3 RESULTS

The simulink results are presented below:

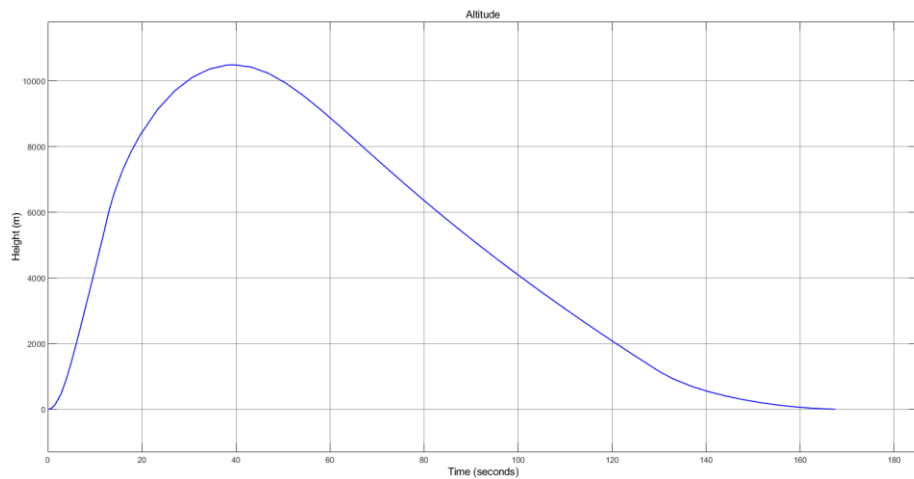


Fig 8. 6Variation of altitude with time

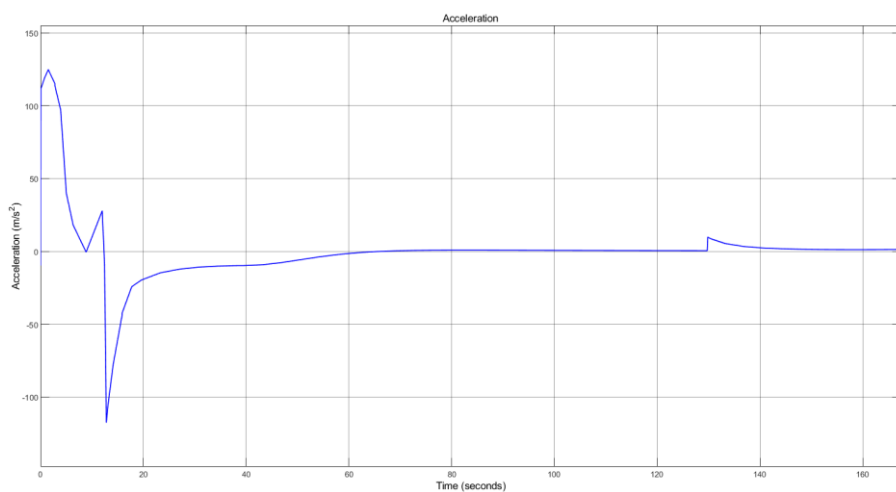


Fig 8. 7 Variation of acceleration with time

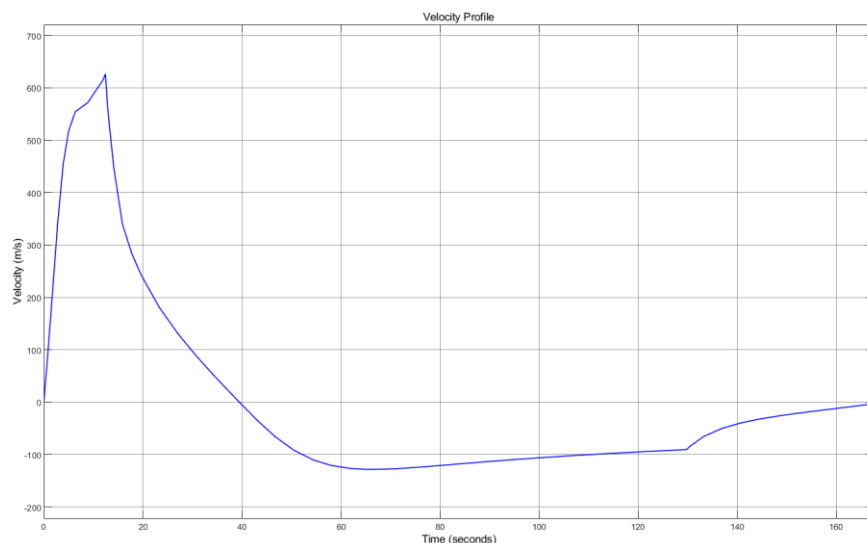


Fig 8. 8 Variation of velocity with time

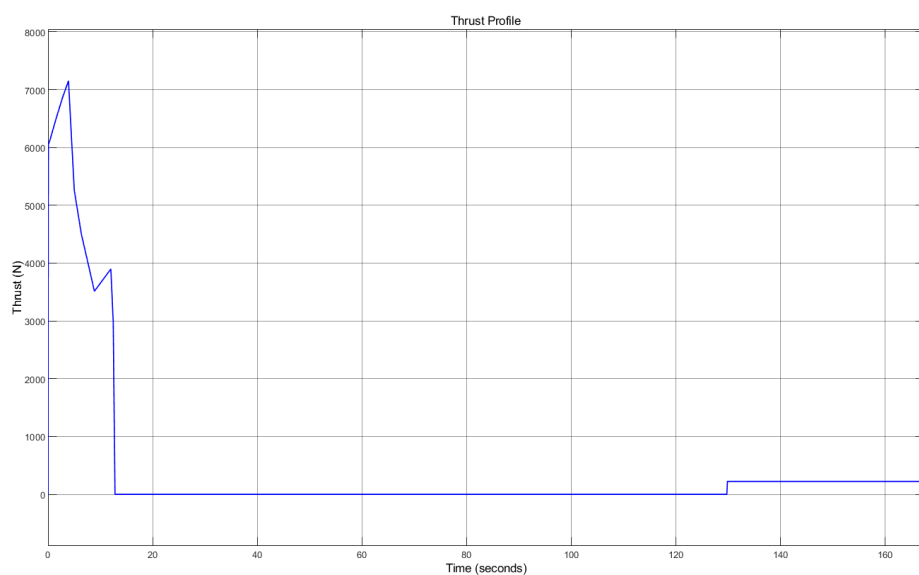
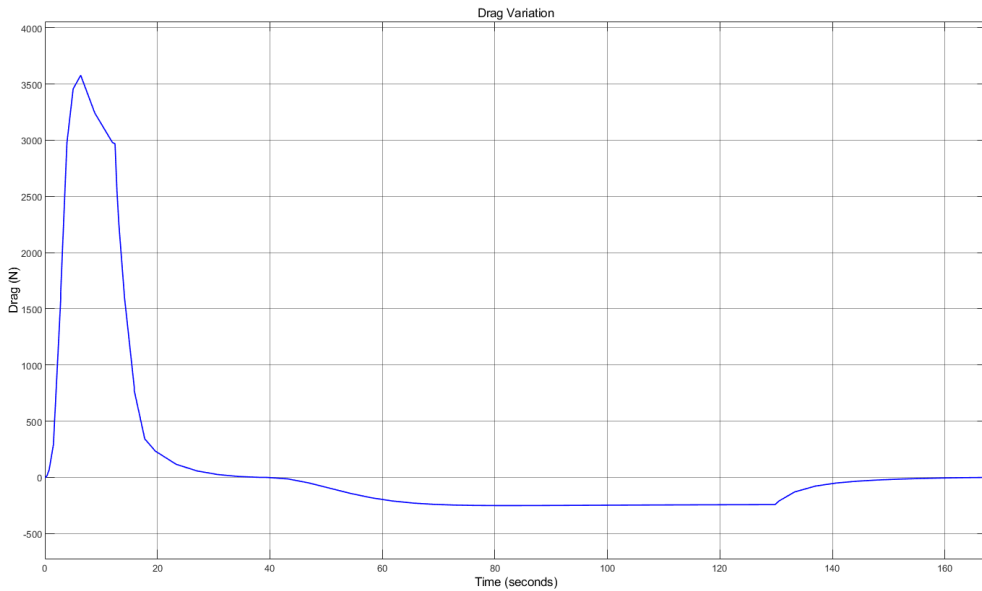
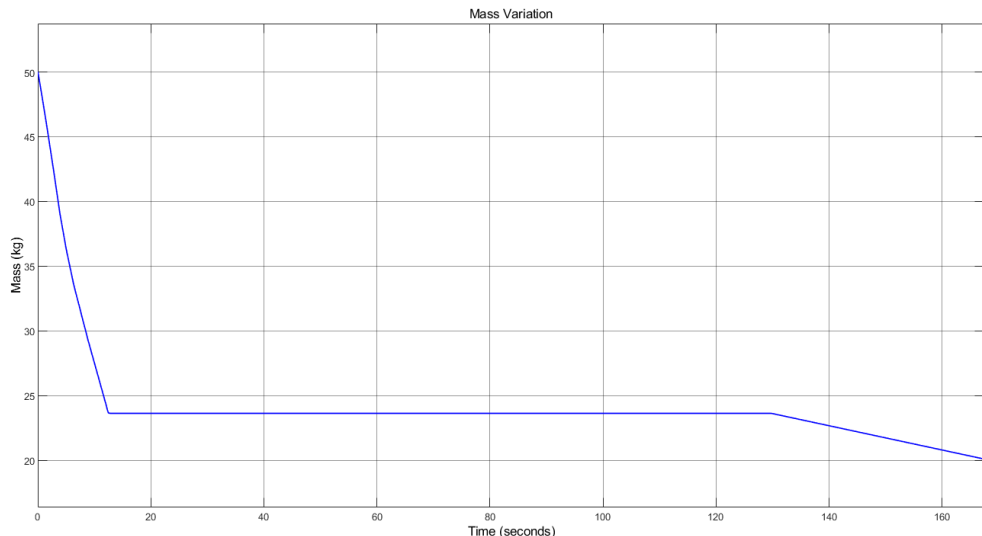


Fig 8. 9 Variation of thrust with time

**Fig 8. 10Variation of drag with time****Fig 8. 11Variation of mass with time**

The Rocket reaches an altitude of 10km in 40 seconds and then begins to descend under gravity. The rocket is under free fall for 128 seconds post apogee. The slow decrease in altitude can be depicted from the graph (fig 8.5) during which the descent motor is operated. The total time of flight is 168 seconds. The maximum acceleration experienced is 120 m/s^2 . It is seen that the acceleration is negative at the time of burnout and then increases gradually due to inertial force (fig 8.6). The flow analysis is done for the rocket body from the velocity plot as shown above (fig 8.7). It is clear that the rocket has zero velocity when the rocket touches ground. Thereby, the rocket is soft landed. The delay time (time at which the descent motor is ignited/operated) is 129.75 s. If the motor is

ignited earlier, then the rocket will reach zero velocity at a higher altitude and if the motor is ignited late, then the rocket will hard land. Therefore, delay time is a crucial aspect to be considered while operating the descent motor. It is assumed that the motor can be ignited at any instant of time, although APCP propellants have difficulty in igniting at a desired instant.

THRUST VECTOR CONTROL

9.1 DEFINITION

Thrust vectoring will be the main control method to keep θ as close to 0° as possible, keeping the rocket upright while following a reference trajectory. Vectoring refers to the gimbaling action of the engine or the flexibility of the nozzle, where the nozzle direction is changed relative to the COG of the rocket. Since the direction of the nozzle dictates the angle at which thrust is exerted, a torque about the COG is created if $\phi \neq 0$ as shown. In reality, the nozzle is moved along 3-dimensions with actuators. Since the simulation developed in this project is in 2-dimensions, only a single rotational movement is needed.

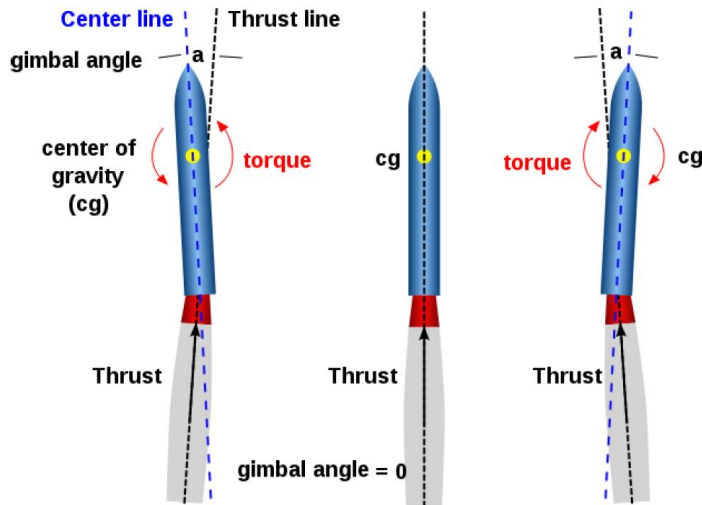


Fig 9. 1Control of rocket body using thrust vector control

The nozzle itself can take many forms, and the generated thrust magnitude and profile are directly dependent on the shape of the nozzle. Thrust reduction and increased wake turbulence can result from a sub-optimal nozzle profile, however, this project will assume ideal thrust profiles utilizing a single flexible nozzle joint. Hence, the gimbal can be represented by a rotary ball joint at the lower end of the rocket. The flow of the thrust will be assumed to act along a single directional vector, F_E .

9.2 TVC MECHANISM WITH SINGLE NOZZLE

Many different mechanisms have been used successfully. They can be classified into four categories:

- Mechanical deflection of the nozzle or thrust chamber.
- Insertion of heat-resistant movable bodies into the exhaust jet; these experience aerodynamic forces and cause a deflection of a part of the exhaust gas flow.
- Injection of fluid into the side of the diverging nozzle section, causing an asymmetrical distortion of the supersonic exhaust flow.
- Separate thrust-producing devices that are not part of the main flow through the nozzle.

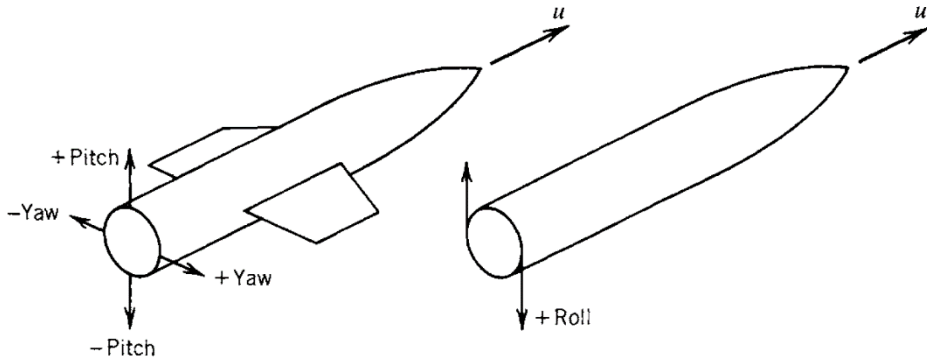


Fig 9. 2 Axis of pitch, yaw and roll motion along rocket body

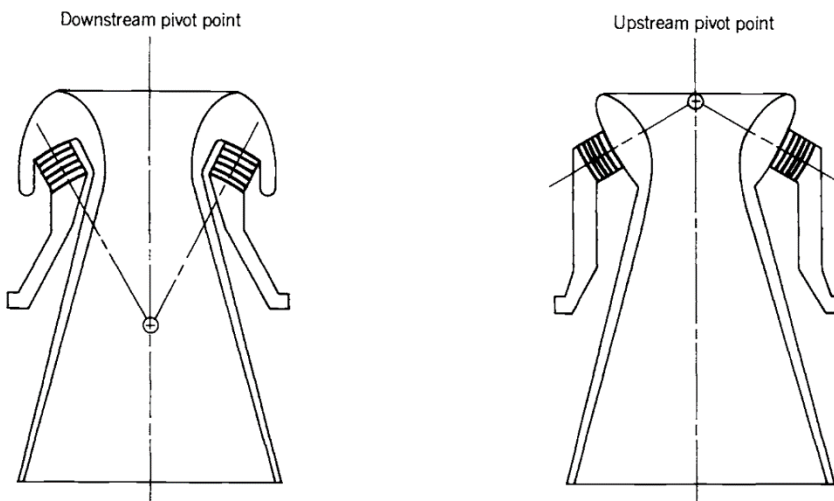


Fig 9. 3 Pivot points for flexible nozzle bearing

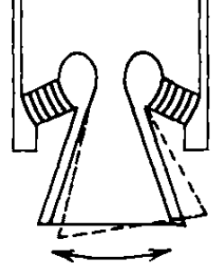
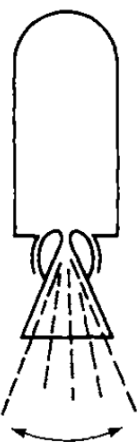
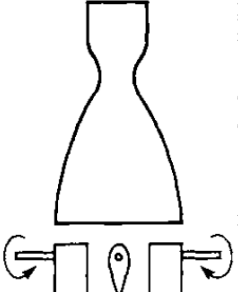
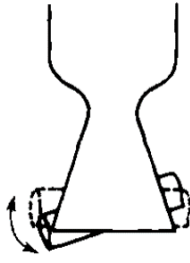
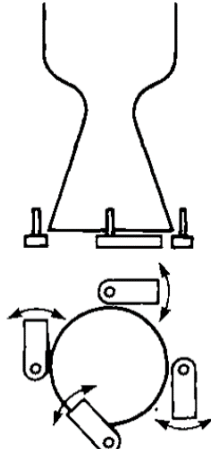
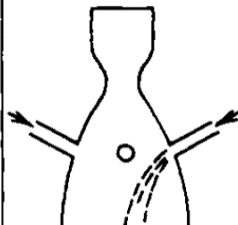
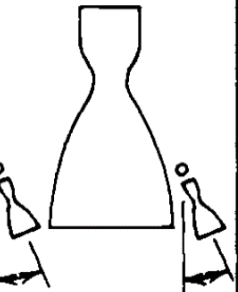
Gimbal or hinge	Flexible laminated bearing	Flexible nozzle joint	Jet vanes
			
Universal joint suspension for thrust chamber	Nozzle is held by ring of alternate layers of molded elastomer and spherically formed sheet metal	Sealed rotary ball joint	Four rotating heat resistant aerodynamic vanes in jet
L	S	S	L/S
Jetavator	Jet tabs	Side injection	Small control thrust chambers
			
Rotating airfoil shaped collar, gimballed near nozzle exit	Four paddles that rotate in and out of the hot gas flow	Secondary fluid injection on one side at a time	Two or more gimballed auxiliary thrust chambers
S	S	S	L

Fig 9. 4Types of thrust vectoring using single nozzle

Flexible laminated bearing nozzle is similar to that of gimbal nozzle and seems to be the best option in case of solid rocket motor although in real life its too hard to maintain for reusability, this has been selected for the ease of construction and easy to work on in the available tie slot. Hence this configuration is adopted in this project. Two methods of using flexible nozzle bearings with different locations for the center of rotation. The bearing support ring is made of metal sheets and polymer resins formed into rings with spherical contours (white) bonded together by layers of molded elastomer or rubber (black stripes). Although only five elastomeric layers are shown for clarity, many flexible bearings have 10 to 20 layers.

9.3 CONTROL ALGORITHM

Closed-loop control systems are the pivot on which such landings are made possible. Both classical control and Artificial Intelligence (AI) techniques rely on state variables to analyze the error with respect to an ideal state and execute corrective measures. A controller's job is to perform these actions in a stable and controlled manner. In classical control, these states must be bound by a well-defined mathematical model, whereas in AI input variables are defined loosely since the method has no knowledge of what the variables represent. This underlines the difference in the approaches of creating a controller. Classical control follows a set of rules and known methodology that have been widely used and tested, whereas AI techniques, such as Reinforcement Learning (RL), are less structured.

9.3.1 PROPORTIONAL INTEGRAL DERIVATIVE (PID) CONTROLLER

A Proportional Integral Derivative (PID) controller is an intuitive controller that is suitable for SISO systems. The PID is a simple yet effective controller that computes the proportional, integral and derivative of the difference between the output and the reference input (error) and outputs a control signal depending on the defined PID coefficients.

9.3.2 OPTIMAL CONTROL

Even though the PID is widely used to control simple systems, it does not guarantee optimal control or stability. Furthermore, problems with coupled variables and MIMO systems increase the complexity and make the manual-tuning of a PID a naïve

approach. To this end, the field of optimal control is introduced. The Linear Quadratic Regulator (LQR) and MPC are two such controllers in this field.

9.3.3 LINEAR QUADRATIC REGULATOR

For a model given by $\dot{x} = Ax + Bu$, the LQR seeks to find a feedback matrix $-K$ that leads to optimal control by minimizing a quadratic cost J .

The disadvantage of LQR is that the optimal feedback is independent of constraints. This poses a problem in processes such as the rocket landing, where all inputs are bounded. The problem can be redefined to include constraints, but more advanced methods, such as MPC, cater for such an issue.

9.3.4 MODEL PREDICTIVE CONTROL

MPC is a relatively new field in control that has only been proven useful thanks to the increased computational power. However, it found widespread use in industry; from precision landings to trajectory planning in missiles. Like LQR, MPC solves a quadratic program by minimizing an objective function. However, unlike LQR, it includes equality and inequality constraints, and the linearized plant dynamics form part of these constraints. This enables the optimizer to find a solution that is optimal for not just the present state, but also future states. The extent of predictability is referred to as the time horizon.

9.4 COMPARISON

The PID is the simplest and most intuitive method, using the proportional, integral and derivative of the error with respect to a reference in order to drive the process. However, the PID is suitable for SISO systems. Therefore, where multivariable, coupled and non-linear systems are presented, the PID can only be implemented to a limited extent on the linearized and decoupled plant. This leads to inaccuracies and sub-optimal control. PIDs are tackled as a baseline.

Unlike PID controllers, LQRs use the state space to find the optimal feedback matrix $-K$. Moreover, whereas the PID acts on the error, the LQR acts on the state. This state is still evaluated with respect to an equilibrium point since any non-linearities need to be linearized for an LQR to be designed. The general form of LQR does not include constraints and the designed LQR will only be optimal at the linearized state.

The shortfall of LQR in dealing with constraints as well as different conditions led to MPC, where the problem is formed as an objective function with constraints. MPC finds the correct input to take by minimizing a cost function with respect to the states and actions. Like LQR, the cost function is quadratic, but it is not solved analytically. Instead, an optimizer is used to find a solution to the objective function. This is also done whilst respecting constraints and following a trajectory. This means that whereas PIDs and LQRs only consider the current state, MPC can incorporate the model in the constraints and simulate future states; enabling it to pick the best actions that maximize not just the current reward, but also future rewards.

The general form of the MPC still needs a well-defined model where the state is found analytically or is estimated. MPC is derived from Bellman's equations and seeks to find the best policy that maximizes future rewards.

9.5 EQUATION OF MOTION

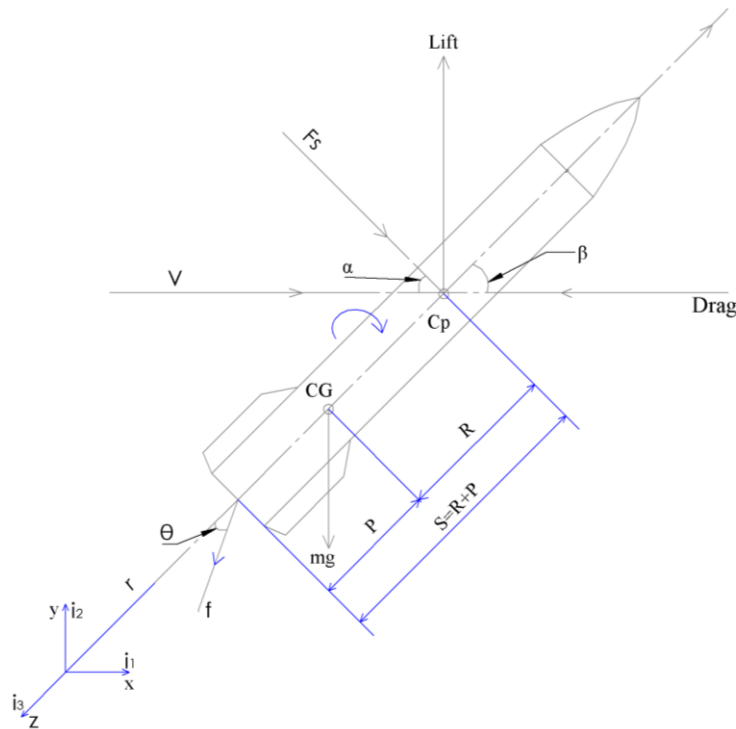


Fig 9. 5Forces acting on rocket body

Equation of motion is derived based on the Fig 9.5, all the forces are assumed to act through the axis line and there is no eccentricity, the assumptions and constants used are as below,

$$L = \text{Lift force} = 0 \quad (9.1)$$

$$D = \text{Drag force} = \text{opposes the motion of vehicle} = \alpha V^2 = (\dot{r}_x^2 + \dot{r}_y^2) \quad (9.2)$$

$$f = \text{thrust force}; |f| = F$$

$$f_w = \text{wind force} = F_w \hat{i}_1 \text{(Assumed to be in i1 direction)}$$

$$F_s' = F_s \cos\alpha \hat{i}_1 + F_s \sin\alpha \hat{i}_2 \quad (9.3)$$

$$f' = F \sin(\alpha-\theta) \hat{i}_1 + F \cos(\alpha-\theta) \hat{i}_2 \quad (9.4)$$

$$f_w = F_w \hat{i}_1$$

$$D' = -D \sin(\alpha + \beta) \hat{i}_1 - D \cos(\alpha + \beta) \hat{i}_2 \quad (9.5)$$

$$e = L \sin\alpha \hat{i}_1 + L \cos\alpha \hat{i}_2$$

$$p = -p \sin\alpha \hat{i}_1 - p \cos\alpha \hat{i}_2$$

$$mg' = -mG \hat{i}_2$$

$$h' = \text{angular momentum} = -J \dot{\alpha} \hat{l}_3 \text{ (clockwise hence negative)}$$

From fig 9.5, we can write three equation of motion in all the three dimensions.

The three equations of motion are

$$m \ddot{x}_1 = F \sin(\alpha - \theta) - D \sin(\alpha + \beta) + F_w + F_s \cos\alpha \quad (9.6)$$

$$m \ddot{y}_1 = F \cos(\alpha - \theta) - D \cos(\alpha + \beta) - mG - F_s \sin\alpha \quad (9.7)$$

$$R' = J \ddot{\alpha} = -D \sin\beta (L) + F p \sin\theta + L F_s - F_w L \cos\alpha \quad (9.8)$$

$$\text{Where } \tan(\alpha + \beta) = \frac{\dot{x}_1}{\dot{x}_2}$$

Linearize with respect to an equilibrium position we will set the linear dynamics of the system for that time. However, we will consider only the vertical flight and then the speed is considered constant

Then $\alpha = \beta = \theta = 0$

$$\dot{x}_1 = 0, \dot{x}_2 = V = \text{constant}$$

$$F = \left(\frac{1}{2} \rho V^2 S C_D \right) + mG$$

$$D \alpha V^2 = \frac{1}{2} \rho V^2 S C_D$$

But $C_D = 2$

$$\text{Therefore } D \alpha V^2 = \rho V^2 S$$

For small α, β, θ ($S_\theta = \theta; C_\theta = 1$ etc.)

$$J \ddot{\alpha} = -D L \beta + F p \theta - L F_w$$

$$m \ddot{x}_1 = F (\alpha - \theta) - D (\alpha + \beta) + F_w$$

$$m \ddot{y}_1 = F - D - mG \Rightarrow m \ddot{y}_1 = \tilde{F} \quad \text{Where } f = F - D - mG$$

Let us disturb the motion such that \dot{x}_1 in small horizontal velocity

That in $V \sin(\alpha + \beta) = \dot{x}_1$

For small $\alpha + \beta$,

$$\dot{x}_1 = V(\alpha + \beta) \quad (9.9)$$

$$\text{Also } \dot{x}_2 - V = \dot{\tilde{x}}_2 \quad (9.10)$$

where ($V = \text{constant}$)

Writing equations removing β and $\alpha + \beta$, using

$$\begin{aligned} \beta &= \frac{\dot{x}_1 - V\alpha}{V} \quad \text{and} \quad \alpha + \beta = \frac{\dot{x}_1}{V} \\ J\ddot{\alpha} &= -(\rho V^2 S)L \left(\frac{\dot{x}_1 - V\alpha}{V} \right) + mG)p\theta - F_w L \\ m\ddot{x}_1 &= F(\alpha - \theta) - \rho V^2 S \left(\frac{\dot{x}_1}{V} \right) + F_w \\ m\ddot{\tilde{x}}_2 &= \tilde{F} = F - D - mG \\ &= F - \rho V^2 S - mG \end{aligned}$$

State space form;

$$x_1 = \alpha; \quad x_4 = \dot{\alpha}; \quad (9.11)$$

$$x_2 = x_1; \quad x_5 = \dot{x}_1; \quad (9.12)$$

$$x_3 = x_2; \quad x_6 = \dot{\tilde{x}}_2; \quad (9.13)$$

$$\dot{x}_4 = \frac{L\rho V^2 S}{J} x_1 - \frac{L\rho V^2 S}{JV} x_5 + \frac{(\rho V^2 S + mG)p\theta}{J} + F_w L \quad (9.14)$$

$$\dot{x}_5 = \dot{x}_1 = \frac{F(\alpha - \theta)}{m} + \rho V^2 S \left(\frac{\dot{x}_1}{V} \right) + F_w = \frac{F}{m} x_1 - \frac{F}{m} \theta - \frac{F}{m} x_5 + \frac{F_w}{m} \quad (9.16)$$

$$\dot{x}_6 = \ddot{\tilde{x}}_2 = \frac{\tilde{F}}{m} = F - \rho V^2 S - mG \quad (9.17)$$

Writing eqn 11-17 in matrix form we get,

$$\begin{aligned} \begin{Bmatrix} \dot{x}_1 \\ \dot{x}_2 \\ \dot{x}_3 \\ \dot{x}_4 \\ \dot{x}_5 \\ \dot{x}_6 \end{Bmatrix} &= \begin{bmatrix} 0 & 0 & 0 & 1 & 0 & 0 \\ 0 & 0 & 0 & 0 & 1 & 0 \\ 0 & 0 & 0 & 0 & 0 & 1 \\ \frac{L\rho V^2 S}{J} & 0 & 0 & 0 & -\frac{L\rho V^2 S}{J} & 0 \\ -\frac{F}{m} & 0 & 0 & 0 & -\frac{\rho VS}{m} & 0 \\ 0 & 0 & 0 & 0 & 0 & 0 \end{bmatrix} \begin{Bmatrix} x_1 \\ x_2 \\ x_3 \\ x_4 \\ x_5 \\ x_6 \end{Bmatrix} + \begin{Bmatrix} 0 \\ 0 \\ 0 \\ \frac{(\rho V^2 S + mG)p}{J} \\ -\frac{F}{m} \\ 0 \end{Bmatrix} \theta + \begin{Bmatrix} 0 \\ 0 \\ 0 \\ 0 \\ 0 \\ \frac{1}{m} \end{Bmatrix} \tilde{F} \\ &\quad + \begin{Bmatrix} 0 \\ 0 \\ 0 \\ -\frac{L}{J} \\ \frac{1}{m} \\ 0 \end{Bmatrix} F_w \end{aligned}$$

This is uncontrollable

Introduce, $F_s = F_R - F_L$ thrust

F_s is acted closer to CPTherefore $F_s \cos\alpha$ will be horizontal direction, $F_s \sin\alpha$ will be in vertical direction.

Thus, the equation is rewritten as

$$\begin{aligned} \begin{Bmatrix} \dot{x}_1 \\ \dot{x}_2 \\ \dot{x}_3 \\ \dot{x}_4 \\ \dot{x}_5 \\ \dot{x}_6 \end{Bmatrix} &= \begin{bmatrix} 0 & 0 & 0 & 1 & 0 & 0 \\ 0 & 0 & 0 & 0 & 1 & 0 \\ 0 & 0 & 0 & 0 & 0 & 1 \\ \frac{L\rho V^2 S}{J} & 0 & 0 & 0 & -\frac{L\rho V^2 S}{J} & 0 \\ -\frac{F}{m} & 0 & 0 & 0 & -\frac{\rho VS}{m} & 0 \\ -\frac{F_s}{m} & 0 & 0 & 0 & 0 & 0 \end{bmatrix} \begin{Bmatrix} x_1 \\ x_2 \\ x_3 \\ x_4 \\ x_5 \\ x_6 \end{Bmatrix} + \begin{Bmatrix} 0 \\ 0 \\ 0 \\ \frac{(\rho V^2 S + mG)}{J} \\ -\frac{F}{m} \\ 0 \end{Bmatrix} \theta + \begin{Bmatrix} 0 \\ 0 \\ 0 \\ 0 \\ 0 \\ \frac{1}{m} \end{Bmatrix} \tilde{F} \\ &+ \begin{Bmatrix} 0 \\ 0 \\ 0 \\ \frac{L}{J} \\ \frac{1}{m} \\ 0 \end{Bmatrix} F_s + \begin{Bmatrix} 0 \\ 0 \\ 0 \\ -\frac{L}{J} \\ \frac{1}{m} \\ 0 \end{Bmatrix} F_w \end{aligned}$$

$F_s \cos\alpha$ and $F_s \sin\alpha$ becomes F_s about x_1 axis and $F_s \alpha$ about x_2 axis

About rotation we get $F_s L$ as moment

Wind force = 0

Lift force = 0

D' is a must = 0

9.6 CONTROLLER DESIGN IN SIMULINK

The controller is designed based on the Equation of motion as derived in section 9.5, The selected controller is a PID controller and it has been coded in MATLAB and the response is tuned for robust and faster controlling of the rocket. The code is then implemented in the SIMULINK environment and the plant is designed, the plant is 6 DOF model and allowance is given to control on the pitch and yaw axis, controlling of the spin is ignored for this simulation. The simulation is done to prove the controlling in the ascend mode and simulated for only during ascent of rocket and the same can also be proved in the decent phase with a proper delay time. The Simulink provides perfect platform to analyze and validate the analytical calculations.

9.6.1 DESCRIPTION OF SIMULINK BLOCKS

The measurements are done using a three-axis accelerometer and three axis gyroscope unit which gives the inertial states of the rocket, the function for testing the PID controller is developed in the MATLAB coder and the response shows it is more robust. The main page contains 4 subsystems as shown in Fig 9.6. They are PID controller, Rocket inertial system and propulsion system, Force and Moment measurement system and 6 DOF quaternion output and results model.

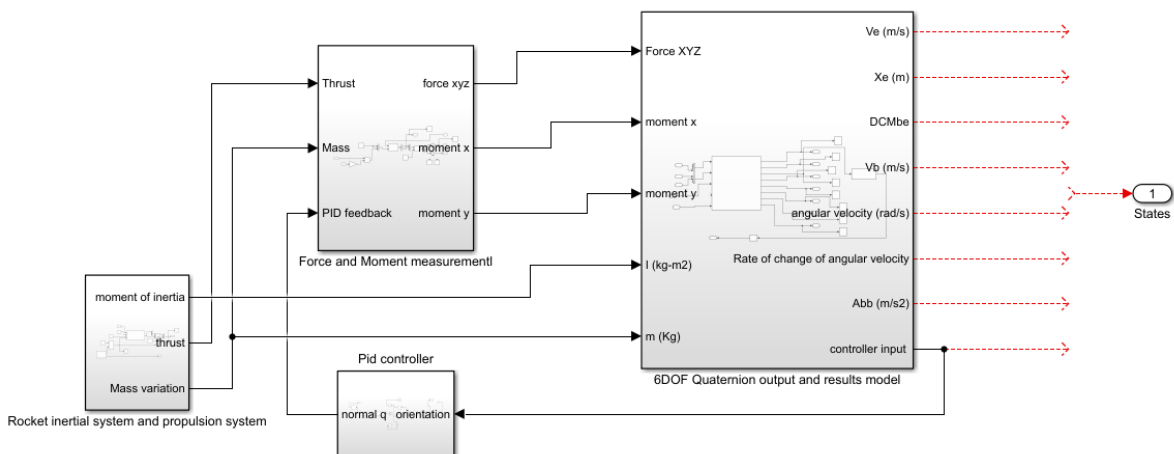


Fig 9. 6 Controller and Simulation model

Rocket inertial system and propulsion system subsystem contains a moment of inertia measurement unit and thrust data measurement unit and a mass calculation unit as shown in Fig 9.7. All the blocks are interconnected to ensure the bus signal has less noise and the signal is not interchanged. Motor configuration subsystem takes the thrust data from workspace at equal intervals of time and outputs the thrust data. And this thrust data is used to calculate the propellant mass as shown in Fig 9.8.

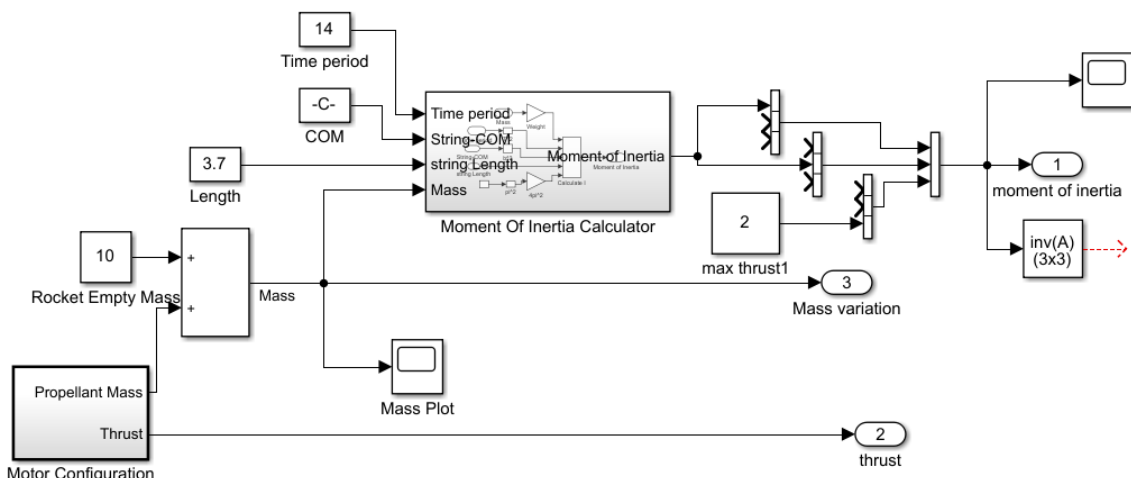


Fig 9. 7 Rocket inertial system and propulsion system blocks

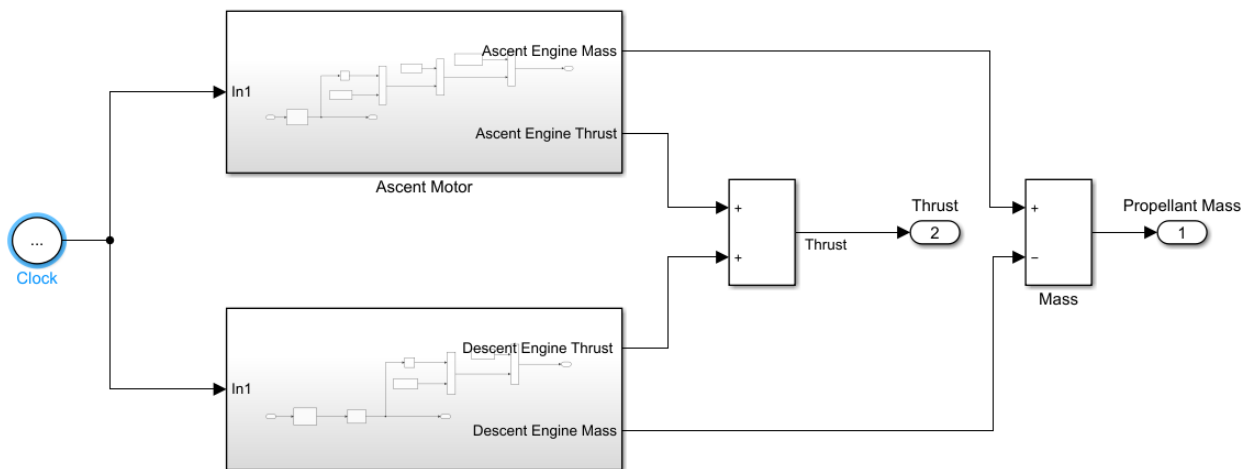


Fig 9. 8 motor configuration subsystem for both ascent and decent

The motor configuration subsystem has two different subsystems for both ascent and decent phase and the subsystem is as shown in Fig 8.2, there is slight difference between both the subsystems where in the decent motor has a delay block for the right ignition as explained in chapter 8. The moment of inertia calculator subsystem is as shown in Fig 9.9, which uses general calculation formula as a base for block building and gives the change in moment of inertia at every instant of time step. This subsystem uses time period, mass variation, center of mass, and the length of the body as input to give one dimensional moment of inertia and the same is done for all the three dimensions although due to symmetry other inertia will be zero.

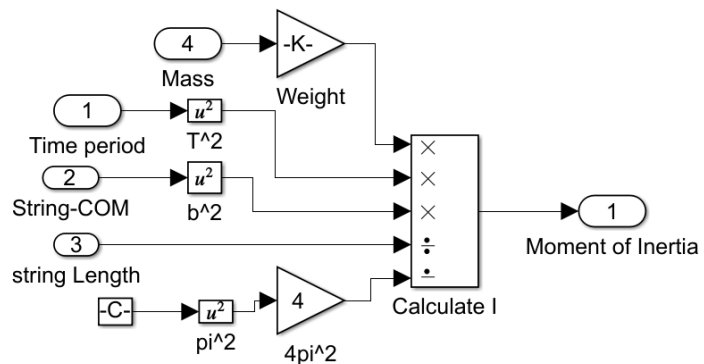


Fig 9. 9 Moment of inertia calculation subsystem

Force and moment measurement subsystem take the input from the inertial subsystem and then it calculates the force in all the three-direction applied on the rocket, the force in the y direction is assumed to be wind disturbance and can be manually changed for different PID response. This force is then calculated in the local frame of reference which includes feedback loop to determine the quaternion error and to calculate

the current force in 3d frame. There are two noise reduction blocks to reduce the noise in the calculation of the moment in xy directions as shown in Fig 9.10.

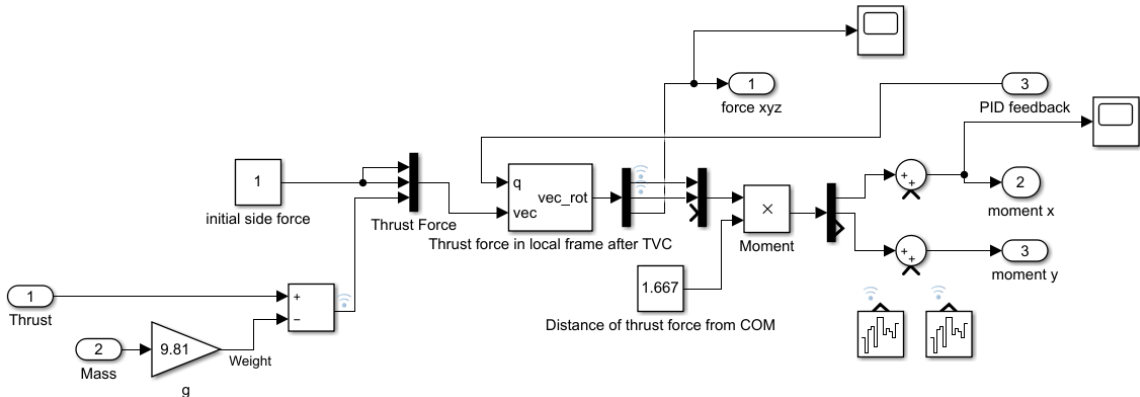


Fig 9. 10 Force and moment measurement Subsystem

The quaternion subsystem is used to determine the rocket state at each time step, this state are used as input for the controllers and the states are converted into angles for the PID input, the ratios are taken in order of XYZ as per the Euler's law of rotation and the equation of motion derivation, this subsystem also contains several scopes to get the output of the simulation. And there is a matrix conversion block is used to make the output quaternions into row vector to facilitate the PID controller.

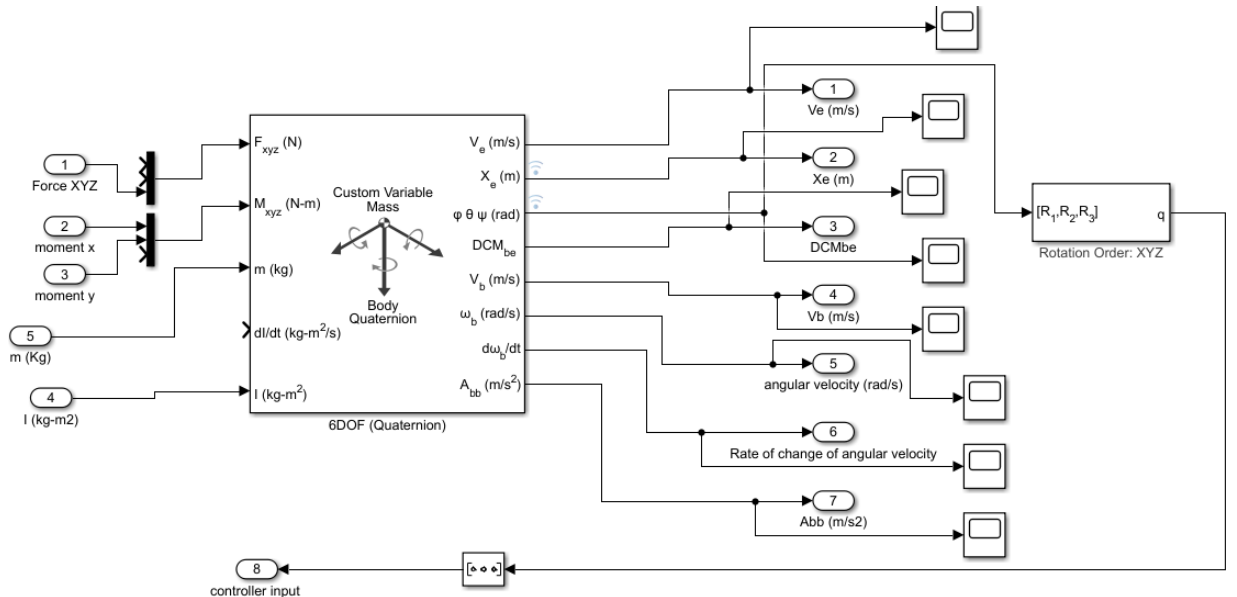


Fig 9. 11 6 DOF Quaternion and Result subsystem

The PID controller subsystem is a inbuild controller system from the SIMULINK environment and this system has also inbuilt tuning app for PID tuning, the inputs from the quaternions are converted to quaternion errors with the help of pre written code in the MATLAB coder, and then the errors are converted to XYZ orientation and fed into

controller to get the PID values and the angle required for rotation in TVC system. And then feedback is designed to get the output in the next timestep.

9.6.2 RESULTS AND DISCUSSION

The PID responses can only be calculated if there is any disturbance, so the controller response is shown in the Fig 9.12, has a degree of rotation in a step input of 1 and 2 degrees and the output is shown, it can be observed that the PID response time is very quick and the PID tuning is more robust.

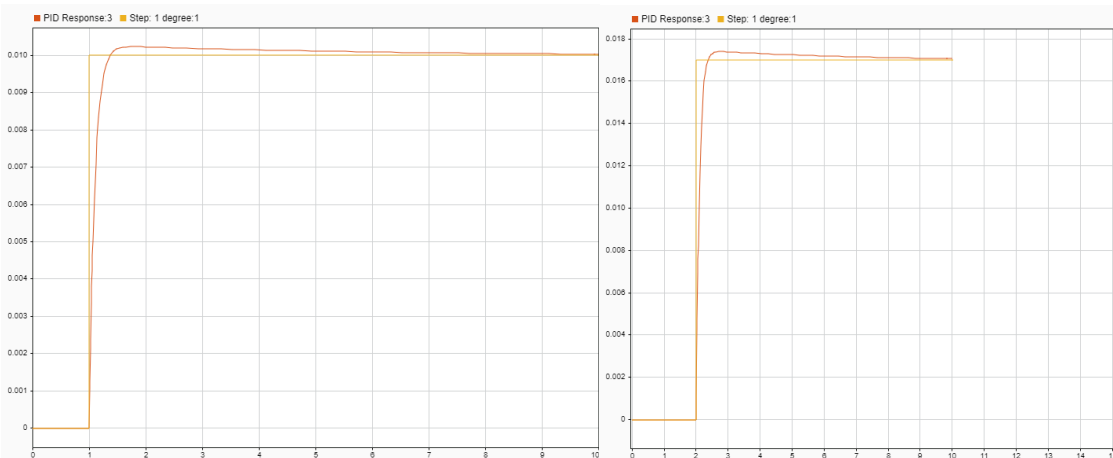


Fig 9. 12 PID response for a step input of 1 (left) and 2 (right) degree of rotation

The velocity profile is as shown in Fig 9.13, it can be observed that the velocity in the other two directions are maintained at almost zero by the controller which is indicated in the blue and red lines, the velocity reaches a maximum at burnout, since there is no drag considered in this simulation the velocity achieved is more than what explained in chapter 8. It is also observed that there is a slight raise in velocity at 4 to 7 seconds of burn out which is due to thrust variation from the solid motor.

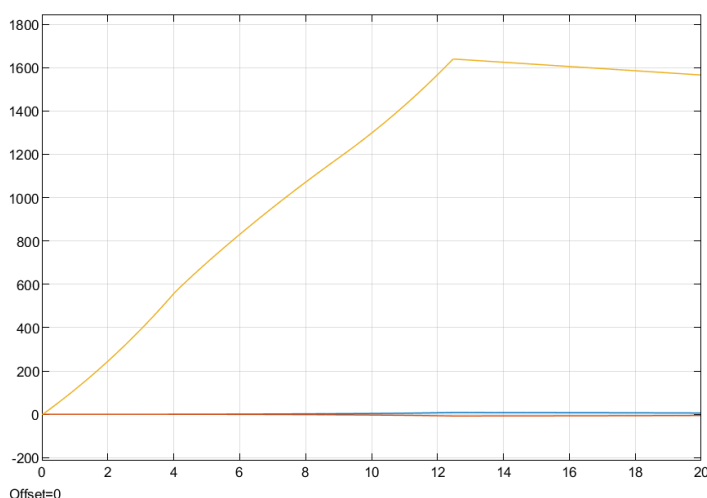


Fig 9. 13 Velocity change in XYZ direction (Red – X, Yellow – Y, Blue – Z)

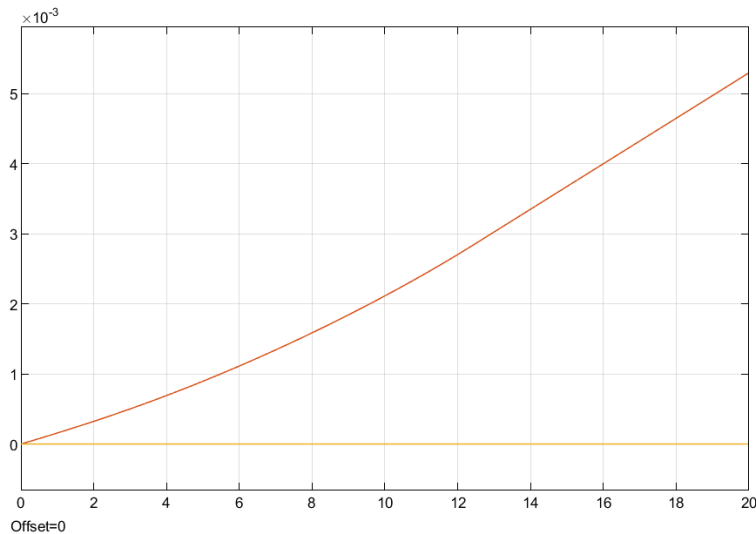


Fig 9. 14 Trajectory of the rocket with respect to Time

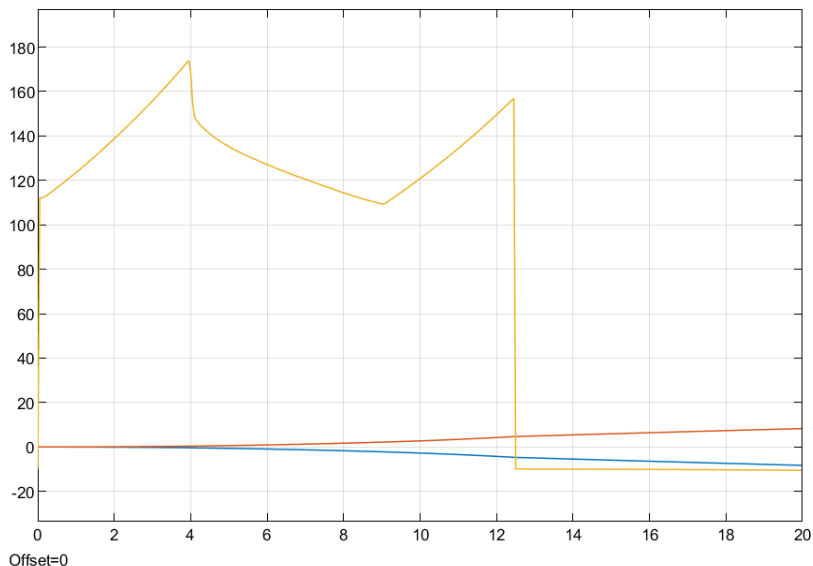
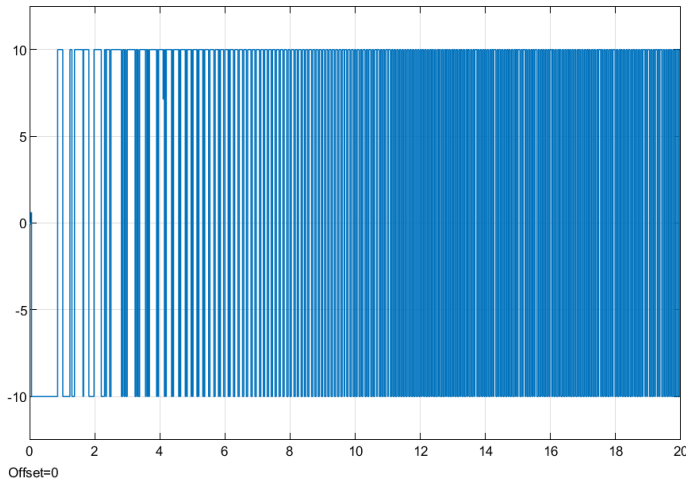
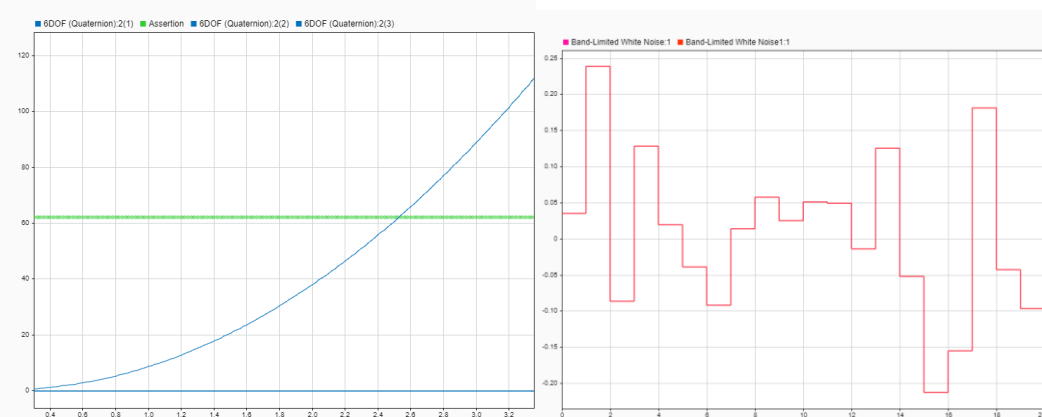


Fig 9. 15 Force variation on the inertial frame of reference of rocket

The trajectory for the rocket is pre-defined and is designed as a boundary value problem, and is optimized using the MATLAB code, Fig 9.14 shows that the rocket follows the trajectory at all the points and the increase in altitude is as desired. Fig 9.16 shows the force applying on the rocket inertial system it is observed that even though a 100N of side force is applied the controller system is able to handle the force and produces good response to keep the rocket upright. The testing is also done for continuous disturbance of the rocket with a continuous step inputs and the results are as obtained in Fig 9.16, it can be observed that there is a maximum deflection of 10 degree for the gimble at extreme conditions and the response shows that the controller can also handle strong gust loads from the atmosphere

**Fig 9. 16 Response output for continuous disturbance****Fig 9. 17 Quaternion response test results – (green implies test passed) ,and the band noise response (right)**

The quaternion errors are used here to control the rocket hence a test is also done in the quaternion subsystem to check the working of the clock and from Fig 9.17 gives the results which indicates in green color that it passes the inbuilt limit which is decided in the MATLAB code. The right side of the figure shows the response of the Band noise block which is used to reduce the noise due to vibrations, From the above results it can be shown that controlling algorithm is more robust and it can be implemented for both ascent and decent phase of rocket Thrust Vector Control systems.

MODEL ROCKET

10.1. INTRODUCTION TO MODEL ROCKET

This chapter illustrates the experimental part of the project. In order to build a rocket powered by a solid rocket motor equipped with thrust vector control, the following aspects has to be considered:

- Mass of the rocket
- Altitude goal
- Burn time
- Time to reach specified altitude
- Stability factor
- Avionics
- Recovery system

1. **Rocket mass:** This is main factor that decides what class of solid rocket motor has to be selected to reach the specified altitude. For our project, we have aimed the rocket mass to be around 1 to 1.5 kg. This is rather the safe mass margin to work with since a F or G class motor can be used whereas, any higher-class motor such as H, Level 1 certification is a must due to the rules and regulations provided by National Association of Rocketry.
2. **Altitude goal:** The rocket is aimed to reach an altitude of 250m.
3. **Burn time:** Commercially available motors such as F-15 provides a maximum burn time of 3.5s. Since we are developing a motor from scratch, we have the control over burn time and design according as it will be discussed in later stage. Burn time also decides the time for which thrust vectoring is active. All the more, we will only be able to control the rocket as long as the motor is active and also restrict us the material to be used for motor casing. Hence this factor is very crucial.
4. **Time to reach specified altitude:** This factor decides the maximum velocity the rocket reaches and therefore characteristics of aerodynamic forces and moments acting on the rocket body.

5. **Stability factor:** A stability factor of 1-1.5 Cal is usually preferred for the rocket to be statically stable that is equipped with fins. Since we are employing active stabilization, we have to aim that the rocket is at least neutrally stable.
6. **Avionics:** Electronics bay consists of a microcontroller that will operate 2 servos for TVC, record flight data and deploy recovery system.
7. **Recovery system:** For the ascend phase the rocket will be recovered by a parachute whereas for the landing phase, a descent motor along with 4 landing legs will try to land the rocket safely.

Considering the above aspects, the next step is to develop the rocket. These steps are as follows:

10.2. PROPELLANT SELECTION

First step is the selection of propellant. Since we are building a F or G class motor, composite propellants such of that implemented in larger rocket for flight simulation cannot be used. They are way more powerful. Hence, the most suitable propellants are that which have relatively lower specific impulse of 100-130 Ns. Most commonly used propellants for this type of model rockets are:

- Black powder
- Potassium nitrate + Sucrose (KNSU)
- Potassium nitrate + Dextrose (KNDX)
- Potassium nitrate + Sorbitol (KNSB)
- RCS – White Lightning
- RCS – Blue Thunder

After careful analysis and availability of raw materials, Black powder and KNSU are selected to power our rocket. Black powder is a mixture of 75% Potassium nitrate (oxidizer), 15% Charcoal (fuel) and 10% Sulphur (burn rate modifier). The composition of Sulphur can be varied to change the burn rate. The final mixture is 1/3rd Black powder and 2/3rd of KNSU, this is done so as to vary the composition of these two propellants to get the desired burn rate. This gives us to control the thrust variation.

For this combination of propellants, the burn simulation is carried out in RoManS (Rocketry Management Software). The mass of the fuel required to carry a maximum mass of 1.5kg of rocket to an altitude of 250m is calculated from Richard Nakka's Spreadsheet. After determining propellant mass, the motor is designed in

RoManSsoftware. This software allows us not only to measure the burn parameters but also carry out 1D point mass simulation. The gain configuration is an end burner as only this configuration gives enough burn time.

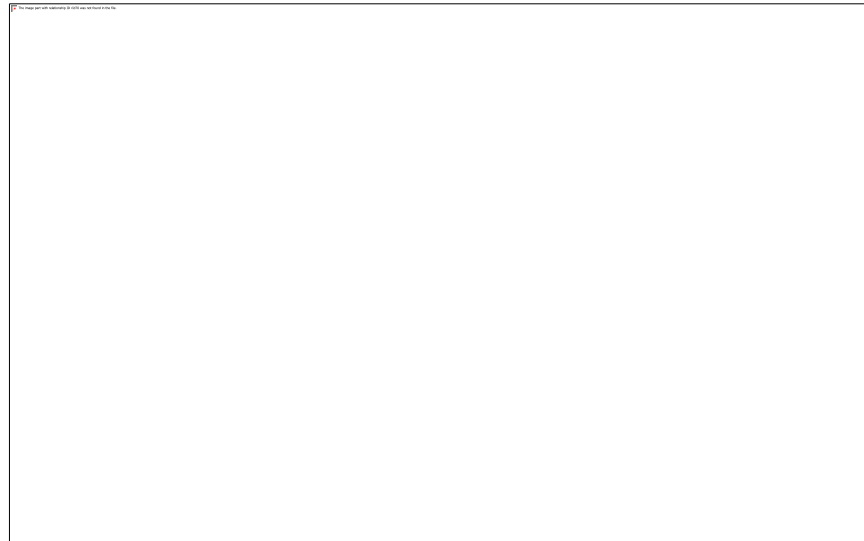


Fig 10. 1Propellants selected for motor test

10.3. SELECTION OF MOTOR MATERIALS AND MOTOR FABRICATION

The motor casing is made of PVC and to protect it from the high flame temperature, a home-made thermal insulation of layer thickness 1.5mm is used. A nozzle made of ceramic powder is used in place of bentonite clay that is most commonly used for SRM. This reduces the nozzle throat erosion drastically. The motor is fabricated as shown below with the help of a hydraulic jack to compress the grain together and a high energy-density motor.



Fig 10. 2Fabricated solid rocket motor

10.4. MOTOR STATIC TEST

Static test is carried out by igniting the motor with the help of an electric igniter. The motor is placed on a load cell to get continuous thrust data. The load cell can bear a maximum load of 10kg and connected to Arduino Nano that writes the test data to an external SD card for later analysis. The motor is then ignited as shown in Fig 10.3 and the thrust data are recorded as shown in Fig 10.4.



Fig 10. 3 Motor static test and its setup

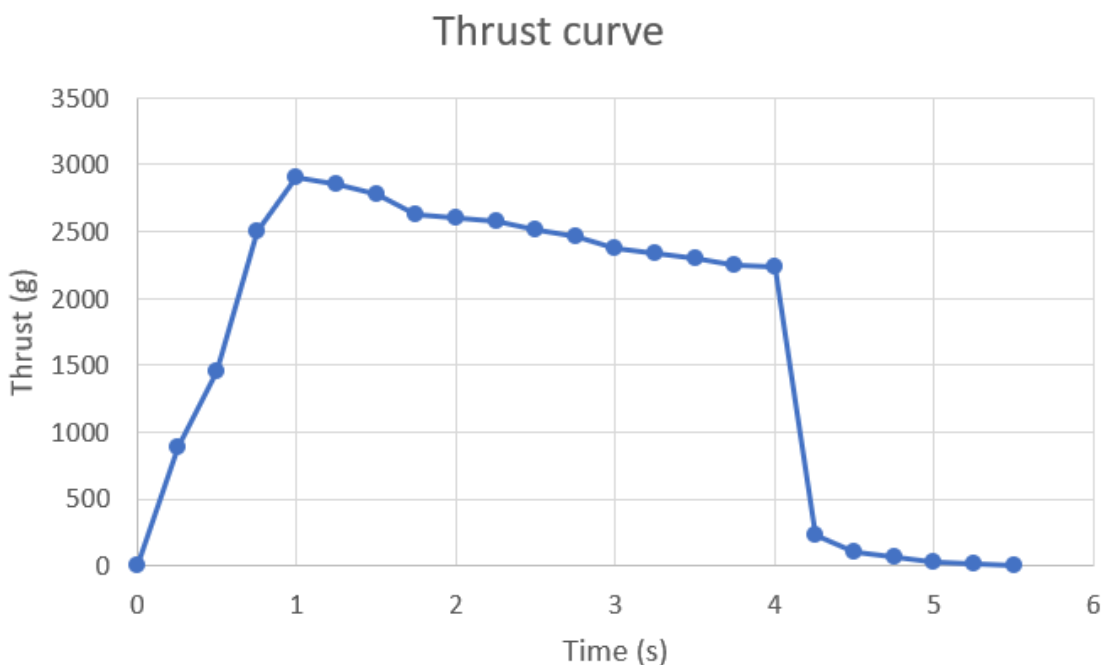


Fig 10. 4 Thrust data recorded with respect to time

10.5. ROCKET BODY MATERIAL SELECTION

The strength to weight ratio plays a major role in the selection of materials for the rocket. High strength cardboard tube is sufficient to handle loads at this scale hence used to make the rocket body. The following are the parts that are housed in the rocket frame:

- Nose cone
- Electronics bay
- TVC
- Landing legs

All the above materials are made of – PLA (3D printed) and the designed parts are shown in below section.

10.5.1 3D DESIGN AND PRINTED PARTS

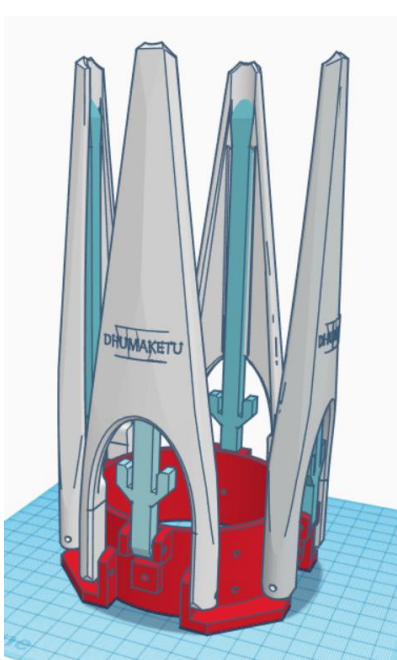


Fig 10. 5Landing legs design and 3D printed part

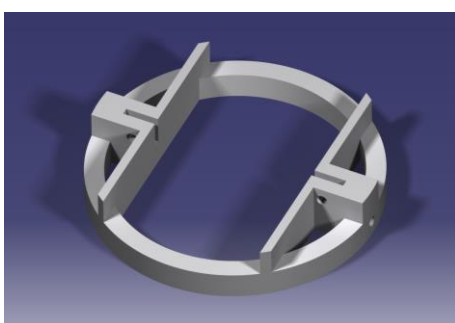


Fig 10. 6PCB mount design and 3D printed part

All the parts are designed in SOLIDWORKS and they are slices in CURA 3D software and then printed with Ender 3 printer with a step height of 0.2mm and an infill percentage of 25. Landing legs are essential for the propulsive landing process of rocket and designed on the basis of selected cylinder diameter as shown in Fig 10.5 and the electronics bay mount is designed to accompany PCB and the battery for control and guidance as shown in Fig 10.6. TVC design derived from reference 11, and they are optimized and recalibrated for our dimensions and a maximum deflection of 30 degree is allowed which can accompany 2 servos as shown in Fig 10.7.

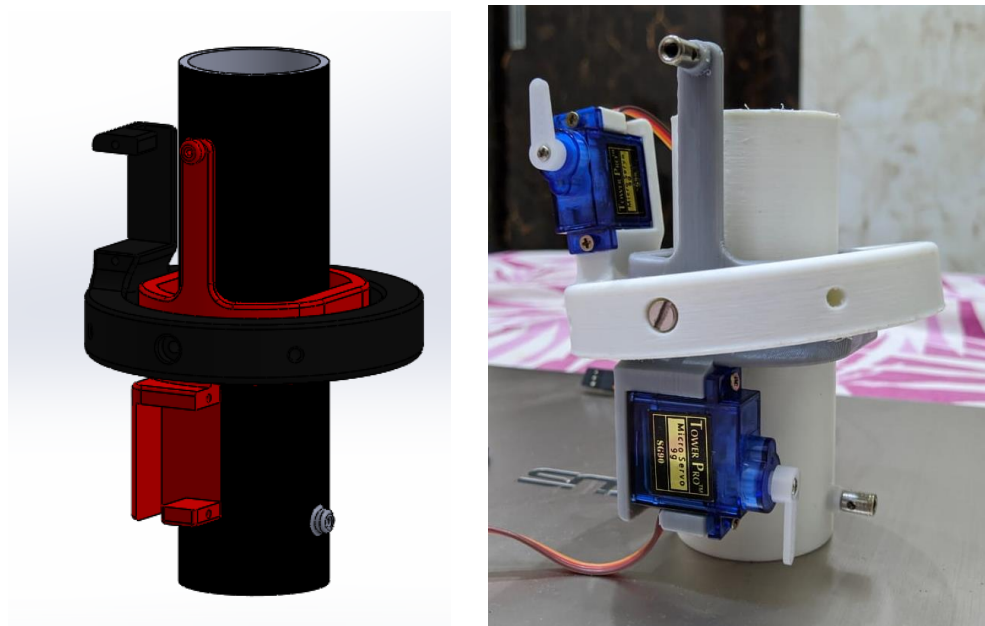


Fig 10. 7TVC design and assembly of the Printed part

10.6. COMPONENT MASS CALCULATION:

Table 10. 1 Mass of various components of rocket

Sl. No	Component Name	Mass (g)
01	Nose cone	61
02	Airframe	190
03	Electronics bay	170
04	TVC	87
05	Landing legs	140
06	Piston ejection system	100
08	Motor	140
07	Total mass	888

10.7. ELECTRONICS

The following are the components used that make up the flight computer

- **Teensy 3.2**



Fig 10. 8Teensy 3.2

TVC requires a powerful microprocessor or a microcontroller. Arduino chips operate at a clock speed of 16MHz which is not recommended since the code that is going to be developed requires higher processing power that does all the quaternion calculations and sends the output to servos. Even the slightest of delay in the control algorithm may hinder the performance the rocket and make it uncontrollable during its flight. Hence, Teensy microcontrollers are used for this purpose.

This chip has a lot of advantages, this board runs at a clock speed of 72MHz and can be overclocked up-to 96MHz there are also there are huge number of digital and analog pins which is necessary for our project. Also, this chip has a higher memory storage capability and internal EEPROM which are necessary to upload heavy codes.

- **MPU 6050 –**

This is most commonly used 6-axis Inertial measurement unit for hobby rockets that houses an accelerometer and a gyroscope. The accelerometer measures linear acceleration along three axis and the gyro measures angular velocity along three axes. The only down point is the lack of a magnetometer that serves as a compass. Other alternatives are MPU 9250 or BNO055 that has magnetometer and hence these are 9-axis measurement units that measures the angle on three axes in addition to acceleration and angular velocity.

MPU 6050 can be used to measure the angle of rotation with small changes to the code by measuring the linear acceleration vector to give the angle of rotation.

- **BMP 280 –**

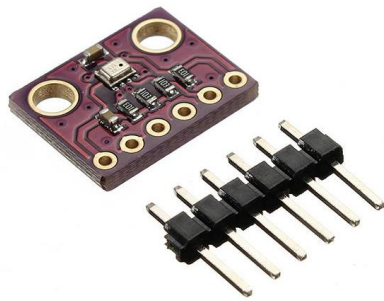


Fig 10. 9BMP 280

This is a barometer used to output altitude by measuring the static pressure. The alternative to this is BMP-180

- **Micro SD card reader**

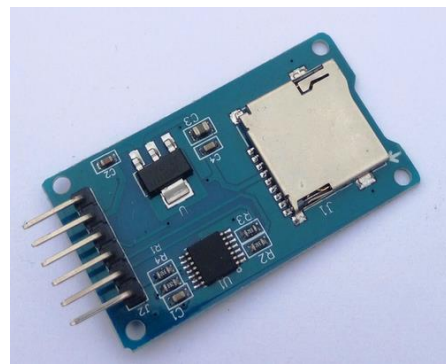


Fig 10. 10Micro SD card reader

We want to store the data at every instance of time. Hence, a flash memory is used to store the flight data. An external EEPROM (Electrically erasable read only memory) can also be used in addition to this for a faster data logging.

- **9g Servos**



Fig 10. 119g servos

These are electro-mechanical actuators that convert electrical signals to mechanical output. These servos have a maximum torque capability of 2kg and a maximum current consumption of 2A. Alternative to this is the metal servos that are stronger and are capable of managing higher torques. But 9g servo are enough to work at this scale. The servos are carefully selected that has a higher response time working on 50Hz.

- **N channel MOSFET**



Fig 10. 12N channel MOSFET

MOSFETs are similar to relays that acts as a switch. Unless the gate is set low the MOSFET is off and if the gate is pulled high, the switch is activated. Here, it is used for pyros that will send high current during the event of parachute ejection or for deploying landing legs. Four MOSFETS are used in the flight computer in the aim for future development.

- **5V regulator**



Fig 10. 135V regulator

Most of the components used requires 5v power supply hence a LM-7805 is used to convert 7.4V to regulated 5V.

- **Buzzer**



Fig 10. 14Buzzer

A 5V, 12mm buzzer is used that acts as an audio indicator and gives the sense of events that the flight computer is processing.

- **RGB LED**

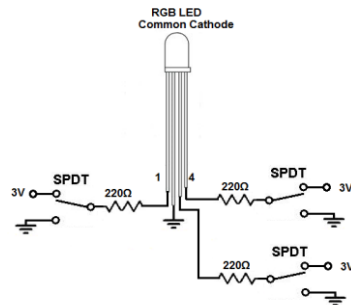


Fig 10. 15RGB light

A common cathode RGB LED is used for visual indication.

- **Resistors**

These are used to limit the current to certain components and also used as voltage divider to measure the voltage of the battery.

- **Capacitors**

These are used as low pass filter to remove any voltage spikes and provide stable DC voltage.

- **Terminal Blocks**

Used to connect 4 pyro channels, to connect battery and a switch

- **Cell LIPO Battery**



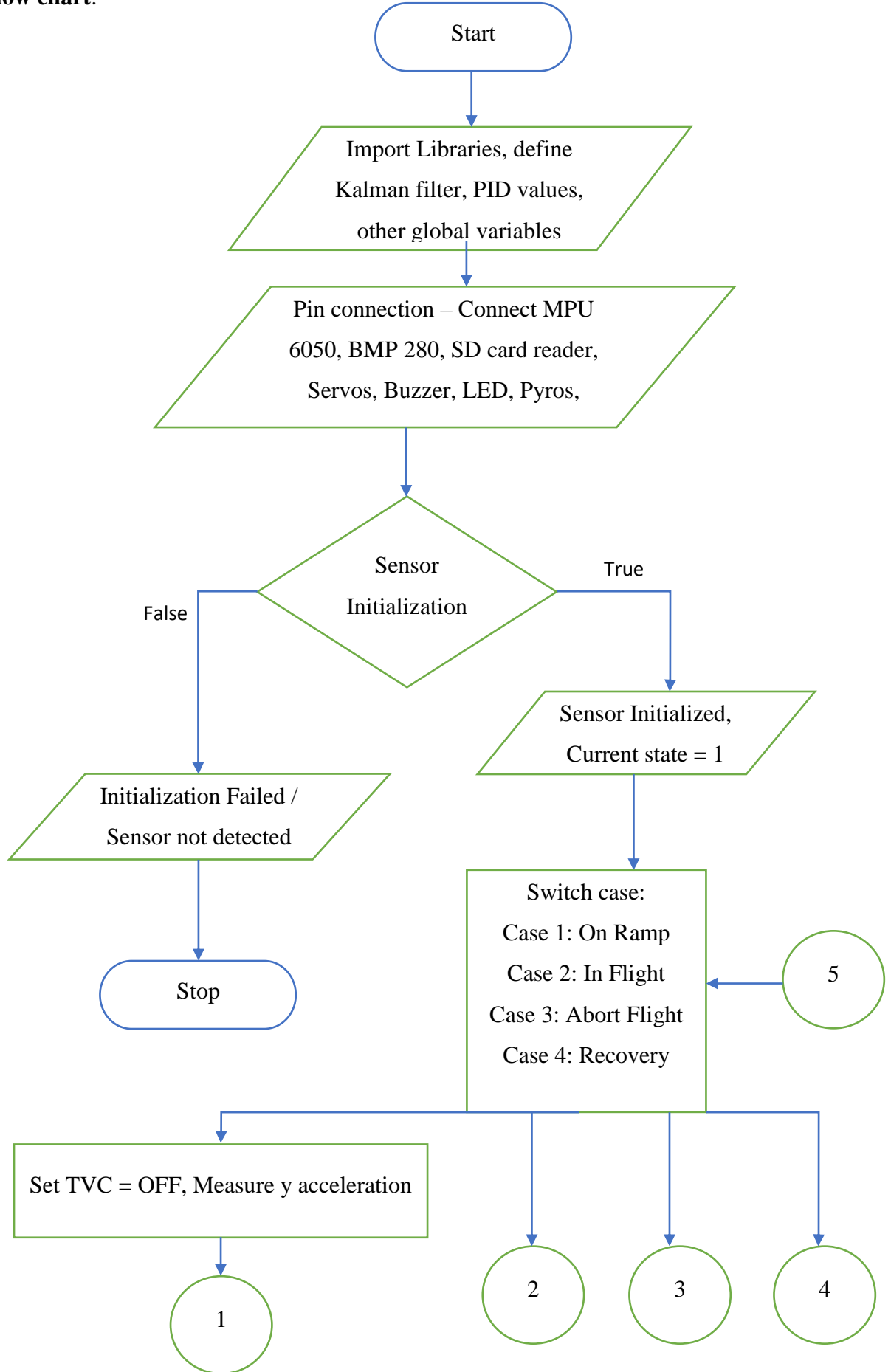
Fig 10. 16LIPO battery

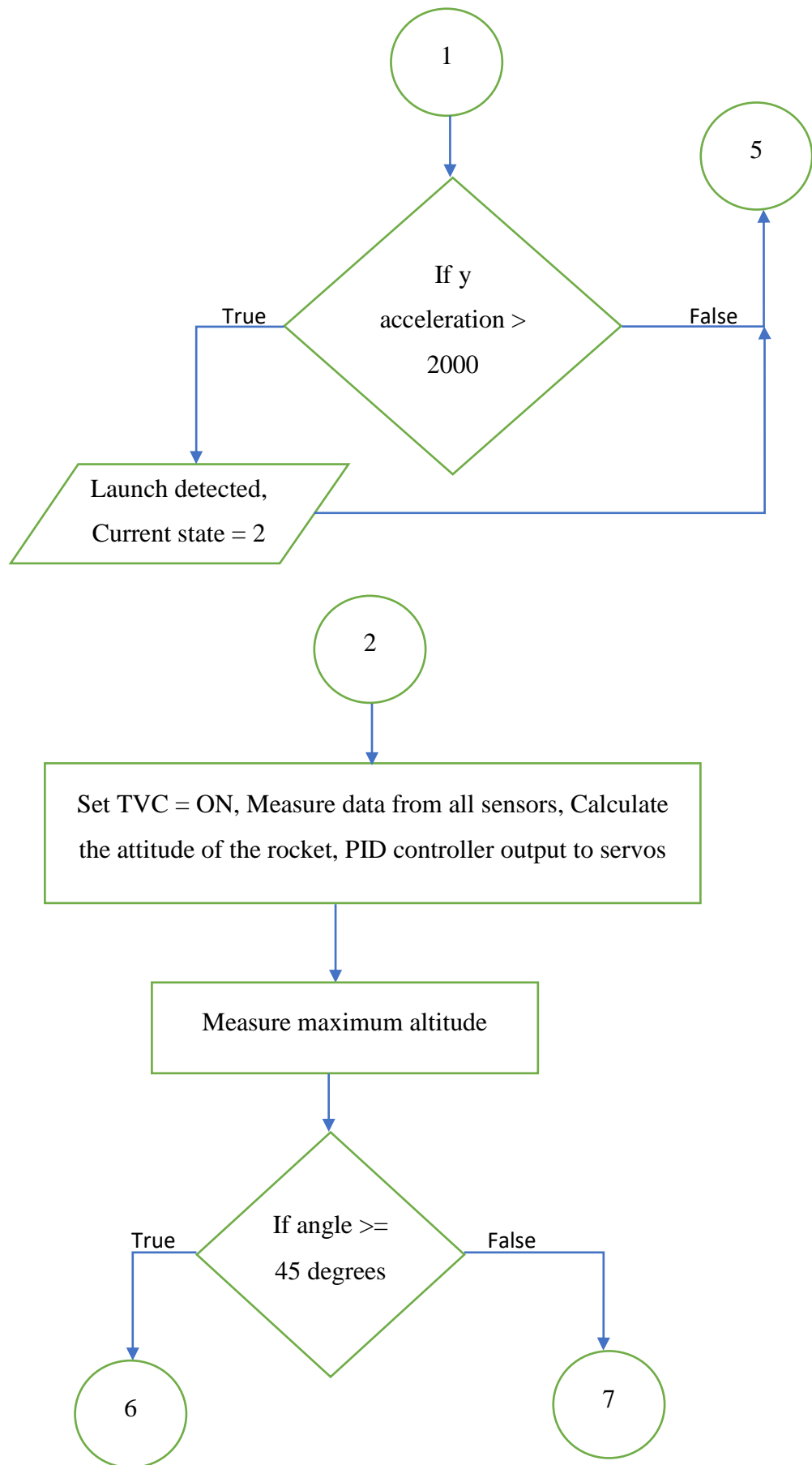
7.4V Lithium Polymer battery is used to power the flight computer and also send high current to pyros when they are activated.

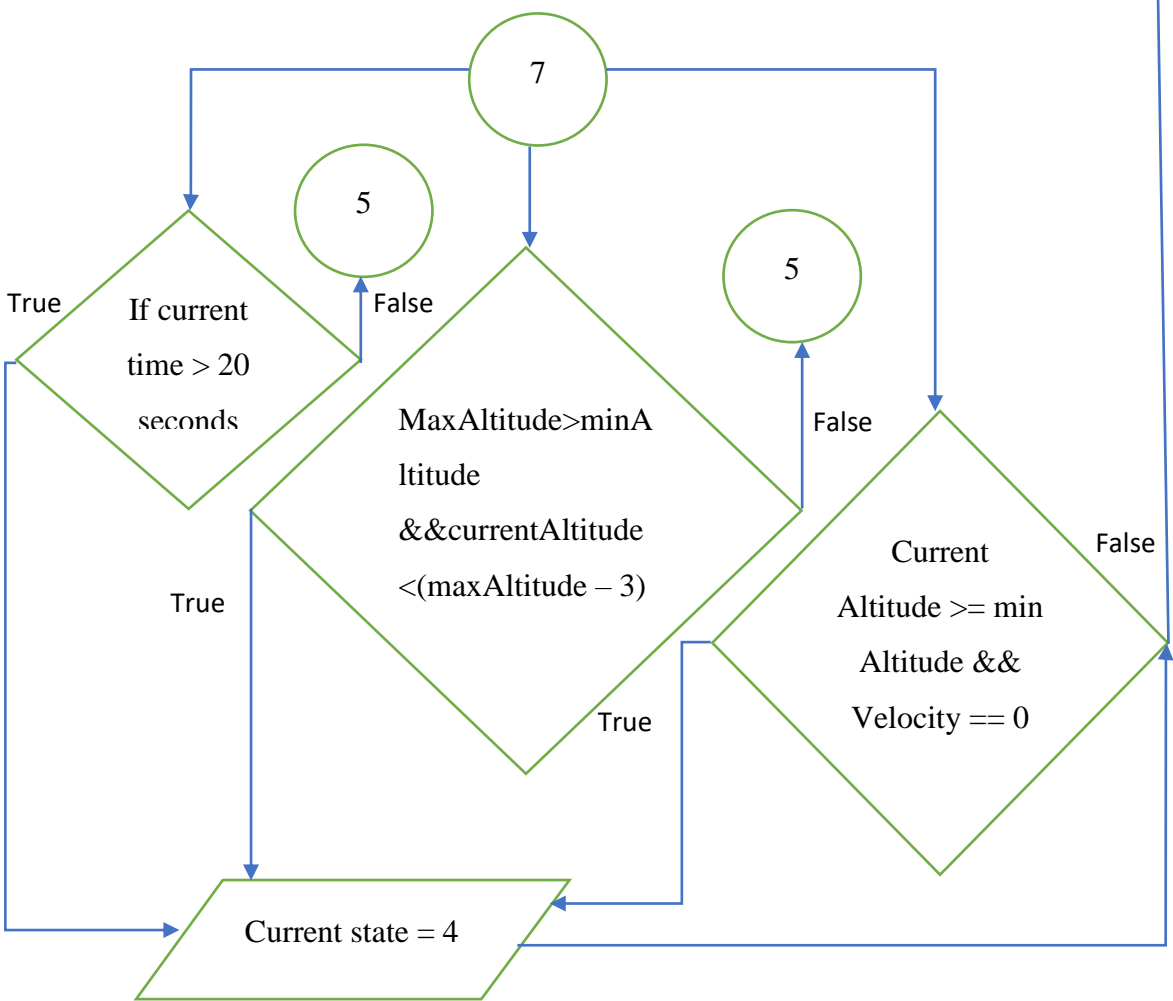
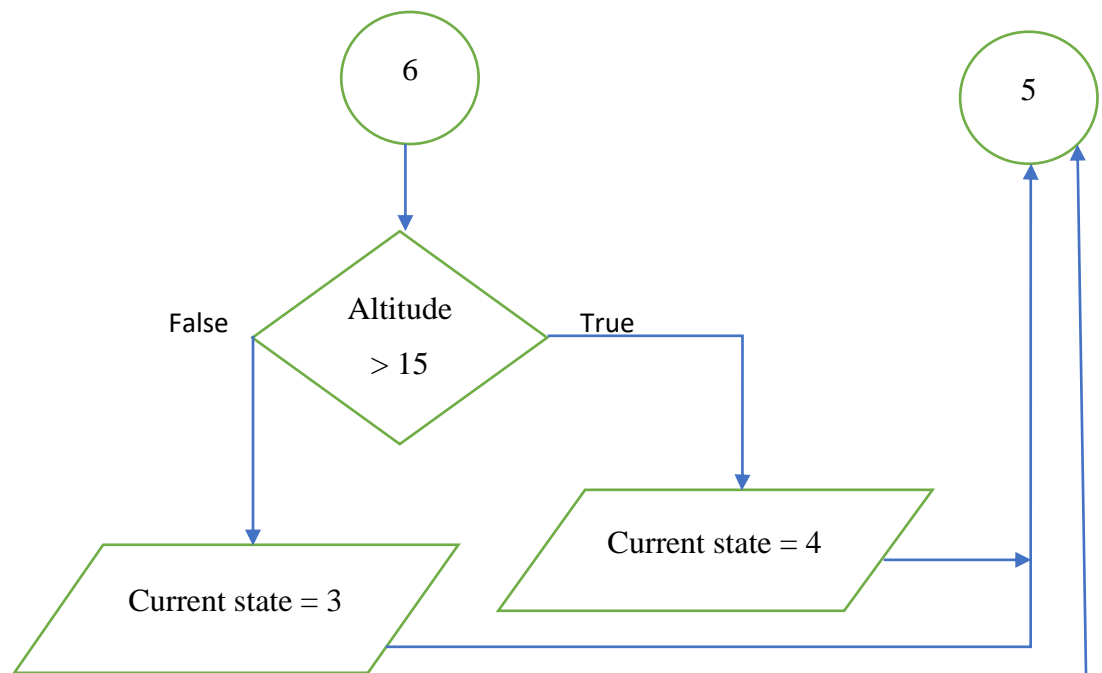
10.8. TVC CODE GENERATION:

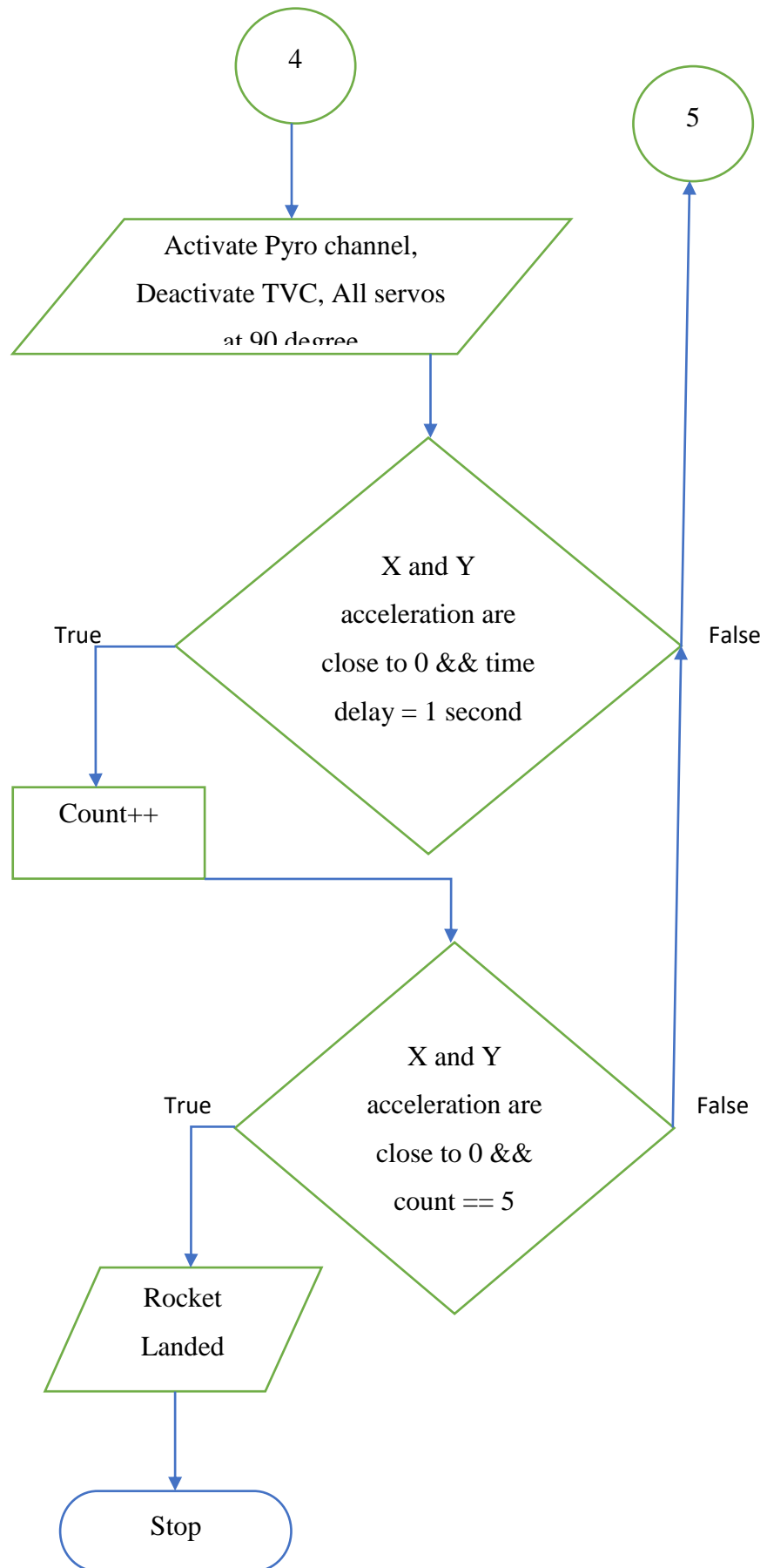
Code is generated in Arduino IDE that is based on C++ programming language and it is depicted in Appendix 4, The code works on the fallowing flowchart

Flow chart:









a) In the first step, the following libraries are imported:

- Arduino.h
- Wire.h
- Servo.h
- I2Cdev.h
- SPI.h
- SimpleKalmanFilter.h
- SD.h
- MPU6050_6Axis_MotionApps20.h
- helper_3dmath.h
- PID_v1.h
- Adafruit_BMP280.h

b) In the next step the pin numbering is done for individual components, bearing in mind to use Pulse Width Modulation pins to RGB LEDs, buzzer and Servos. Since both MPU 6050 and BMP 280 work on I2C protocol, they can be connected to the same Serial Clock and Serial Data pins on the Teensy board. Because the SD card reader works on SPI bus, that is faster than I2C protocol, separate pins are defined for MOSI and MISO and Chip select pins.

A PID controller will be implemented to control 2 servos. A simple Kalman filter will be used to filter out the noise from the raw values of MPU and give stable reading. After this, the PID values along with quaternion vectors are defined. In the end other global variables required to execute the code are initialized.

c) Next step is to setup in which pins will be defined, sensors connection will be checked and initialized’.

d) In the loop section, a switch case is used to detect 4 states of the rocket namely:

- i. ‘On Ramp: This state of the rocket indicates, that the rocket is placed on the launch pad and is ready for takeoff. The thrust vectoring is set to off in this mode.

It continuously calculates the acceleration in y direction and if this acceleration is beyond 2000, the launch is detected then the current state of the rocket is now In-Flight mode.

- ii. In Flight: In this mode, the flight computer continuously logs all the data from the available sensors. It then processes the data to calculate the

attitude of the rocket and passes it to the PID controller. The PID controller then outputs the data to servos and stabilizes the rocket.

This mode also aborts the flight if the rocket is tilted to 45 degree or more. If everything is well and good then code is written to calculate the maximum altitude that depends on the reading of the barometer. If the current altitude is lower than the previous altitude of the sample then the apogee is detected and this altitude is stored.

There are 3 types of recovery mode for the rocket. The first one is a predetermined time interval after the launch is detected. When this time is elapsed the current state changes to Recovery mode. The second one is an and function between maximum altitude is greater than minimum altitude specified in the code and if the current altitude is lesser than (maximum altitude minus 3m). The third one is also an and function of (if current altitude is greater than or equal to minimum altitude) and velocity is negative. This is one of the safest modes to activate Recovery mode.

- iii. Abort Flight: The flight is aborted and if the height is lesser than 15m, pyros are deactivated. Else if the altitude is greater than 15m, recovery mode is activated.
- iv. Recovery: If this mode is activated then the pyro channels are activated and the parachutes are deployed. Thrust vectoring is stopped and the servos are position to 90 degrees.
- v. Land detection is also programmed in which the computer checks acceleration in x and y to be close to zero and waits are 5 count of these values. If the count is 5 then the land is detected and data logging is stopped

10.9. PCB DESIGN

PCB design is done in AUTODESK's EAGLE software. First the schematic design is done where each connection is made for the components. Then the board is designed according to the schematic. The board is sized 115 * 65 cm. The schematics and board design are shown below.

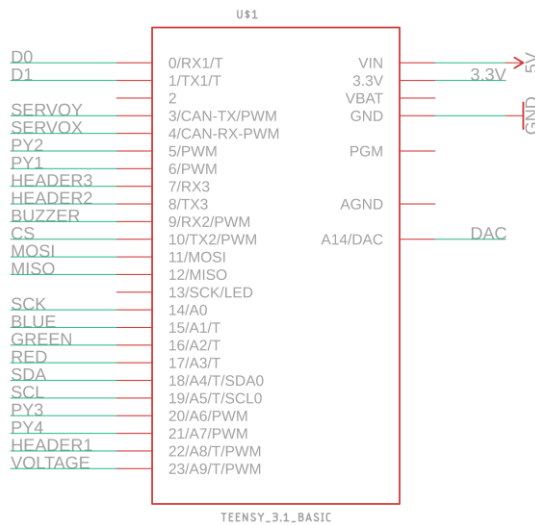
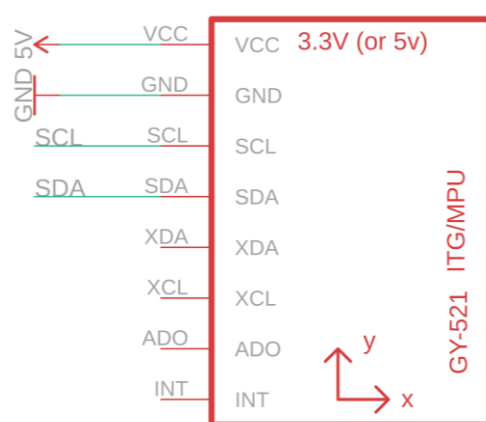

Fig 10. 17Teensy 3.2

Fig 10.17 shows the buzzer along with two servos ServoX and ServoY requires pulse width modulation (PWM) pins. Hence Buzzer is connected to Digital pin 9 and The two servos are connected to pin 3 and 4 respectively of the Teensy micro-controller. Pin 5,6,20 and 21 are connected to 4 pyro channels. Chip-select (CS), Master out Slave in (MOSI), Master in Slave out (MISO) and Serial clock (SCK) of SD card reader, are connected to Digital pins 10, 11, 12 and 14 respectively. LED terminals are connected to Analog pins A1,A2 and A3. Serial data and clock are connected to pin 18 and 19 respectively. Voltage measure pin is connected to Analog pin A9. The header pins are connected to 7,8 and 22 for the requirement of any Serial communication in future projects.


Fig 10. 18MPU 6050

MPU 6050 and BMP 280, work on I2C protocol and requires only SCL and SDA pins that are connected to Teensy and are shown in Fig 10.18 and Fig 10.19

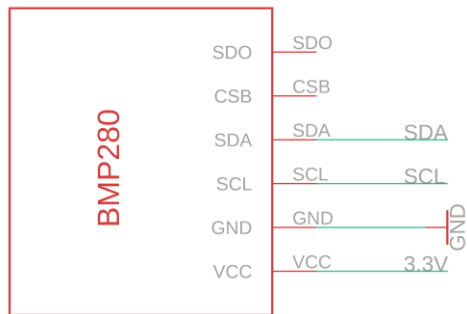
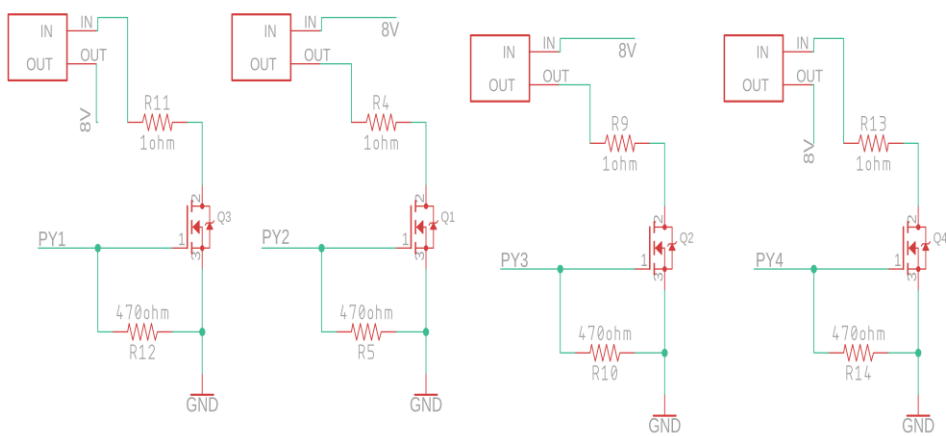

Fig 10. 19BMP 280

Fig 10. 20Micro SD Card Reader

SD card reader works on SPI (Serial Protocol Interface), hence requires 4 pins these are Chip-select (CS), Master out Slave in (MOSI), Master in Slave out (MISO) and Serial clock (SCK) as shown in Fig 10.20. The pyro signals consisting of Terminal block, N channel MOSFET, pull-up and pull-down resistors are shown. The PY is the pyro signal that connects Gate terminal to Teensy as shown in Fig 10.21


Fig 10. 21Pyro channels

Capacitors are used to filter out noise during voltage stepdown in Voltage regulators and their schematic is as shown in Fig 10.22, Schematic for servo is shown in Fig 10.23, where SERVOX or SERVOY is the signal connection to Teensy.

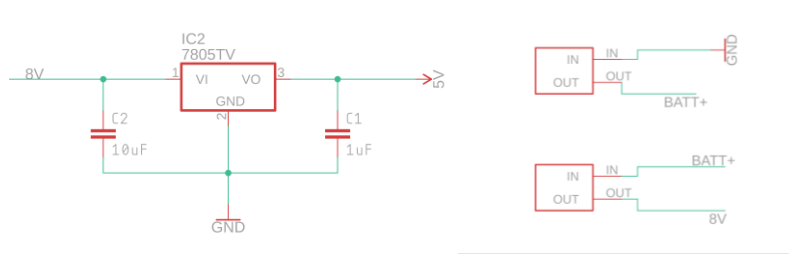
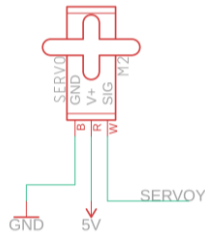
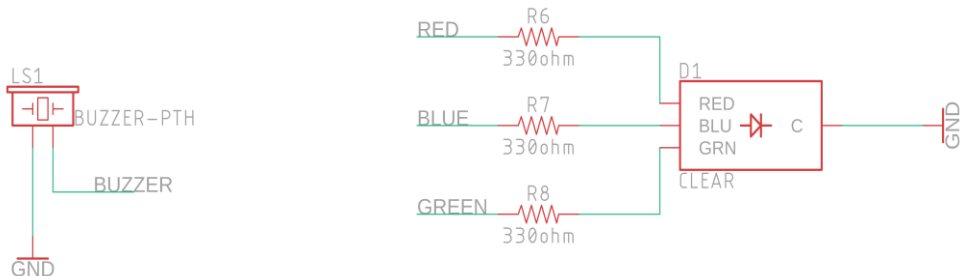
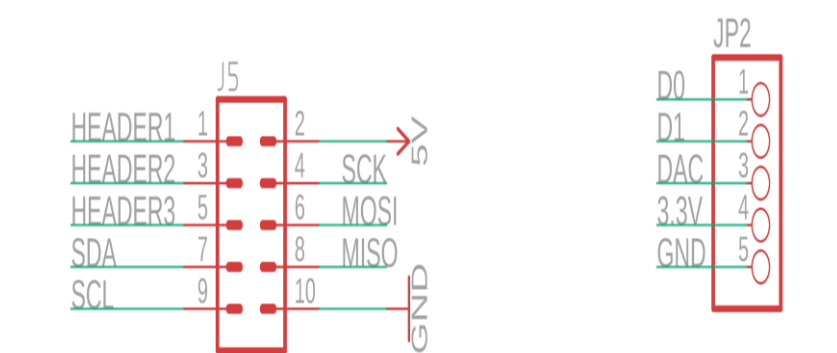

Fig 10. 22Voltage Regulator, Battery Terminal and Switch

Fig 10. 23Servo

Fig 10.24 shows the Buzzer and RGB LED schematic, LED requires current limiting resistors to prevent damage to LEDs hence, three 330-ohm resistors are used for each terminal whereas buzzer does not require any. Fig 10.25 Header pin block J5 and JP2 are extra terminals that can be used to connect any peripherals that work on SPI or I2C protocol.


Fig 10. 24Buzzer and RGB LED

Fig 10. 25Header Pins

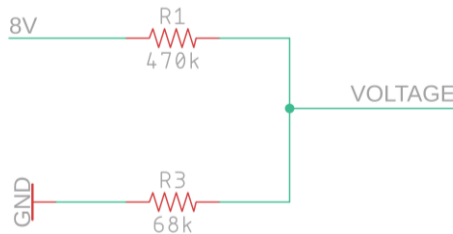
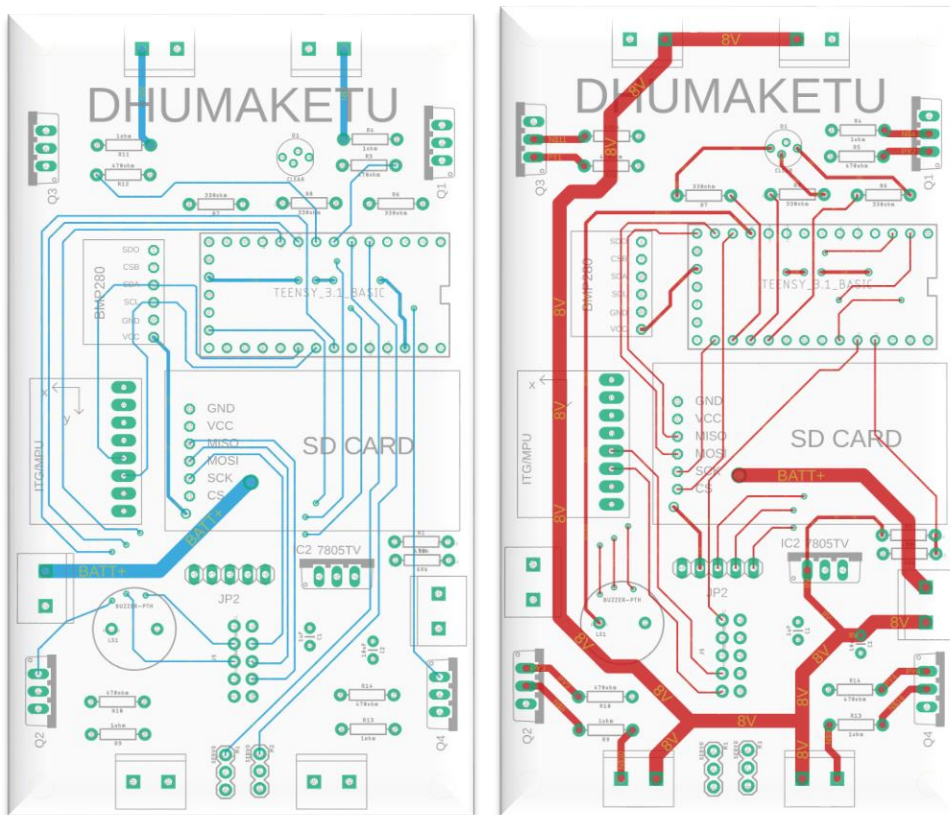

Fig 10. 26Voltage Measure

Fig 10.26 shows the schematic of voltage measure; Voltage divider rule can be used to measure the battery voltage. 470k ohm and 68k ohm resistors are used for this purpose and the voltage across 68k ohm resistor is measured which is then multiplied by a factor in the code to determine the actual voltage


Fig 10. 27Top and Bottom layer of PCB board

The board contains 2 main layers of copper. Top layer – 5V and Bottom layer – Ground. The placement of components is a result of several iterations that is convenient for the sensors. From the schematic design, the components are already connected to their respective pins through what is known as air-wires in Eagle. In the board design, Copper traces of suitable width has to be drawn following these wires. Holes known as ‘Via’ can be used to jump from bottom of the board to the top and vice versa. For the battery

terminal and to power all the pyros, the width is 2mm which is calculated from the current and temperature rise through this path. For all the rest of the signal connections, the width is 0.25mm. The board design is as shown in Fig 10.27, the red and blue paths represent top and bottom layer traces respectively. The same schematic is connected in the Breadboard to test the servo response as shown in Fig 10.28.

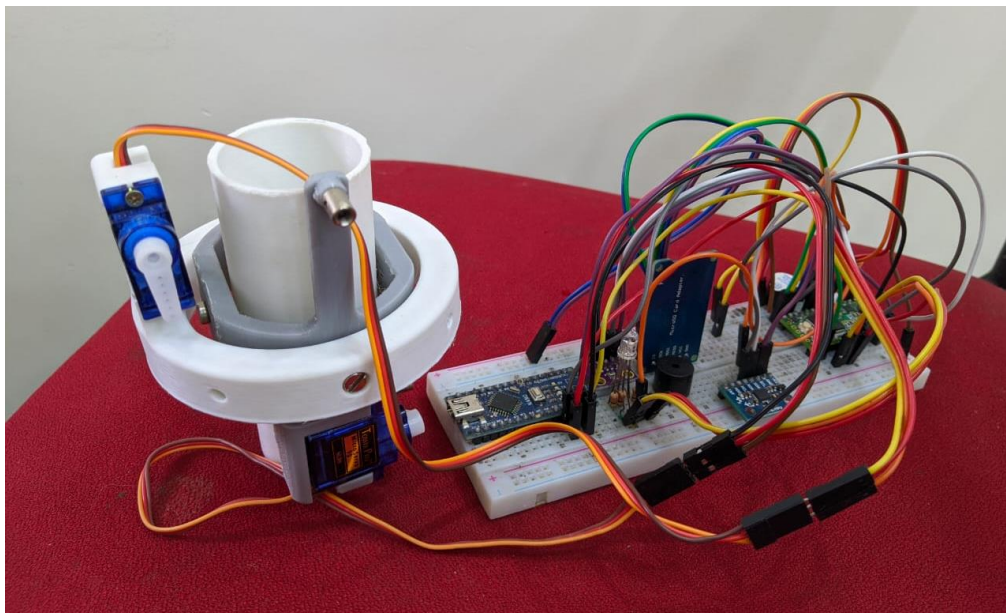


Fig 10. 28 Electronics connections arranged in breadboard for response outputs

The PID response for the Arduino code is recorded and is shown in Fig 10.29 blue line signifies launch detection signal, red line shows detection signal, orange and green line shows the PID response signal for two servos for the applied orientation.

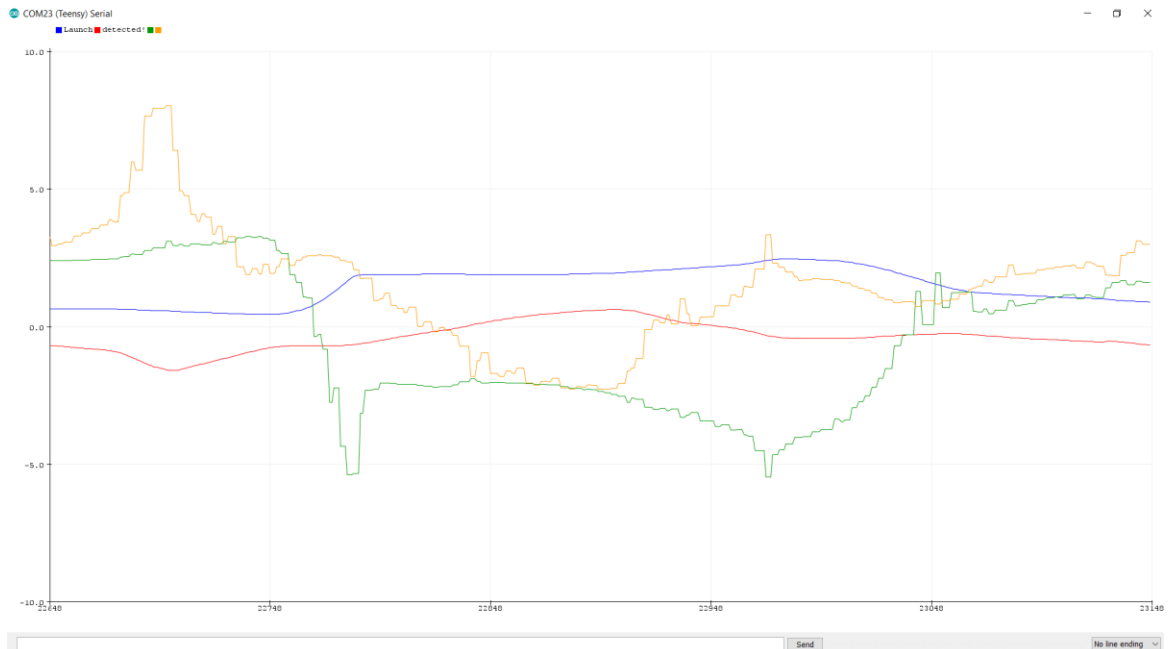


Fig 10. 29 PID response signal and launch detection signal

CHAPTER 11

CONCLUSION

11.1 CONCLUSION

Based on the requirement of reaching an altitude of 10km with a payload of 3.6 kg and then to achieve soft landing, a rocket consisting of two solid rocket motors (ascend and descend motor) has been designed and flight simulation has been carried out. It was found that, Ammonium perchlorate composite propellant with Aluminium as fuel has one of the highest specific impulse among solid propellants and several experimental data were available. Due to these reasons, this propellant is used in both the ascent and descent motor. First, the best mass of the rocket along with propellant required to reach an altitude of 10km and then to soft is determined. It was found that the best total mass of the rocket to satisfy this need was 53.5 kg that includes 26.348 kg + 3.711 kg of fuel. Then the burn simulation has been carried and the design parameters are determined. This process is carried out simultaneously with the MATLAB program that determines the optimal nozzle configuration. Finally, the simulation resulted in the descent motor to have an end burner configuration to satisfy low thrust and long burn duration.

Next, a vertical flight simulation was performed in MATLAB® and Simulink® which resulted in the rocket reaching to desired altitude and then landing safely (zero velocity when altitude is zero). With the confirmation of these results, the rocket body consisting of motor equipped with TVC and landing legs were designed. Suitable materials were selected for these components to stay within the mass margin. A stability analysis was performed to keep the rocket at least in neutral stability. Flow analysis has been carried out one for the maximum velocity (supersonic) and the other in the subsonic region.

The flight data was then merged with a controller and equations of motion was then derived. Although, MPC is a better choice for these applications, there was uncertainty in the controller results. Hence, a PID controller was implemented. The developed MPC controller needed a lot of computation power to tune it for right values as the controller is completely AI based and need to learn itself from mistakes.

A model rocket was then developed to demonstrate the TVC with a PID controller. It was desired that the model rocket to weigh between 1 and 1.5kg. Based on this, a burn simulation was carried out with mixture of Black powder and KnSU as propellant to determine the propellant mass required to reach an altitude of 250m. Next, rocket motor was fabricated and static test was performed. Parts of the rocket such as Landing legs, TVC mount and nose cone was designed and 3D printed. Later, Arduino code was developed based on the selection of micro-controller, sensors and other electronic components to implement a PID controller for TVC. When the code was executed, the serial plotter showed all the sensors along with the controller output to servo motors, performed as desired. Finally, to develop a flight computer, PCB board was designed and the connections were made according to the Arduino code. Although testing of the rocket is not done due to COVID – 19 pandemics, the results obtained are satisfactory to conclude that the model rocket works. Model rockets is gaining interest day by day and will continue to grow in future. One can build a rocket on his own following the guidelines presented in this project and save expenses of buying a rocket kit.

It is also found that the controller developed is very robust and can be easily implemented for the propulsive landing of boosters, it is also found that for propulsive landing a set of small thrusters are required to control the rocket from the equations, and to propulsive land a solid rocket we require small liquid thrusters to ignite after the burnout of the solid boosters for soft landing and thus the thrust vector control can be applied on the Solid Rocket Motors with the explained constraints and this makes the rocket industry more reliable and economic.

11.2 FUTURE SCOPE

The design process and methodology employed in this project to develop a rocket that can reach an altitude of 10km can be further extended to develop similar rocket for low earth orbit satellite launches. Although reuse of solid rockets has not been yet developed, the ease of manufacturing, availability of experimental data and good knowledge on solid propellants attracts many researchers to this field. If at all, a concept of constructing reusable solid rockets are of interest in future, then this project analysis is of great deal in designing such rocket motors.

A better alternative to solid rockets is the hybrid rocket where either fuel or oxidizer can be varied to get various thrust levels similar to liquid propellants. Since these concepts are still developing, the lack of availability of data makes it inconvenient to work on hybrid rockets.

An advance control algorithm such as LQR and MPC can be implemented to the landing phase of rocket that greatly enhances the performance. But the downgrade is that MPC requires several iterations of simulation to get it right. Selection of weight parameters is not universal and is purely based on individual choice.

As far as model rockets are concerned, the concepts developed in this project works best for the hobby scale. This is due to local regulations and cost restrictions. But the same can be improved with a better rocket motor, micro-controller and high response servos.

PUBLICATIONS

- [1] Anutha M., Aishwarya K., Kavya Patil., Prajwal Nayak., and Prajwal P., “Development of Solid Rocket Motor For Ascent Andsoft Landing In Vertical Flight”, IJCRT, pp. 2093-2106, Volume 8, Issue 4, April 2020.

REFERENCES

- [1] Reuben Ferrante., “A Robust Control Approach for Rocket Landing,” Master of Science, Artificial Intelligence, School of Informatics, University of Edinburgh, 2017.
- [2] Jet propulsion laboratory., “Study of Selected Thrust Vector Control Systems For Solid Propellant Motors,” space-general corporation 9200, California, Report No. 884 FR-I, August 2, 1965.
- [3] Dings, A., Cooper., “Design and Integration of a High-Powered Model Rocket,” Worcester Polytechnic Institute, March 2019.
- [4] Samuel S. Bowman1., “Two-Stage, High-Altitude Rocket with Internal Skeleton Design Entered in Advance Category of 7th ESRA IREC”, California Polytechnic State University, San Luis Obispo, CA, 93407.
- [5] Anoop Thankachen and Santosh Kumar., “Design Optimization and Analysis of Rocket Structure for Aerospace Applications,” International Journal of Engineering Trends and Technology (IJETT), Vol. 24., Number6., June 2015.
- [6] M. S. EL-Wazerya., M. I. EL-Elamya., and S. H. Zoalfakarb., “Mechanical Properties of Glass Fiber Reinforced Polyester Composites,” International Journal of Applied Science and Engineering, pp. 121-131., Vol. 14., 2017.
- [7] Md Akhtar khan1., B.K Chaitanya., Eshwar Reddy Cholleti., “Conceptual Design and Structural Analysis of Solid Rocket Motor Casing,” IJERCER, ISSN (e): 2250 – 3005., Vol. 07., Issue. 02., February, 2017.
- [8] Eric Hardester and Philip Kinghorn., “Rocket Fin Design,” February 15, 2013.
- [9] Ashraf Fathy Ahmed and Suong V Hoa., “Thermal insulation by heat resistant polymers for solid rocket motor insulation,” Journal of Composite Materials, pp. 1549–1559, Vol. 46, Issue. 13., 2011.
- [10] George P. Sutton., “Rocket Propulsion Elements,” John Wiley & Sons, Inc., New York, 1964.

APPENDIX

APPENDIX 1: MATLAB CODE FOR THEORETICAL CALCULATION

```

clc;
clear all;

%%propellant constants%%

a = 0.0482;                                     %burn rate co
efficient (in/s)
al = a*25.4;                                     %burn rate co
efficient (mm/s)
n = 0.3607;                                      %pressure exp
onent
rho = 0.054352;                                   %propellant d
ensity (lb/inch^3)
rho1 = rho*27679.9;                               %propellant d
ensity (kg/meter^3)
cstar = 2651;                                     %characterist
ic velocity (ft/s)
cstar1 = cstar*0.3048;                            %characterist
ic velocity (m/s)
k1 = 1.117;                                       %specific hea
t at chamber
k2 = 1.1165;                                      %specific hea
t at exhaust
M1 = 55.381;                                      %molecular we
ight at the chamber (kg/kmol)
M2 = 55.805;                                      %molecular we
ight at the exhaust (kg/kmol)
R = 8314;                                         %gas constant
(J/kmol-K)
Pa = 14.7;                                         %ambient pres
sure (psi)
Pal = Pa*6894.75729;                             %ambient pres
sure (pascal)
Tc = 2059;                                         %Flame temper
ature (kelvin)

```

dimensions of motor %%

```

ril = 5; hf1 = 0; bf1 = 0; nf = 0;                %grain config
uration in mm
ri = ril/25.4
hf = hf1/25.4
bf = bf1/25.4
L1 = 150;                                         %propellant 1
ength (mm)
L = 150/25.4;                                     %propellant 1
ength (inch)
Dep = 1.14173;
Dep1 = 29;                                         %propellant extern
al diameter (mm)
Dt1 = 7;                                           %throat diame
ter (mm)

```

```
Dt = Dt1/25.4; %throat diameter
ter(inch)
De1 = 21;
De = De1/25.4; %exit diameter
r (inch)
```

ri =
0.1969

area calculations and different cross sections%%

```
Acs = pi*ri^2+hf*bf*nf; %cross-section area
Ab = ((2*pi*ri)+(2*nf*hf))*L; %burn area (inch^2)
Ab1 = Ab*645.16; %burn area (mm^2)
At = (pi*(Dt^2))/4 %throat area (inch^2)
At1 = At*645.16; %throat area (mm^2)
Ae = (pi*(De^2))/4 %exit area (inch^2)
Ae1 = Ae*645.16; %exit area (mm^2)
```

At =
0.0597

Ae =
0.5369

motor performance calculation %%

```
Pc = ((rho*Ab*a*cstar)/(32.1741*At))^(1/(1-n)) %chamber pressure (psi)
Pcl = Pc*6894.76; %chamber pressure (pascal)
Kn = Ab/At %burn to throat ratio
```

```

at area
rb = (a*((Pc)^n))                                %burn rate (i
n/s)
rb1 = rb*25.4;                                    %burn rate (m
m/s)
M = sqrt((2/(k1-1))*(((Pc/Pa)^((k1-1)/k1))-1))    %mach number
at exit
Te = Tc/(1+(((k1-1)*M^2)/2))                      %temperature
at exit
r = R/M1;                                         %gas constant
/molecular weight in chamber
Ve = sqrt(((2*R*Tc)/(M2*(k2-1)))*(1-(Pa/Pc)^((k2-1)/k2)))   %velocity at
exit(m/s)
Vel = M*sqrt(k2*r*Te);                            %alternate fo
rmula
Pt = Pc*((1+((k1-1)/2))^(-k1/(k1-1)))          %throat press
ure(psi)
Pt1 = Pt*6894.76
Tt = Tc/(1+((k1-1)/2))                           %throat tempe
rature
mdot = ((Pc1*At1)/sqrt(Tc))*sqrt((k1/r)*(((k1+1)/2)^(-(k1+1)/(k1-1)))*10e-6) %mass flow ra
te (kg/s)
mdot1 = 2.205*mdot                                %lb/s
T = (mdot*Ve)                                     %thrust
Cf = sqrt(((2*(k1^2))/(k1-1))*(((2/(k1+1))^((k1+1)/(k1-1)))*(1-((Pa/Pc)^((k1-1)/k1)))))%th
rust coefficient
Isp1 = T/(mdot*9.81)                               %specific imp
ulse
Isp2 = (Cf*cstar1/9.81);                          %alternate fo
rmula
AR = (Ae/At)                                       %area ratio
PR = (Pa/Pt)                                       %pressure rat
io
mp = (1504*((pi*(Dep1^2)/4)-Acs)*L1)*10e-6      %mass of prop
ellant required
PRT = Acs/At                                       %port to thro
t ratio
mfluxt = mdot/At                                    %mass flux at
the throat

```

Pc =

167.6862.....

Published with MATLAB® R2019b

APPENDIX 2: NOZZLE DIMENSION CALCULATION MATLAB CODE

```
clc;
clear all;

rt=0.5;
rc=1.8;
re=1.8;

for theta=20:1:45
    theta
    xc=(rc-rt)/(tand(theta))

end

for alpha=12:1:20
    alpha
    xd=(rc-rt)/(tand(alpha))

end
```

APPENDIX 3: 1D FLIGHT SIMULATION MATLAB CODE

```
%motor data%
clc;
clear all;
%thrust as a function of time%

%Ascent Motor%
Thrust = xlsread('C:\Users\HP\Desktop\controlling\point mass\AscentMotor.csv','B2:B253');
Time = xlsread('C:\Users\HP\Desktop\controlling\point mass\AscentMotor.csv','A2:A253');

Total_impulse = 62000;
Propellant_mass = 26.35;
Engine_int_mass = 35;

%Descent Motor%
time = xlsread('C:\Users\HP\Desktop\controlling\point mass\DescentMotor.csv','A2:A795');
thrust = xlsread('C:\Users\HP\Desktop\controlling\point mass\DescentMotor.csv','B2:B795');

total_impulse = 8848; %Ns%
propellant_mass = 3.711; %kg%
engine_ini_mass = 5; %kg%
```

Published with MATLAB® R2019b

APPENDIX 4: TVC ARDUINO CODE COMPILED OUTPUT

The code is developed in C++ language on Arduino IDE platform and the developed code is made public in the following link, <https://github.com/PrajNasa/Thrust-Vector-Control-of-Model-Rockets>, the output of the code is as below

Dhumaketu-Mk2 firmware 05-04-2020

MPU6050 Calibration Sketch

Your MPU6050 should be placed in horizontal position, with package letters facing up.

Don't touch it until you see a finish message.

MPU6050 connection successful

Reading sensors for first time...

Calculating offsets...

...

...

...

Sensor readings with offsets: 0 -1 16387 -1 0
-1

Your offsets: -1119 878 1366 59 0 10

Data is printed as: acelXacelYacelZgyroXgyroYgyroZ

Check that your sensor readings are close to 0 0 16384 0 0 0

If calibration was successful write down your offsets so you can set them in your projects using something similar to `mpu.setXAccelOffset(youroffset)`

Gimbal in use

Initializing MPU 6050 device...

Testing device connections...

MPU6050 connection successful

Initializing DMP

Enabling DMP

BMP Initialized

MEASURE INITIAL ALTITUDE: 820.52m

-720
-670
-734
-724
. . .
2944

Launch detected!

0.39	-2.69	-1.58	9.80
0.39	-2.69	-1.58	9.80
.			
.			
.			
0.44	-2.71	-1.82	9.68

Maximum altitude: 54.24

Parachute ejected!

Current altitude: 54.24

Current vertical velocity: 0.00

. . .

(Count 5)

LANDED!